SOLUTE TRANSPORT IN A LAYERED FIELD SOIL

A thesis presented in partial fulfilment of the requirements
for the degree of
Doctor of Philosophy
in
Soil Science
at Massey University

Valerie Olga Snow

1992

Massey University Library
Thesis Copyright Form

Title of thesis: Solute Transport in a Layered Field Soil

(1) (a) I give permission for my thesis to be made available to readers in Massey University Library under conditions determined by the Librarian.

~~(b) I do not wish my thesis to be made available to readers without my written consent for ... months.~~

(2) (a) I agree that my thesis, or a copy, may be sent to another institution under conditions determined by the Librarian.

~~(b) I do not wish my thesis, or a copy, to be sent to another institution without my written consent for ... months.~~

(3) (a) I agree that my thesis may be copied for Library use.

~~(b) I do not wish my thesis to be copied for Library use for ... months.~~

Signed A Snow

Date 17/2/92

The copyright of this thesis belongs to the author. Readers must sign their name in the space below to show that they recognise this. They are asked to add their permanent address.

NAME AND ADDRESS DATE

ABSTRACT

Although concern about the effects of movement of chemicals through soil has brought about a need for greater understanding of solute transport, the question as to where best to focus the research effort remains open.

Initially a philosophical framework was presented that described in a general sense how research into solute transport has been conducted. It was argued that we must combine modelling with experimentation for effective progress in understanding, and that the efforts in field versus lab experimentation and process- versus non-mechanistic modelling should be balanced. Currently there is a need for more field experimentation, but the preferred direction of the modelling effort is less clear. Both process-based and non-mechanistic models are considered in order to deduce the effect of soil layering on solute transport.

Field experiments were carried out on a soil consisting of three layers of distinct texture. This soil was instrumented with porous cup samplers at four depths at twenty sites. There was also a 2 m^2 lysimeter within the plot.

In the first experiment irrigation was used to supplement rainfall in order to leach a surface application of solid KCl through the soil. Porous cup samples of the soil solution were collected on numerous occasions and soil cores less often. The experiment of the following year was similar in design except that no irrigation was used. Finally, in the third year, the lysimeter was instrumented with porous cup samplers and the same experimental design repeated on a smaller scale.

A convection-dispersion (CDE) model was applied to the lysimeter data. This was successful, provided that the surface soil and assumed Dirac delta solute input were not included in the calibration. Layering within the profile appeared to have little effect on solute transport. The transport porosity was revealed to be two-thirds of the water-filled porosity, thus a substantial part of the water-filled porosity did not transport solute. The CDE modelling of the field data was not particularly

successful, probably due to the spatially variable nature of solute transport and water application.

The Aggregated Mixing Zone (AMZ) model was also used. This model subdivided the transport porosity into convective and dispersive components, and also allowed for non-interacting flow paths. Although the AMZ model was conceptually appealing, parameterisation of the model was found to lack discrimination. Little further understanding of solute transport was gained from this model.

Textural differences in the soil seem to be overwhelmed by both small-scale heterogeneity of water application and solute movement in the soil, especially near to the surface. It was apparent that processes occurring in the surface soil require much more attention than they have been afforded in the past.

Both process-based modelling and field experimentation will increase our understanding of solute transport. It also seems that an increased effort in improving measurement techniques will be advantageous.

ACKNOWLEDGEMENTS

Funding for the work done in this thesis was provided by two organisations that, as a result of recent restructuring, no longer exist. They were the Ministry of Works and Development and the Department of Scientific and Industrial Research.

Thanks are due to Professor Bob White, now at School of Agriculture and Forestry at the University of Melbourne, who was chief supervisor for much of the time. He initiated the work and sought the initial funding.

Dr Dave Scotter, of the Department of Soil Science, provided background guidance and thoughtful discussion throughout the thesis, and later became chief supervisor. Thanks for this as well as the discussions of choice tramping spots in the Ruahines.

Dr Brent Clothier (Environmental Physics Group, HortResearch) found himself co-opted informally, and then formally onto the supervision team. During this study he gave freely of his time and provided much zestful argument, as well as friendship. Brent also was closely involved in the final writing of the thesis. Without his inspiration, encouragement and guidance the thesis probably would not have been completed within the deadline. He deserves, and has, my great appreciation.

The last appointment to the supervisorial team was Dr Paul Austin, then of the Department of Production Technology at Massey University, but now at Cambridge Control, Cambridge, United Kingdom. Paul encouraged a line of research that probably would otherwise have been ignored and, as well as his modelling skills, brought a different perspective to many discussions. I hope he appreciated the ensuing debate.

At various times the following people assisted in the field work.

Katy Grainger and Hugh Forlong helped instrument the field. Hugh also carried on with the experimental work while I was ill in 1988.

Most of the students in the Department of Soil Science in 1989 helped spread fertiliser on the plot.

Malcolm Boag, Dave Scotter, and Alister Pickens tried to help me get the irrigation system started in 1989, fought over who would get to wear the Gortex raincoat, and provided solace when it wasn't needed.

Ross Wallace and especially Ian Furkert helped with those jobs that just couldn't be done by one person, such as mowing the 0.35 ha plot with standard lawnmowers.

John Julian deserves special mention. He helped organise equipment, coaxed the irrigation pump, did all sorts of jobs that made the field work possible, and terrified me with his cross-country driving.

Thanks to all these people and to those whose, although not included formally here, efforts are nevertheless appreciated.

Thanks to Dave Barker for the final proof reading of the thesis. This was much appreciated.

Jacque Rowarth, Prue Williams, Peter Kemp, and Robyn Simcock all proved to be wonderful friends during this study. Thanks also to the members of the Manawatu Tramping and Skiing Club with whom I spent too many sanity-preserving days, both enjoyable and miserable, in New Zealand's wonderful forests, rivers, and mountains.

TABLE OF CONTENTS

Chapter Three
RESULTS AND DISCUSSION

Chapter Four
CONVECTIVE-DISPERSIVE MODELLING OF SOLUTE TRANSPORT

Chapter Five
THE AGGREGATED MIXING ZONE MODEL

Chapter Six
DISCUSSION AND CONCLUSIONS

List of Figures

List of Tables

List of Symbols

a_i	parameter in A	-
b_i	parameter in B	-
c	soil solution concentration	$M\ L^{-3}$
c^f	flux concentration	$M\ L^{-3}$
c^r	resident soil solution concentration	$M\ L^{-3}$
c^ϕ	field-scale soil solution concentration	$M\ L^{-3}$
c_i	input solute concentration	$M\ L^{-3}$
c_o	output solute concentration	$M\ L^{-3}$
c_p	concentration in rainfall	$M\ L^{-3}$
c_r	concentration in irrigation	$M\ L^{-3}$
e	error, deviation of model from data	-
f	solute travel-time probability density function	T^{-1}
f	defined by equation (A.8)	-
g	solute life-time probability density function	T^{-1}
g	defined by equation (A.9)	-
i	dummy variable	-
j	number of intervals of cumulative drainage	-
j	dummy variable	-
k_i	AMZ model parameter, defined by (5.14)	-
l	dummy variable	-
n	dummy variable (Appendix B)	-
n_a	number of a_i parameters in A	-
n_b	number of b_i parameters in B	-
n_c	number of c_i parameters in C	-
n_d	number of d_i parameters in D	-
n_f	number of f_i parameters in F	-
n_i^z	number of tanks in i^{th} series at depth z	-
n_k	number of delays on the ARMA input	-
q^{-1}	delay operator	-
s	slope of the saturated water vapour curve	$M\ L^{-1}\ T^{-2}$
s	Laplace variable (Ch. 5)	-

t	time	T
v	pore-water velocity	$L\ T^{-1}$
x	number of pathways	-
x_i	proportion of water passing through i^{th} path	-
z	depth or calibration depth	L
A	cross-sectional area	L^2
A	ARMA equation polynomial	-
B	ARMA equation polynomial	-
C	ARMA equation polynomial	-
C	Laplace transform of c	-
C_i	Laplace transform of c_i	-
C_o	Laplace transform of c_o	-
C_r	count ratio	-
D	dispersion coefficient	$L^2\ T^{-1}$
D	ARMA equation polynomial (Ch. 5)	-
E	evapotranspiration rate	$L^3\ L^{-2}\ T^{-1}$
F	ARMA equation polynomial	-
F	defined by equation (A.2)	-
H	total solute uptake by herbage	$M\ L^{-2}$
I	cumulative drainage density	$L^3\ L^{-2}$
$\overline{I}$	average drainage density	L
I^{ϕ}	field-average drainage	$L^3\ L^{-2}$
J^{ϕ}	field-average solute flux	$M\ L^{-2}\ T^{-1}$
J_w	water flux	$L\ T^{-1}$
L	calibration depth	L
M	amount of applied solute	$M\ L^{-2}$
N	number of samples	-
P	rainfall	$L^3\ L^{-2}$
Q	water flow rate	$L^3\ T^{-1}$
Q	cumulative drainage	L^3
Q_{in}	solute mass entering soil volume	M
Q_{out}	solute mass leaving soil volume	M
R	irrigation	$L^3\ L^{-2}$

R_n	net radiation per unit area and time	M T^{-3}
V_c	convective volume	L^3
V_m	mixed volume	L^3
V_t	total volume	L^3
Z	prediction depth	L
α_i	AMZ model parameter, defined by (5.12)	-
β_i	AMZ model parameter, defined by (5.13)	-
γ	psychometric constant	M L^{-1} T^{-2}
θ	volumetric water content	L^3 L^{-3}
$\hat{\theta}$	estimated volumetric water content	L^3 L^{-3}
θ_{st}	transport porosity	L^3 L^{-3}
θ_{im}	porosity inactive in solute transport	L^3 L^{-3}
θ_{TDR}	θ measured with a TDR	L^3 L^{-3}
λ	dispersivity	L
λ	latent heat of vaporisation of water (Ch. 2)	L^{-2} T^{-2}
μ	mean of the lognormal distribution	-
μ_{field}	field average mean of lognormal distribution	-
ρ_b	bulk density	M L^{-3}
ρ_s	Spearman correlation coefficient	-
ρ_w	density of water	M L^{-3}
σ	standard deviation of the lognormal distribution	-
σ_{field}	field average of the lognormal distribution	-
τ	input time	T
$\mathcal{L}$	Laplace operator	
E	expectation	
E_f	expectation at field scale	
E_l	expectation at local scale	
E_{field}	expectation of field-average BTC	
Var	variance	
Var_f	variance at field scale	
Var_l	variance at local scale	
Var_{field}	variance of field-average BTC	
Cov	covariance	

Chapter One

INTRODUCTION

1.1 INTRODUCTION

Concern about deleterious effects upon the environment consequent to the movement of chemicals through soil has lead to an unprecedented interest by both scientists and the lay-community about matters related to solute movement.

Late in the 19th century when soil physics research was very much in its infancy, F.H. King, a soil physicist at Madison, Wisconsin, encouraged his mathematician colleague, Charles Sumner Slichter, to become engaged in the study of ground water. He combined an expression of mass balance with Darcy's Law, and produced the equation for steady flow of water through a soil. Slichter noted that this was a

> "... familiar equation occurring in nearly all branches of applied mathematics, known as Laplace's equation ... it seems remarkable that the fact that the solution of any problem in the motion of ground waters depends upon a differential equation has not been pointed out before."

So the process-based modelling bias of soil physics was established early in its history.

Slichter was not only concerned with communication between the scientific and lay-communities but had an avid interest in field measurement techniques. This is aptly demonstrated by the following quote, recorded by a non-scientist, from a talk given by Slichter to a local club in the late 19th century.

> "The flow of water exercised our speaker's ingenuity. He makes a pair of holes in the ground, puts some nasty stuff in the water of one and makes his attendant drink from time to time the water of the other. Noting the expression of his face, he determines the moment when the water of one hole appears in the other, and ultimately its rate of progress - some 8-20 feet - or was it miles - per diem."

This also indicates that very early on Slichter aimed to increase understanding by an approach which combined both experimentation with analytical modelling.

While our techniques of chemical analysis may have become more sophisticated during the intervening century, the basic experimental approach has not altered a

great deal. However the models thus far developed to explain and predict solute movement are a great deal more complex than those in vogue 30, or even 15, years ago. Many of these models have not however been rigorously tested against field data.

This lack of testing is of concern as recently Clause 60 of the Resource Management Act has charged Regional Councils with the responsibility to ensure that any

> "... discharge of a contaminant onto land ... which may result in that contaminant ... entering a water body ... [the Regional Council] shall be satisfied that none of the following effects are likely to arise in the receiving waters, ... the rendering of fresh water unsuitable for consumption by farm animals: ... any significant adverse effects in aquatic life."

In addition, Regional Councils are required to monitor compliance with, and the effects of, resources consents (Clause 31) and have an "obligation to adopt best practical option to prevent or minimise adverse effects of discharges" (Clause 13). This, in effect, means that modelling solute transport is required by planning legislation. Thus the lack of fully tested solute transport models capable of application to real-world problems, and capable of predicting solute transport to the satisfaction of the lay community, is of some concern. This also highlights that the need for communication between the scientific and lay communities has, if anything, grown since Slichter's day.

Although the need for greater understanding of solute transport is well established, the question as to how best to focus the research effort remains open. In an effort to answer this question a brief history of solute transport research is presented. Here only the general trends will be highlighted as the purpose of the section is to establish a philosophical framework. Specific questions will be posed in Section 1.3 and the following section will outline the experimental approach taken later in the thesis. This introductory chapter will then conclude with a brief summary. Literature relevant to the experimental and modelling work undertaken in this thesis will be reviewed in the appropriate chapters.

1.2 A HISTORICAL PERSPECTIVE OF SOLUTE TRANSPORT

Late last century, Slichter not only established solute transport research as a field-based experimental discipline but he derived the underpinning equation. Little further progress was made until 1953 when Sir Geoffrey Taylor published a paper describing dispersion in a capillary tube. The equation developed by Taylor, justifiably described more recently by Knight (1988) as 'beautiful', was the classic convection-dispersion equation (CDE). So by the late 1950's our ability to understand and predict the movement of water, at least on the Darcy scale, had greatly improved. These advances set the scene for an increased research effort starting early in the 1960's.

In 1967, Biggar and Nielsen coupled Taylor's (1953) CDE equation with laboratory-based miscible-displacement experiments and started a research approach which dominated solute movement for almost two decades. During this time we learned much about how ionic strength, pore-water velocity, anion exclusion volumes and many other fairly small-scale phenomena affected solute transport. This increased the general understanding of solute transport such that the time came when it was feasible to attempt to apply laboratory-based existing understanding to the field.

Attempts to transfer the existing understanding to field-based problems were not however, in general, successful. We learned that small-scale heterogeneities in the soil structure can have a large effect on solute movement. This indeed enhanced our understanding, even if it was of the harsh realities of the field. However as far as modelling of field-based transport was concerned, we may have only advanced a little. Late in the 19th century, Moore (1898), referring to the land disposal of sewage, stated that,

> "Where the land is of a stiff clayey nature ... cracks one and two inches wide and five feet deep are sometimes met with ... [these result in] the direct passage of sewage and surface water into [the cracks] ... so that the effluent is not purified as intended."

The almost exclusively laboratory-based research of the previous decade had resulted in a mismatch of our understanding of solute transport with reality. Thus demonstrating that overall understanding will not result without a balance of both experimental and modelling approaches.

During the late 1970's and 80's solute transport modelling had remained largely process-based, yet ignored the effect of preferential flow on solute transport. The CDE was adapted to allow for spatial variation in its parameters (Dagan and Bresler, 1981), and the mobile-immobile CDE was also proposed (van Genuchten and Wierenga, 1976), yet still preferential flow was largely ignored. However as data from more field-based experimentation became available it became evident that, at least in some cases, the CDE was inappropriate to describe field-scale transport.

In response, Jury (1982) proposed that a non-mechanistic model might enhance our ability to describe solute transport and the Transfer Function Model (TFM) was launched, at least within soil science. Earlier, Raats wrote that his

> "... transfer function approach to the transport of solutes was ... inspired by the analogous treatments of certain industrial processes ... and of tracers in hydrological systems ..."

and in 1978 he published two papers, one on transfer function theory, and another of example problems. However the concept of the TFM lay dormant in soil science until the pair of papers, Jury (1982) and Jury *et al.* (1982), were published. These not only outlined the theory, but coupled that theory with data from field experimentation, thus demonstrating the necessary linkage of modelling with experimentation for effective progress.

The success of the TFM at predicting solute transport behaviour from Jury *et al.*'s (1982) data led to the realisation that solute had been transported through the soil with little lateral mixing. When Jury (1988) re-examined Taylor's (1953) paper it was revealed that Taylor had stipulated that the CDE was appropriate only where sufficient time had elapsed for mixing to smooth lateral variations in solute concentration. So as a non-mechanistic model, the TFM had indeed enhanced our understanding of solute transport.

Later, White *et al.* (1986), and then Jury and Roth (1990), assigned a mechanistic interpretation to the TFM model by interpreting the TFM in terms of *a priori* knowledge of the structured soil. This demonstrated our preference for process-based models as a framework with which to ponder upon solute transport.

From the above discussion it is possible to create a schematic diagram of the process or cycle that solute transport research has been through, and will go through, in its quest for ever greater understanding of the underlying processes.

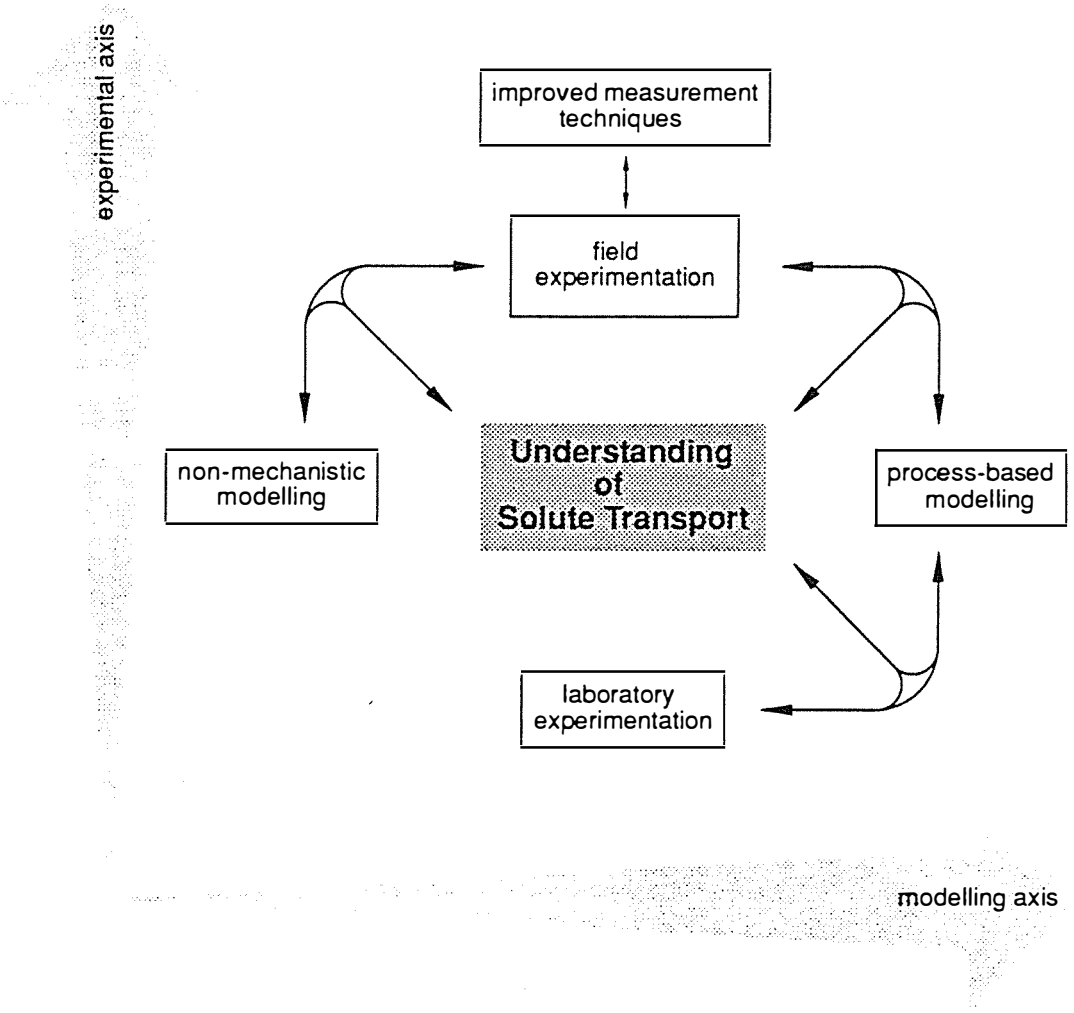

Figure 1.1 A philosophical framework for the understanding of solute transport.

In this schematic the process of gaining understanding of solute transport has been mapped onto its two principle axes, those of experimentation and modelling. Each of these axes have their extremes; field versus lab experimentation, and of process versus non-mechanistic modelling. The systems of arrows on Figure 1.1 show the vital tripartite collaboration of understanding, experimentation, and modelling. Our understanding of solute transport can only improve via the association of experimentation and modelling. Well-designed experiments will result only from the

combination of understanding and modelling. Finally, successful models of solute transport will be those that result from an alliance of understanding and experimentation.

Studies of the late 19th and early 20th century commenced on the upper end of the experimental axis, with field-based research, but little in the way of any model of solute transport. Little progress was made until the 1960's. Then there was a synergism between laboratory experimentation and process-based modelling which greatly enhanced our basic understanding of solute transport. Thus, during the 1960's and 1970's, solute transport research was placed firmly at the lower end of the experimental axis and the upper end of the modelling axis.

Understanding gained by the partnership of process-based modelling with laboratory experimentation, coupled with the availability of improved techniques to monitor *in situ* solute and water transport, allowed advances in field experimentation. This experimentation revealed that understanding developed in the laboratory was not entirely applicable in the field. This reveals that understanding resultant from effort concentrated exclusively at either extreme of the experimental or modelling axis will be biased, and will not be a faithful rendition of reality.

Experience has shown that there is a need to balance our efforts in modelling with those in experimentation. It is questionable if the large number of untested computer models published in the last decade have truly enhanced our understanding of solute transport. Philip (1991) succinctly referred to this as a "...shadow-boxing surrogate for science ...". In the last decade or so, the modelling and experimental efforts have not necessarily been balanced.

Perhaps the direction, from laboratory- to field-based experimentation or from process to non-mechanistic modelling, should change from time to time. But a balance should be maintained for effective progress.

Is there presently greater need for modelling or for experimental work? On each of the axes depicted in Figure 1.1, in which direction should we be moving? Towards non-mechanistic in preference to process-based modelling? Should we favour field-based experimentation in neglect of laboratory experimentation?

Currently there seems to be little doubt that modelling efforts have not been sufficiently complemented by experimental studies. Most reviewers of solute transport research, and also authors of modelling-based papers, lament the paucity of good data. Given our ability to predict solute behaviour in the laboratory this would suggest that the experimental effort should be towards the field. As stated by Feynman in 1967,

> "One of the ways of stopping science would be only to do experiments in the region where you know the law."

Practically, there is a need to resolve field-based problems in the real world. While laboratory-based experimentation may enhance our understanding, it has so far done little for the solution of real-world problems.

The experimental need for field research is well recognised. What about the preferred direction of the modelling effort? This is less clear. This is partly because the distinction between non-mechanistic and process-based modelling has become rather blurred. There are, for example, mechanistic interpretations of some non-mechanistic TFM's. As it is not immediately obvious which direction to take both will be examined, this may reveal the better direction for future work.

This section has attempted to develop a philosophical framework in which to pose general questions relating to solute transport. In the following section specific questions will be posed. These will be brought together again in the concluding chapter, where the scheme presented in Figure 1.1 will be re-examined.

1.3 ISSUES OF SOLUTE TRANSPORT ADDRESSED IN THIS THESIS

The convection-dispersion equation has long been the basis of our understanding of solute transport. This model states that the dispersivity, or the ratio of the spread of the solute breakthrough curve to its velocity, will remain constant with time. However, following the field work of Jury and co-workers (Jury *et al.*, 1982 and Butters and Jury, 1989) it seems that the linear growth in the dispersivity previously seen in aquifers, may also occur in soils. This growth in the dispersivity arises as a result of local correlation of the velocities caused by poor lateral dispersion in relation to the measurement time.

From this then the question arises that if this correlation exists, what is the result when a sharp soil layer interface is encountered? Will any correlation be destroyed, or will it persist? As the persistence of any correlation will ultimately affect the shape of the breakthrough curve, this has practical implications for the movement of contaminants downwards to ground water.

A review of the literature relevant to the effect of soil layers on solute transport reveals that this topic has been more the subject of theoretical studies than of experimentation. Even then, most of the experimental evidence is from repacked, rather than intact, soils.

There are many theories of solute movement allegedly pertaining to layered soils (Bruch, 1970; Shamir and Harleman, 1967; Selim *et al.*, 1977; Al-Niami and Rushton, 1979; Barry and Parker, 1987; Gureghian and Jansen, 1985; Dyson and White, 1989; Dyson *et al.*, 1990; Jury and Roth, 1990; and Leij *et al.*, 1991). These models were usually based on the assumption that the order of the different soil layers did not affect solute movement, and also that solute movement in the two layers was independent. That the former assumption was justified was affirmed by the experimental work of both Selim *et al.* (1977) and Dyson and White (1989). Dyson *et al.* (1990) and Jury and Roth (1990) developed theory to deal with the circumstance where solute transport in the layers could not be assumed to be independent. This might arise for example where solute movement was rapid at one particular place in the soil because water application was consistently high there also (Jury and Roth, 1990).

Field soils are layered. However except where the layering is in the form of distinct horizons of substantial thickness, changes in solute transport within these layers can not in itself be studied, but becomes part of the overall heterogeneity of the soil. Starr *et al.* (1978) and Starr *et al.* (1986) conducted ponded leaching experiments in a layered soil, where the upper layer was less permeable than the lower soil. The experiment was designed specifically to examine the effect of the instability that was produced at the interface between layers. The experiments were not carried out with the intention of examining the correlation of solute transport across an interface and the data presented in the paper were not amenable to this type of analysis. Large continuous macropores would have been water-filled during this saturated flow regime, but would be empty during the unsaturated flow conditions

that more commonly prevail during solute transport in the field. So saturated flow experiments are not necessarily the most appropriate method by which to study the effect of layering.

Here the effect of the interfaces between soil layers on solute transport is the main subject of a combined experimental and modelling research approach. Ancillary questions will be related to the validity of modelling transient processes as if they were rather of a simpler steady-state nature. An elementary examination of the spatial variability of solute transport is also presented.

1.4 EXPERIMENTAL APPROACH ADOPTED IN THIS THESIS

Outlined in the previous section was the rationale for studying the effect of soil layering on solute transport. This section will outline the general approach of the experimental work.

As indicated, in both the title and Section 1.3, the experimental work of this research was field-based. To set the scene for discussions as to the layout of the experimental work, the design was decided in the latter part of 1987 and instrumentation of the field began later that year. At this time the results of the experiment of Jury *et al.* (1982) had already been published. But the differences between the predictions given by the CDE and the TFM, plus the effect of a textural change on the growth of dispersivity, were not revealed until publication of a report by Butters and Jury in 1988.

The Manawatu fine sandy loam consisted of three differing layers of soil located well above the water table. This soil, which will be described fully in Chapter Two, consisted of approximately 500 mm of structured sandy loam, 400 mm of structureless fine sand, and several meters of gravelly coarse sand. The texture of the soil within each layer was relatively uniform and the interfaces between the layers were sharp. Clothier (1977) studied the water transport properties of this soil in detail so the requisite knowledge of the water movement in the soil existed.

In order to study the effect of the interfaces it was necessary to monitor the solute concentration on either side of each interface. Because of spatial variability, it was

desirable that repeated measurements be taken. Since soil cores obviously cannot be used for repeated measurement, porous cups were decided upon as the primary method for assessing the soil solution concentration. The experimental design consisted of many sites within what hopefully would be a relatively uniform extent of soil, each instrumented at several depths with porous cup samplers. Additionally this design would allow an examination of the spatially variable pattern in the breakthrough curves.

The purpose of the first experiment, in 1988, was to provide a data set to allow the development and initial testing of models describing and predicting the transport of non-reactive solutes, in particular anions, through a field soil with distinct soil layers. Leaching of a pulse input of solute under steady water flow was considered amenable to analysis, and also relatively easily managed in the field. Irrigation was used to supplement rainfall to attempt to produce approximately steady-state water movement.

Any models developed as a result of the 1988 experiment would require independent validation. A rigorous test for any model is successful application to conditions different from the calibration and it would appear that Jury *et al.* (1990) are the only researchers to have published work like this. If the 1989 experiments were carried out under natural rainfall then this would provide an ideal data set upon which to validate any model. Additionally it would be possible to compare the 1988 and 1989 experimental results to examine the effects of transient versus steady-state water flow on solute transport.

A further experiment was carried out in 1990, at the smaller scale of a field lysimeter of the same soil. This more-controllable environment was thought likely to yield useful information. As the surface area of the lysimeter was only 2 m^2 it was feasible to irrigate this area by hand, thus allowing greater control of the application rate and variability than might be possible with a conventional irrigation system.

1.5 SUMMARY

These initial sections have presented a philosophic framework of solute transport research, and specific questions to be addressed later in this thesis have been posed. Not only should this thesis provide some insight to the questions posed in Section 1.3, but it should also examine the usefulness of the framework presented in Figure 1.1 and thereby indicate where future work should be directed.

The thesis is now divided into chapters dealing with the experimental details, presentation of the results, process-based modelling of the results, as well as non-mechanistic modelling of the data. Based on these, Figure 1.1 will be revisited in the final chapter.

Chapter Two

SOIL, SITE AND EXPERIMENTAL METHODS

2.1 SITE AND SOIL

The experimental work described in this thesis was done within a paddock of the Massey University Number One Dairy Farm where the soil type was the Manawatu fine sandy loam. In 1986, following a crop of turnips, the paddock was sown in prairie grass (*Bromus willdenowii* Kunth cv. Matua), white clover (*Trifolium repens* L. cv. Pitau), and red clover (*T. pratense* L. cv. Pawera). Since that time the paddock has been grazed as part of the normal rotation of the seasonal-supply dairy farm. By 1988, the pasture had reverted to a mixture of predominantly prairie grass, a perennial ryegrass (*Lolium perenne* L.), and small-leaved genotypes of white clover, with red clover, crested dogstail (*Cynosurus cristatus* L.), browntop (*Agrostis capillaris* Sibth.), and a range of temperate C4 species as minor pasture components (G. Lynch, pers. comm., 1990).

2.1.1 Soil description

A recent soil of alluvial origin, the Manawatu fine sandy loam, comprises six soil horizons (see Table 2.1) to a depth of approximately 1 m, the depth relevant to this study. However the profile can be seen to consist of three morphologically and hydrologically very distinct layers. The description of the horizon nomenclature follows FAO-Unesco (1974). The upper layer consisted of the Ap and Bwj horizons, and will be referred to as the sandy loam layer. The Cu1 and Cu2 (which was not present consistently) horizons were bulked together as the fine sand layer, while the 2C and 3C horizons formed the coarse sand layer. The depth of the interface between the 2C and 3C horizons was highly variable.

Within the section of the paddock on which the experimental work was done, henceforth referred to as the plot, the upper layer of sandy loam had an average depth of 0.4 m, with range 0.3 to 0.5 m. The second layer of fine sand extended to an average depth of 0.85 m, with range 0.7 to 1 m. This layer was underlain by the coarse sand layer which extended for several more meters. The hydraulic behaviour

Table 2.1 Soil Description (Clothier, 1977).

Horizon	Depth (mm)	Description
Ap	0-230	Dark greyish-brown (2.5 Y 4/2) fine sandy loam to silt loam; friable, moderately-developed medium and sub-angular blocky structure; very few faint reddish-brown mottles in lower parts of horizon, many roots, distinct wavy boundary.
Bwj	230-510	Greyish-brown (2.5 Y 5/2) fine sandy loam; friable; weakly developed medium sub-angular blocky structure; few roots; distinct wavy boundary.
Cu1	510-740	Olive grey (5 Y 5/2) fine sand; very friable; weakly developed medium blocky structure; no roots; distinct wavy boundary.
Cu2	740-870	Olive (5 Y 4/3) fine loamy sand; very friable; weakly developed medium blocky structure; many distinct fine reddish-brown mottles; thin sand layers throughout and thin iron coatings at base; sharp wavy boundary.
2C	870-1020	Olive (5 Y 4/3) coarse sand; loose; single grained; very wavy distinct boundary.
3C	1020 (+)	gravelly coarse sand (5 Y 3/2).

of the soil is determined by the fine sand/coarse sand interface (Clothier *et al.*, 1977b). A full description of the soil morphology may be found in Clothier (1977) and Clothier *et al.* (1978). The physical properties may be found in Clothier (1977) and Clothier *et al.* (1977a).

Soil cores of known volume were collected for determination of bulk density, ρ_b [M L^{-3}] of each soil layer. The results are given in Table 2.2. The nature of the coarse sand layer was such that it was possible to obtain only one intact core. Because of such difficulties, that value must be viewed with caution.

Table 2.2 Soil bulk density (ρ_b), standard deviation (sd), number of samples (N) taken for the three layers of the Manawatu fine sandy loam.

Layer	Horizons	ρ_b (sd) Mg m^{-3}	N
sandy loam	Ap and Bwj	1.47 (0.06)	4
fine sand	Cu1 and Cu2	1.40 (0.04)	9
coarse sand	2C and 3C	1.25	1

2.1.2 Lysimeter description

In 1967, a weighing lysimeter was installed with the soil carefully repacked to the same depth layering and bulk density as found in the surrounding soil. Previously this lysimeter had been used both as a non-weighing drainage lysimeter (Clothier, 1977; Clothier *et al.* 1977a and 1977b) and as a weighing lysimeter for water balance experiments (Green, 1983; Green *et al.*, 1984). Field *et al.* (1985) also used the lysimeter for an experiment involving the leaching of simulated cattle urine. During the periods when the lysimeter was not been involved in experimental work it was fenced off from the remainder of the paddock to exclude stock and machinery. The pasture in the lysimeter enclosure was not harvested during these 'non-experimental' periods. This resulted in a composition more prairie grass dominant than the paddock.

A full description of the lysimeter had been given by Green *et al.* (1984). Briefly, the lysimeter had a surface area of 2 m^2 and was 1 m deep. The soil profile consisted of 500 mm of sandy loam above 400 mm of fine sand. Beneath these two layers was 100 mm of gravelly coarse sand. Porous ceramic tubes, air entry pressure 20 kPa, were installed in the base of the gravelly sand layer. The ceramic tubes were connected to a vacuum pump which produced a suction of approximately 35 kPa when measured at the pump. This suction was greater than the air-entry value of the ceramic tubes. But, as a single tube was used to both apply the suction and remove the leachate, the suction actually applied to the tubes was not known. A

liquid trap situated between the pump and tubes allowed the collection of the lysimeter leachate.

2.2 INSTRUMENTATION

2.2.1 Field plot layout

An infra-red photograph taken of the paddock in 1983 at a time of developing crop water stress was used to identify an area close to the lysimeter which was thought to have a reasonably uniform depth of sandy loam plus fine sand. Within this area, 33 holes for neutron probe access tubes were augered on a 10 m × 10 m grid during November 1987. The depths of the interfaces between the soil layers were noted, and 20 holes chosen to have the depth of the layering as uniform as possible. Each of these chosen holes will be referred to as a measurement site. The depths of the interfaces at the selected sites are given in Table 2.3, while Figure 2.1 shows the relative position of the sites as well as the layout of the instruments within each site.

2.2.2 Neutron probe measurements

Access tubes, to allow soil water content measurement by a neutron moisture meter, were installed by augering a hole with a 48 mm diameter bucket auger and inserting an access tube. The hole was augered to either 350 mm below the level of the coarse sand, or until a stone large enough to halt further augering was encountered. The lower ends of the 48 mm internal-diameter aluminium access tubes were sealed with a rubber bung and silicon-based sealant. The upper end of the tubes were installed flush to the soil surface and covered with a rubber cap. When measurements were to be taken an extension was fitted to the tube in order that the cams locking the radioactive source to the shield could be released.

The scaler of the neutron probe was a Troxler Laboratories model 2601. The probe was a Troxler Laboratories model 104A with a 100 mCi Americium-Beryllium source. Data required for calibration of the neutron probe were collected during

Table 2.3 Interface depths, and depth of the deepest sampler.

Site	Depth of interface (mm)		Depth of '1000 mm' sampler (mm)
	sandy loam - fine sand	fine sand - coarse sand	
1	300	880	1050
2	450	800	990
3	420	780	1050
4	450	920	1000
5	420	860	900
6	490	850	1000
7	370	840	960
8	350	940	1010
9	330	920	1020
10	320	910	1050
11	350	1000	1050
12	380	840	920
13	480	730	860
14	306	780	1010
15	430	790	980
16	390	830	1050
17	350	800	1050
18	350	870	1100
19	300	850	950
20	330	950	1050

installation of additional access tubes close to the experimental site. As the hole for the access tube was deepened, the soil from the auger was collected and the depth from which it was taken noted. Gravimetric water content was determined on these samples. Immediately after access tube installation the neutron probe was used to take readings of the count ratio, C_r, at the depths from which the soil samples had

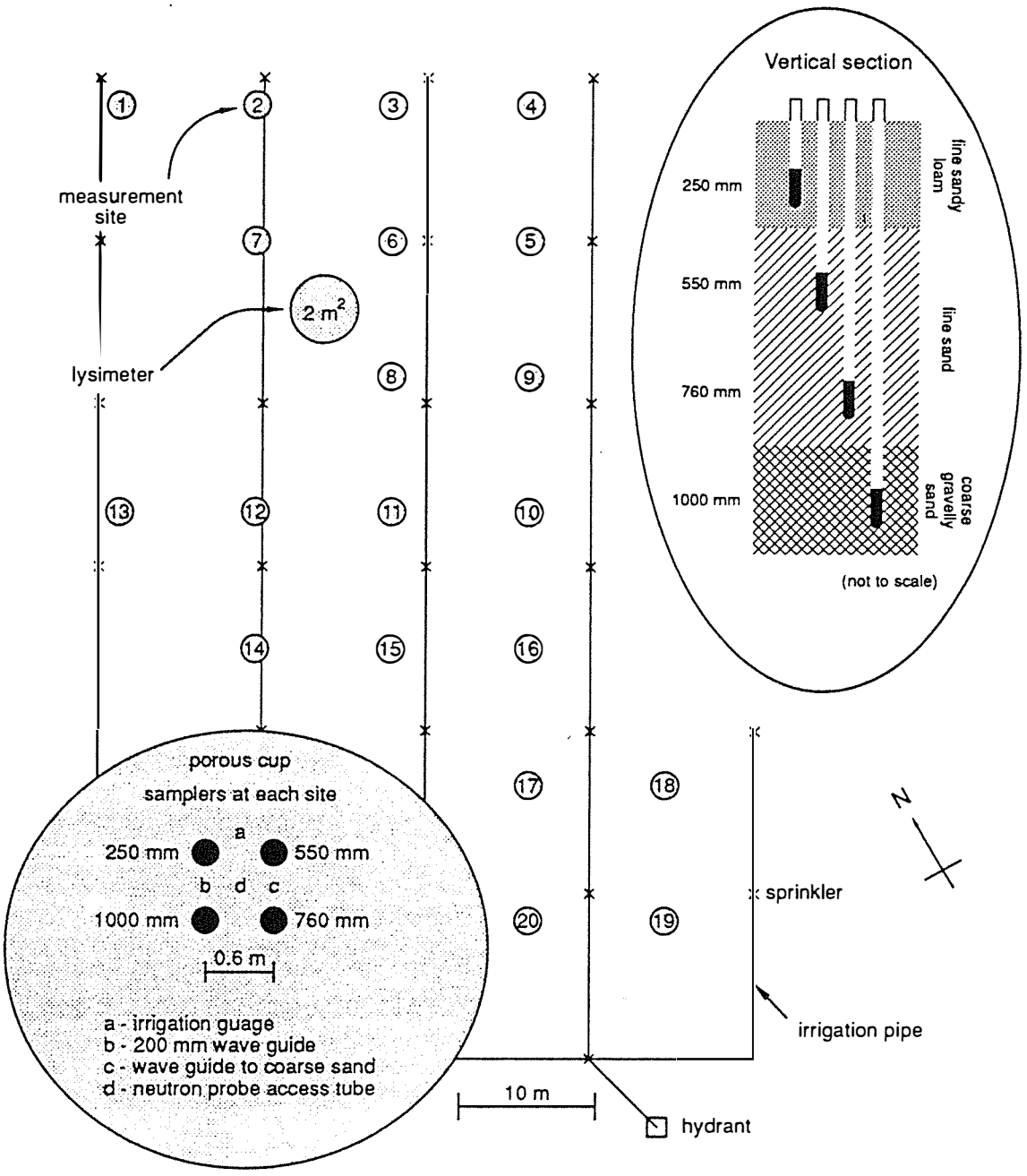

Figure 2.1 Field plot layout.

been collected. Soil bulk density was used to convert the gravimetric water content of the samples to a volumetric basis. The single measurement of ρ_b for the coarse sand soil layer is probably low, and this will have affected the calibration. As the water content determined from the neutron probe measurements will be used only to confirm that the water content of the soil remained constant, any error caused by the effect of the coarse sand ρ_b on the calibration was unimportant.

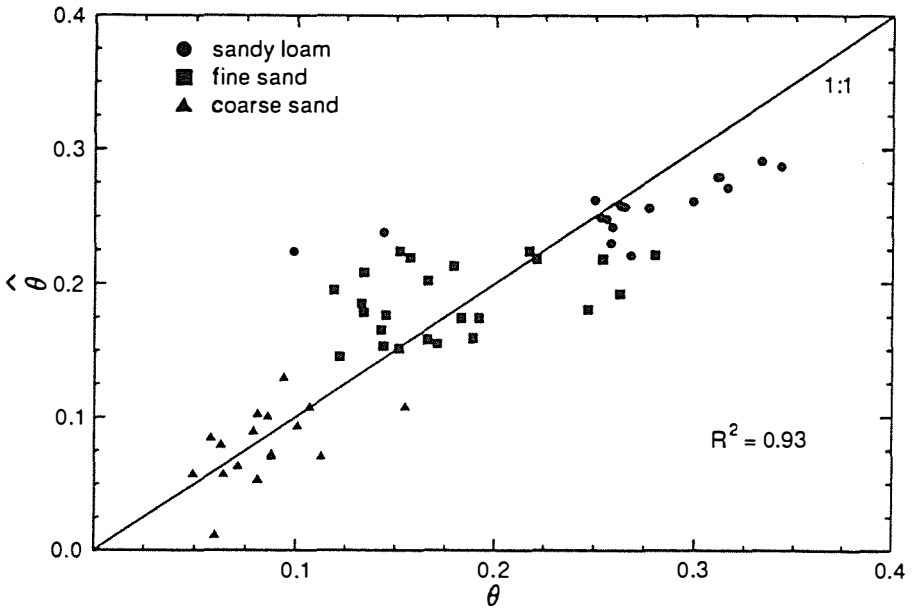

Figure 2.2 Scatter plot of θ measured by gravimetric sampling against that from equation (2.1).

The equation relating C_r to volumetric water content, θ, was determined by linear regression of measured θ on C_r and ρ_b using the REG procedure of SAS. A separate regression for each soil layer was investigated but the regression for the bulked data was found to be adequate. The calibration was,

$$\hat{\theta} = -0.74 + 0.19C_r + 0.56\rho_b \quad , \tag{2.1}$$

where $\hat{\theta}$ is that determined from neutron probing and θ is that measured gravimetrically. Figure 2.2 shows the relationship between θ and $\hat{\theta}$. In order to avoid soil surface effects, measurements were not taken within 200 mm of the surface.

2.2.3 Soil solution sampling

Much of the data presented in this thesis comes from samples of the soil solution collected through porous cup samplers. In this sub-section the construction and installation of these samplers are described. The sub-section concludes with a description of the method by which the samples were collected.

Construction

Porous cup soil solution samplers comprise a ceramic cup attached to a PVC barrel which has some form of attachment to allow the imposition and maintenance of a vacuum. The porous cups were obtained from SoilMoisture Equipment Corporation and had an air entry value of approximately -100 kPa. The barrel of the sampler was of 15 mm class E PVC pipe and the suction cup was connected to the pipe with a PVC adapter. The PVC-PVC joints were bonded with PVC cement and the PVC-Ceramic joints with 24-hour Araldite. When not in use the open end of the PVC barrel was covered with a 15 mm irrigation pipe end cap. A 5 mm length of the PVC pipe was forced into the cap to prevent the tapered cap becoming jammed onto the barrel.

To allow application and maintenance of a vacuum the sampler was fitted with a rubber bung joined to a 300 mm length of anaesthetic-machine rubber tubing. The vacuum was sealed by bending the tubing back on itself and clamping it off.

Installation

Prior to installation the samplers were leached with at least 100 ml of distilled water. Two augers were required for installation. First a pilot hole was drilled to the required depth with a 19 mm auger, which was then enlarged to the required diameter with a 22 mm auger. A slurry, made of soil from the sandy loam layer and distilled water, was then poured down the hole and the pre-wetted sampler inserted.

At each site four samplers were installed. These were at 250 mm depth in the sandy loam, at 550 mm and 760 mm in the fine sand, and at about 1000 mm in the

coarse sand. Not all the samplers were installed to the same depth in the coarse sand, because at many sites the presence of a large stone prevented insertion to the intended depth of 1050 mm. The actual depths of the '1000 mm' samplers have been given in Table 2.3.

Sample collection

A vacuum of approximately -80 kPa was applied to each sampler with a SoilMoisture Equipment Corporation hand test vacuum pump. The sampler was then sealed and the sample of soil solution allowed to collect for approximately 1 hour. The sample was retrieved from the sampler using a 60 ml syringe and a length of flexible PVC tubing. If insufficient sample had collected then the vacuum was re-applied and sample accumulation was allowed to proceed for a further hour. Thirty ml of the collected solution was stored in a vial and the remainder discarded. Samples collected during the 1988 and 1990 experiments were stored at 3 °C, while those from the 1989 experiment were stored frozen.

2.2.4 Time domain reflectometry

A time domain reflectometer (TDR) was used to measure the water content of the top 200 mm of soil, so as to complement the neutron probe measurements of soil water content below this depth. This device also was used to assess the storage of water at each site to the depth of the fine sand to coarse sand interface. The TDR used was a SoilMoisture Equipment Corporation IRAMS Trase System I soil moisture analyzer.

Stainless steel wave guides were installed at each site in the positions shown in Figure 2.1. The length of the wave guides used to determine the water storage in the soil above the coarse sand was taken from the known depth of the fine sand to coarse sand interface rounded to the nearest 50 mm. Average water content to 200 mm was taken every time the neutron probe was used. Measurements to the depth of the coarse sand were taken more frequently, as needed to establish the time trend of water storage.

This TDR device required some calibration to represent the water content of the soil satisfactorily. Calibration of this particular instrument was carried out by Rahardjo (1989) and found to be,

$$\hat{\theta} = 1.18\ \theta_{TDR} - 0.014 \quad , \tag{2.2}$$

where θ_{TDR} is the volumetric water content as displayed by the TDR.

2.2.5 Meterological measurements

Rainfall was measured in the paddock using a 100 mm diameter plastic rain gauge. During the 1988 experiment the gauge was located some 50 m from the plot at 0.75 m height. During the 1989 and 1990 experiments the gauge was within the area of the plot at 300 mm height. Samples were collected from time to time for measurement of the chloride concentration. Sunshine hours and air temperature, used in the estimation of evapotranspiration, were taken from the DSIR meterological site, approximately 1 km from the plot.

In order to schedule the daily irrigation during the 1988 leaching experiment it was necessary to estimate quickly evapotranspiration. This was not possible with the DSIR meterological data, so an Algin Scientific Evapotranspiration Meter was used. This meter logs air temperature and solar radiation at half hourly intervals, accumulates these measurements throughout the day, and then calculates the potential evapotranspiration using the formula of Priestley and Taylor (1972). Although the Evapotranspiration Meter provided quick estimates of E, they were not accurate enough for use within the water balance and were used as a guide only to determine the amount of irrigation water to be applied. The more accurate estimate of E from the DSIR meterological measurements was used within the water balance calculation.

Evapotranspiration calculation

Potential evapotranspiration was estimated by the Priestley and Taylor (1972) equation as,

$$\lambda E = 1.26 \frac{s}{s + \gamma} \frac{R_n}{\rho_w} , \qquad (2.3)$$

where λ is the latent heat of vaporisation of water [L^2 T^{-2}], E is the rate of evapotranspiration [L^3 L^{-2} T^{-1}], R_n is the amount of net radiation received per unit area of surface in unit time [M T^{-3}], s is the slope of the saturation vapour curve at the mean temperature [M L^{-1} T^{-2}], γ is the psychometric constant [M L^{-1} T^{-2}], and ρ_w is the density of water.

Net radiation was estimated from sunshine hours, date, and latitude, as described below.

- First the angle of declination was found from the number of days between the current day and the nearest equinox using equation 1.12 in Rosenberg (1974, p15).
- The half-day length, in degrees, may then be calculated from equation 3.3 in Sellers (1965, p15).
- From this, the half-day length was used to calculate the maximum possible duration of sunshine, and from this the maximum number of hours measurable by a sunshine hour recorder can be calculated (de Lisle, 1966).
- Hence, the amount of solar radiation arriving at the earth's atmosphere per day may be found from equation 3.7 in Sellers (1965, p16) and from Table 2.2 in Robinson (1966, p16) to determine ratio of the instantaneous to the mean distance from the earth the sun.
- Finally, the solar radiation at the earth's surface was found from de Lisle (1966, equation 4) and, from that, net radiation according to Scotter *et al.* (1979).

The Priestley and Taylor (1972) estimate of evapotranspiration has previously been demonstrated to work for well-watered pasture in the Palmerston North weather

(Scotter *et al.*, 1979; Green, 1983; Green *et al.*, 1984). The use of a more complex equation, for example the Penman equation, was not really justified (Green *et al.*, 1984).

2.2.6 Irrigation system

The irrigation system consisted of four 100 mm diameter aluminium pipe lines running the length of the plot (see Figure 2.1) connected to a header pipe. The header pipe was, in turn, connected to a hydrant. The hydrant was supplied with water from the Turitea Stream via a diesel motor-driven water pump.

Although there were 24 outlets for sprinklers on the irrigation pipes, the pump had the capacity to operate only 12 sprinklers at any one time. At the beginning of an irrigation session sprinklers were placed in alternate outlets and moved along one outlet half way through the session. The sprinklers were again moved at the beginning of the next irrigation session. As each irrigation sprinkler exhibited a different application pattern and rate, this movement of the sprinklers lead to a more uniform total application of water to the plot.

Input of water to the sites from the irrigation system was considered to be variable enough to make necessary the measurement of this input at each site. This was accomplished with the use of plastic catch cans, of diameter 62 mm, at a height of 0.75 m. These catch cans were situated at each site and also close to the lysimeter. The application rate for the irrigation system averaged over the plot area was 5 mm hr^{-1}. Samples were taken for chemical analysis.

2.3 1988 LEACHING EXPERIMENT

It was argued, in Chapter One, that field experimentation should form a vital part of the current research effort in solute transport. Without this experimentation, and associated modelling, effective progress will not result. The 1988 experiment was to provide a data set which would reveal the nature of solute transport in the

layered soil. Leaching of a pulse input of solute under steady water flow was readily amenable to analysis, and this type of experiment was also considered relatively easy to manage in the field.

Chloride was used as the solute because it was present in only low concentrations naturally in the soil, it is neither produced nor consumed in the soil, except by plant uptake with transpired water. Further, it is readily available in a cheap form as solid KCl fertiliser, which is easily spread. Finally, chloride is relatively easy to measure.

In deciding upon the irrigation application rate several factors were considered. These included the ability of the soil to conduct water, the expected duration of the experiment, and the potential for plant uptake of chloride-laden water.

With a saturated hydraulic conductivity of 110 mm day^{-1} (Clothier, 1977), the sandy loam is the least conductive of the three soil layers. Given this high conductivity, the choice of the application rate could then safely be determined by other factors. A drainage rate of 10 mm day^{-1} and an assumption of piston displacement of solute lead to the expectation of the solute peak reaching the 250 mm sampler after 7 days and the 1000 mm sampler after 30 days of irrigation. Allowing for significant solute spreading it was considered that it may be necessary to continue the experiment so there was up to three times the amount of drainage estimated to move the solute to the 1000 mm sampler, that is for 90 days. This length of time was considered practicably manageable, yet giving a slow enough passage of the solute to allow initially daily sampling to provide sufficient data to characterise solute movement at the 250 mm depth. Additionally, it was reasonable to expect that the bulk of the solute would have passed beyond the reach of the plant roots within 15 days. Given an average E of 3 mm day^{-1}, this would amount to a loss of 45 mm of transpired water. If the average solute concentration was, for example 200 g m^{-3}, then the plants, through passive uptake of chloride, would remove only 9 g m^{-2} of chloride from the soil. A further consideration was the length of time necessary to operate the irrigation system. With a maximum expected E of 5 mm day^{-1}, a daily irrigation duration of 3 hours would be required to produce 10 mm of drainage. This was

considered to be the greatest duration of irrigation practicable in relation to the length of time needed to collect and process soil solution samples.

During the course of the experiment the plot was grazed as part of the rotation of the farm. Various efforts were made to protect the instruments from the cows during grazing, but some damage necessitating sampler replacement occurred at each grazing.

The aim in this experiment was first to establish an approximately steady water flow of 10 mm day^{-1} through the soil, and determine the pre-existing concentration of chloride in the soil solution. Following a heavy application of solid KCl on the plot numerous sets of soil solution samples would be taken plus a few sets of soil core samples removed, still under a regime of 10 mm day^{-1} drainage. The removal of soil cores, though considered to be useful for the interpretation of solute movement through the soil, was thought to create too great a potential for altering water and solute movement to permit many samples to be collected. Drainage from the lysimeter was also collected. Approximately steady drainage was maintained by accounting for rainfall with less irrigation water the day following the rainfall. As the fastest changes in chloride concentration were expected to occur in the initial stages of leaching, soil solution samples were at first collected daily, and then less frequently.

As indicated above, steady drainage of 10 mm day^{-1} was first established, and soil solution samples were collected to measure the initial chloride concentration in the soil solution. Then, on 26 April 1988, a Sisas precision fertiliser spreader was used to apply KCl. The aim was to apply 200 g KCl m^{-2} in two perpendicular passes of the plot in an effort to enhance the uniformity of application. The application rate and uniformity were measured by placing 11 catch cans beneath the path of the spreader. Before fertiliser was spread, at each of the 20 measurement sites, an area, 0.75 × 0.75 m, masking the porous cup samplers was covered by plastic sheeting. This allowed the area immediately above the samplers, and also the lysimeter, to have fertiliser applied more accurately by hand.

Unfortunately the spreader broke down approximately halfway through the first pass, and was not operational again until 28 April 1988, more than 48 hours later. During the 72 hours since the last irrigation, there was no rainfall, some dewfall, and no irrigation. However during that time the smaller granules of fertiliser were observed to dissolve and the surface of the soil dried under the approximately 12 mm of evapotranspiration. The final application rate was 193 g KCl m^{-2} (92 g Cl^- m^{-2}) with a standard error (se) of 16 g KCl m^{-2} (8 g Cl^- m^{-2}). Also on the 28 April 1988, the plastic-covered area surrounding each site, and the 2 m^2 of the lysimeter were spread with KCl at a rate of 200 g m^{-2} (95 g Cl^- m^{-2}).

Immediately following the final application of fertiliser, irrigation was restarted. No attempt was made to catch up the previous 2 days irrigation allocation of more than 30 mm that was missed.

A set of soil solution samples were collected following the 28/4/88 irrigation (day 1). Soil solution samples were then collected daily for the next 8 days. Following day 9, samples were collected approximately every second day for 12 days.

On day 16, soon after the paddock had been grazed for the first time, it became evident that the soil structure at the surface had deteriorated and that, during irrigation, some surface ponding was occurring. The most probable initial cause of this was decreased earthworm activity. In the first few days after the KCl application, the concentration of salt in the top of the soil was quite high; the osmotic potential may have been as low as -5 bar. While this was considered unimportant as far as plant growth is concerned, it was likely to be harmful to the earthworms present in the soil. Reduced casting activity and some dead earthworms were observed on the soil surface. However the effects of this were not evident until after the plot was grazed when the combination of the wet soil and heavy stock at a relatively high density, caused sealing of surface-vented macropores as well as alteration of the properties of the soil surface. Under 'normal' conditions the active earthworm population would soon have created new openings and restored the surface conductivity. Mid-way through the experiment there was renewed surface casting activity, but at a lower rate than observed in the neighbouring unfertilized soil.

After the decreased conductivity of the surface soil became evident, the frequency of irrigation was decreased and then ceased altogether as the ponding would have led to substantial areas of saturated flow. This was considered undesirable as it was likely to enhance considerably the variability of water, and solute, movement through the plot. Cumulative drainage, I [L^3 L^{-2}] at this time averaged 181 mm. Assuming piston displacement, this would place the solute peak at over 500 mm deep at this time. Therefore solute flow was unlikely to have been unduly affected by the surface conductivity changes.

After day 22, rainfall was the only water input to the plot. The movement of solutes slowed considerably and samples were taken less frequently. The days on which soil solution samples were taken, and the average drainage of water through the sites at these samplings, are given in Table 2.4.

Table 2.5 1988 soil coring dates. N is the number of samples at each depth.

Date	Day	I (mm)	N	Depths (mm)
28 April	1	6	10	0-100, 100-200, 200-300
12 June	46	390	20	0-250, 250-450, 450-650, 650-850, 850-1050
25 October	181	790	20	

Soil cores were taken from the plot as shown in Table 2.5. The water content of the soil was measured infrequently during the time when the irrigation was being applied. The need was to establish only that the drainage rate was steady. Once irrigation was stopped, the TDR was used to assess the water storage to the depth of the coarse sand. If necessary, this would allow for the effect of changes in water storage on solute transport to be taken into account.

At first, the lysimeter was drained every day. Once irrigation was stopped it was drained only after significant rainfall.

Table 2.4 1988 soil solution sampling dates, and average cumulative drainage on that day.

Date	Day	I (mm)
28 April	1	6
29 April	2	13
30 April	3	22
1 May	4	35
2 May	5	42
3 May	6	52
4 May	7	70
5 May	8	85
6 May	9	95
9 May	12	146
11 May	14	161
13 May	16	181
16 May	19	197
19 May	22	206
24 May	27	269
29 May	32	316
3 June	37	337
10 June	44	390
6 July	70	510
26 July	90	580
23 August	118	645
20 September	146	734

2.4 1989 LEACHING EXPERIMENT

For the reasons discussed in Chapter One, the 1989 experiment was to be carried out under natural rainfall. Because drainage through the plot in 1989 was to be derived from rainfall only, solute was expected to be present at high concentration within the root zone for some length of time. It was thought this would have two effects of immediate concern. Firstly it would be necessary to reduce the KCl application rate so that plant growth and earthworm activity were not unduly affected. Secondly, as the chloride would be within the reach of the plant roots for some time, that taken up by the plants might be significant and would need to be assessed.

The plot had been retained in the farm grazing rotation for the duration of the 1988 experiment. However the damage caused to the instruments made it desirable that the cows be excluded from the plot during the 1989 experiment. Instead the plot was mowed and the clippings removed.

Before any solute was applied to the plot in 1989 it was necessary to collect both soil cores and soil solution samples so that the initial chloride level in the soil could be assessed. The first full set of soil solution samples was collected on 23 July 1989 and a set of soil cores were collected the following day. On 25 July 1989 KCl was applied. For the 1989 experiment the application rate was reduced to 50 g KCl m^{-2} (24 g Cl^- m^{-2}). This application rate made hand-application possible.

The plot was marked into 10 × 10 m squares and the appropriate amount of fertiliser for each square was weighed into two bags. If a square contained a measurement site, the 1.2 × 1.2 m square around this site was separated from the larger square and the fertiliser applied separately. The amount of fertiliser for the larger square was appropriately adjusted. The fertiliser was applied by hand in two passes.

Chloride uptake by the pasture, and so removed from the plot by mowing, was assessed by measuring the amount of, and the chloride content in, the herbage. The amount of herbage was assessed by cutting 0.1 m^2 quadrats of pasture to ground

level with clippers. Quadrats were taken both before and after mowing and the herbage then dried at 60 °C for 48 hours. The method for determining the chloride content of the herbage is detailed in Section 2.6.

Table 2.6 1989 soil solution sampling dates.

Date	Day	I (mm)
26 June	5	9
7 July	16	30
13 July	22	44
15 July	24	48
19 July	28	64
3 September	74	83
10 September	81	89
15 September	86	91
17 October	118	103

Time domain reflectometry measurements of water storage to the depth of the coarse sand layer were taken each time soil solution samples were collected. Water content measurements using the neutron probe were taken less frequently as the depth distribution of water in this soil has been described already by Clothier (1977). The lysimeter was drained, and soil solution samples collected, after each major rainfall event. Soil cores were taken infrequently. Details of the timing of the soil solution sampling and soil coring are given in Tables 2.6 and 2.7 respectively.

During the 1988 experiment the excess of rainfall over evapotranspiration was approximately 500 mm. Given this it was reasonable to expect considerable movement of the applied solute past the soil solution samplers in 1989. Although leaching may not have reached the depth of the 1000 mm samplers, it should have been more than sufficient to characterise solute movement through the paddock. Unfortunately however, rainfall was far less than the normal, and over the 120 days

Table 2.7 1989 soil coring dates. N is the numbers of samples at each depth.

Date	Day	I (mm)	N	Sampling Depths (mm)
24 July	33	66	20	0-100, 100-200, ···, 900-1000
4 August	44	68	20	0-100, 100-200, 200-300
9 August	49	70	20	0-100, 100-200
30 August	80	72	20	0-100, 100-200
25 September	96	91	20	0-100, 100-200, ···, 900-1000
17 October	118	72	20	0-100, 100-200, 200-300

of the experiment rainfall exceeded evapotranspiration by less than 100 mm. Later in the trial, when it became obvious that there was not likely to be sufficient rainfall, it was decided to re-install the irrigation system to supplement rainfall and thereby move the solute at least to the depth of the 760 mm sampler. Unfortunately the irrigation pump was subject to continual breakdown, and with the onset of spring and higher E, the experiment was terminated.

2.5 1990 LEACHING EXPERIMENT

Although the abortive 1989 experiment was to have been the final experiment, it was considered desirable to have a completely independent set of data to compare with the 1988 experiment. So a further smaller experiment was carried out in 1990.

It was not possible to repeat the basic design of the 1988 and 1989 experiments and sample the whole field. Instead the lysimeter was instrumented with three soil solution samplers, at 250, 550, and 760 mm depth, and also with TDR probes. Natural rainfall was not to be relied upon, so the lysimeter was irrigated when

necessary. As the surface area of the lysimeter was only 2 m^2 it was feasible to irrigate it by hand, thus allowing greater control of the local application rate than might be possible with a conventional irrigation system.

The basic experimental design was little different from the previous two experiments. The lysimeter was pre-irrigated and samples obtained from the porous cup samplers and also from the drainage from the lysimeter in order to establish antecedent solute concentrations. On 23 July 1990 (day 1) 30 g $Br^- m^{-2}$ in the form of solid reagent grade KBr was applied to the surface of the lysimeter. Bromide was used in preference to chloride as it was not initially present in the soil.

At first irrigation was applied using a 4 litre hand operated pressure sprayer. Approximately 20 min were required to apply the 2 mm of water held in the sprayer's reservoir to the lysimeter. During application no ponding was observed. At day 38, after 162 mm of drainage from the lysimeter, the method of water application was changed to a watering can. The pressure sprayer, while being excellent as far as the prevention of ponding was concerned, was slow. The watering can held 5 litres of water and it took approximately four minutes to apply this amount. Once the watering can was emptied, the soil was allowed to rest for 6 minutes before the next 5 litres were applied. The result was an instantaneous application rate of about 38 mm hr^{-1}, but overall the rate was just 15 mm hr^{-1}. Some short-term ponding was observed, but this water always disappeared well before the next 5 litre application was applied. The solute peak was at a depth of approximately 550 mm before the application method was changed. It is unlikely that changing the water application method at the surface at this time had any effect on solute movement.

2.6 CHEMICAL ANALYSES

Concentrations of chloride and bromide were, at various times, measured from soil solution samples, soil core extracts, and herbage extracts. The sample preparation and analytical methods are described below.

2.6.1 Soil solution samples

In general, the soil solution samples needed no processing prior to chemical analysis. However, occasionally from the 250 mm samplers, a cloudy sample was obtained. The cloudiness was assumed to be due to suspended mineral or organic matter. These samples were filtered through a Whatman #40 filter paper. Usually this filtering had little effect on the visual quality of the sample. The effect of filtering was tested on a clear sample and found not to affect the chemical composition of the sample, but was considered desirable in case the suspended matter caused blockage of the extremely narrow bore tubes in some of the analytical equipment.

Soil solution samples were, at various times, analyzed for chloride and bromide. Details of the analysis of the samples are given below.

Chloride

The majority of the soil solution samples were analyzed for chloride using the Tecator FIA Star Analyzer. The method used was as detailed in the Tecator Application Note number AN 63/83 based on the method of Florence and Farrar (1971). Essentially, the chloride ion, when reacted with mercuric thiocyanate in the presence of ferric ions, produced the red-coloured complex, ferric thiocyanate. The concentration of this complex was determined photometrically. The calibration determined by the analyzer was found to be unreliable so the millivolt reading from prepared standards was used to determine the calibration by regression against the known concentration in the standards.

From 1989, a Corning Chloride Analyzer model 925 Chloride Titrator was available. This instrument titrated the chloride ions in the sample against silver ions, determining the endpoint potentiometrically. The few samples which did not conveniently fit into the concentration ranges of the flow injection analyzer were analyzed on the titrator. Sufficient samples were analyzed on both the FIA and the Titrator so as to obtain cross-validation.

Bromide

Bromide concentration was determined using an Orion Research Bromide Specific Ion Electrode (model 94-35A). Standards were prepared to determine the relationship between the millivolt reading and bromide concentration. It was necessary to sort the samples to be measured in anticipated ascending order of concentration, and measure standards frequently to minimise instrument drift and hysteresis. All determinations were carried out with a background concentration of 0.15 M $NaNO_3$ as an ionic strength adjuster.

2.6.2 Soil cores

Chloride was extracted from soil samples with 0.05 M K_2SO_4. Although water adequately extracted the chloride in the soil, it was easier to filter the supernatant when K_2SO_4 was used.

The extraction method was as follows.

- Field moist soil was placed in a 50 ml polypropylene screw-capped centrifuge tube along with extractant to produce a known soil:solution ratio of approximately 1:3. Blanks, comprising extractant only, were also prepared and processed identically to the samples.
- Soil and extractant were shaken on an end-over-end shaker for 30 min and the mixture centrifuged for 2 min at 8000 rpm.
- Following this, the supernatant was filtered through a Whatman #40 filter paper into a vial and stored at 3 °C.

Moisture content was determined on a sub-sample of the soil at the same time as the extraction, thus allowing solute concentration in the soil solution to be calculated.

Chloride

The chloride concentration in the extractant was analyzed on the flow injection analyzer as for the soil solution samples but with 0.05 M K_2SO_4 as the carrier. Standards were also prepared in 0.05 M K_2SO_4.

2.6.3 Herbage

Collected herbage was dried in a forced-air oven at 60 °C and then ground in a hammer mill with a 1.5 mm sieve size. Bromide or chloride was extracted from the herbage by a method similar to that of White and Ayoub (1983) and Heng (1991). One gramme of the ground, dried herbage was placed in a conical flask with 60 ml of distilled water and heated to 90 °C for 4 hours. Blanks of distilled water were also prepared. Once cooled the digested herbage was filtered through a Whatman #41 filter paper into a volumetric flask and the solution made up to 100 ml with distilled water. The filtered solution was analyzed for chloride concentration with the chloride titrator, or bromide using the specific ion electrode.

Chapter Three

RESULTS AND DISCUSSION

A wealth of data was obtained from the experiments described in Chapter Two and now these data will be presented and some of the general implications discussed. Here the first three sections present the data collected in the three years of experimental work. The succeeding four sections discuss the relationships between samples collected by porous cups and soil cores, the calculation of the field solute flux, spatial variability of solute transport, and finally compare the breakthrough curves (BTC's) of solute obtained from the lysimeter during both 1988 and 1990.

3.1 1988 DATA

As explained in Chapter Two, the rationale behind the first field experiment was to provide data concerning solute concentration versus cumulative drainage with which to characterise the solute transport properties of the soil. In order to remove effects due to unsteady water flow, an irrigation system was used to supplement rainfall, initially on a daily basis, to obtain approximately steady water flow.

Firstly the irrigation regime, and the water balance for the field as a whole, are examined in some detail. The primary method for assessment of the soil solution solute concentration was through the collection of soil solution samples via suction cups. These data, along with the data from the lysimeter are presented in Section 3.1.2, followed by results from the collection of soil cores. The final sub-section examines the mass balance of chloride during the 1988 experiment.

3.1.1 Water Balance

Under the irrigated regime of the 1988 leaching experiment, the significant inputs of water to the soil were rainfall and irrigation water. Outputs of water were drainage and evapotranspiration. Thus the water balance of the soil may be expressed mathematically as,

$$\theta(t) = \theta(0) + \frac{R(t) + P(t) - E(t) - I(t)}{z} , \qquad (3.1)$$

where t stands for the time at which the water balance is to be assessed, $\theta(t) - \theta(0)$ is the change in depth-averaged water content over the interval 0 to t, $R(t)$ is the total amount of irrigation water that was applied [L], $P(t)$ is the amount of rainfall [L], $E(t)$ [L] and $I(t)$ [L] are the amounts of water lost through evapotranspiration and drainage respectively. Finally, z is the depth of soil under consideration [L].

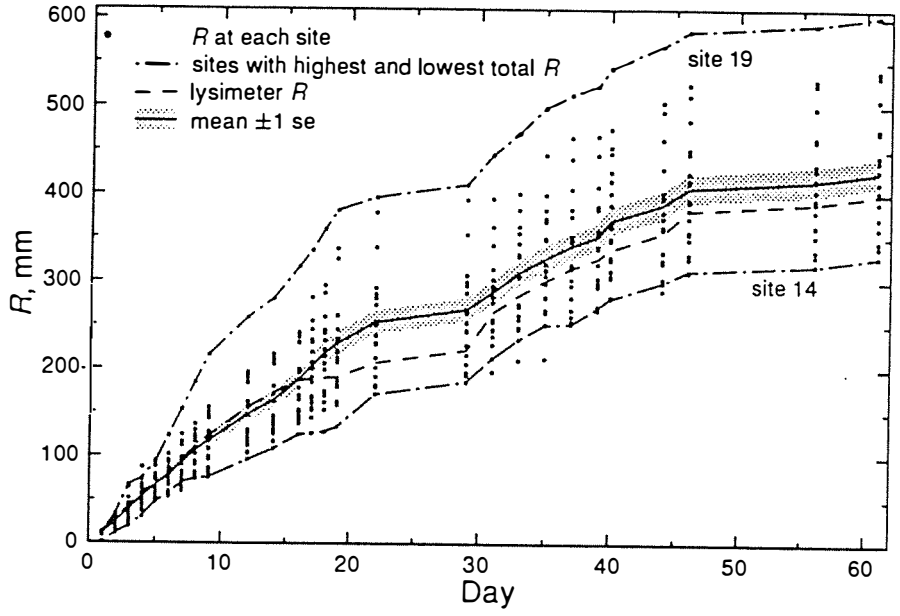

Figure 3.1 Cumulative irrigation input to each site and the lysimeter. Day 0 was 27 April 1988.

Below, individual components of the water balance will be quantified for the 1988 experimental period. Finally the overall water balance will be discussed.

The cumulative irrigation input, R, at each site is shown in Figure 3.1. For any particular irrigation event, the spatial distribution of R is better described lognormally, than by a normal curve. The lognormal mean and standard error (se), shown on Figure 3.1, were calculated by the method of Sichel (1952). When each

site was ranked with regard to its cumulative irrigation input, the rankings remained reasonably constant with time. For example the sites receiving the highest total (site 19) and the lowest total (site 14) amount of irrigation water are identified in Figure 3.1. Such temporal invariance reflects the non-changing pattern of irrigation, so indicating that in this instance using the field average irrigation input for each site would lead to a significant error in the drainage estimate.

The difference between the highest and lowest sites was 274 mm. This was approximately 30% of the total water input at the end of the period. The uniformity coefficient (Christiansen, 1942) varied between 70% and 80% for individual irrigation events.

Although the percentage variation in the amount of irrigation water received was substantial, the rate at which that water was applied was likely to have been even more variable. This may have resulted in spatial variation of the timing of incipient ponding and total amount of free surface water ponding. This will be examined further in more detail in Section 3.7.

The temporal pattern of rainfall over the experimental period is shown in Figure 3.2. When considered on a medium-term basis, say over 10 days, the amount of rain falling was reasonably constant. Exceptions to this were the periods between days 21 to 23 and on day 88, when 54 mm and 76 mm of rain fell respectively.

The daily evapotranspiration was calculated from sunshine hours and air temperature as described in Section 2.2.5. The pattern of E over the period can be seen in Figure 3.2. Between the end of April and July, from approximately the beginning of the experiment and day 100, the daily amount of evapotranspiration can be seen to be reasonably constant. After this time, the rate of evapotranspiration increased as spring approached.

Cumulative measured drainage from the lysimeter, seen in Figure 3.2, remained relatively constant at the desired 10 mm day^{-1} for approximately the first 20 days. After this the drainage rate declined to about 3 mm day^{-1} as the irrigation input was decreased.

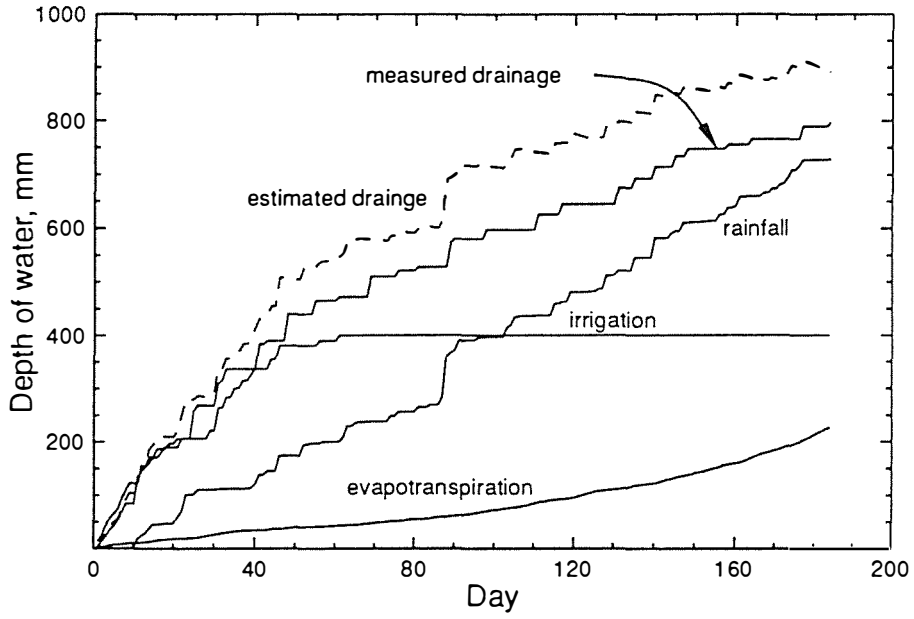

Figure 3.2 Water balance for the 1988 experiment showing evapotranspiration, irrigation, and rainfall, as well as measured and estimated drainage.

In calculating the water balance for the lysimeter, it was assumed that there was no change in water content of the soil. This expectation was justified by measurements of the amount of water stored above the coarse sand layer, which remained relatively constant even after irrigation ceased. This is a reflection of both the soil layering (Clothier *et al.*, 1977b) and the low E. Thus, equation 3.1 can be simplified so that drainage can be estimated as the sum of irrigation and rainfall minus evapotranspiration. The results of this calculation are shown as the dashed line in Figure 3.2.

The estimated amount of drainage was almost always higher than the measured drainage. By the end of the experiment the difference between the two drainage amounts rose to 95 mm, or 12 % of the measured drainage. This discrepancy may be caused by either an over-estimation of irrigation input, over-estimation of rainfall, or an under-estimation of evapotranspiration. Both rainfall and irrigation were indeed highly variable. However the rain gauge and the catch cans used for

measuring the input of irrigation water were more likely to under catch than the reverse.

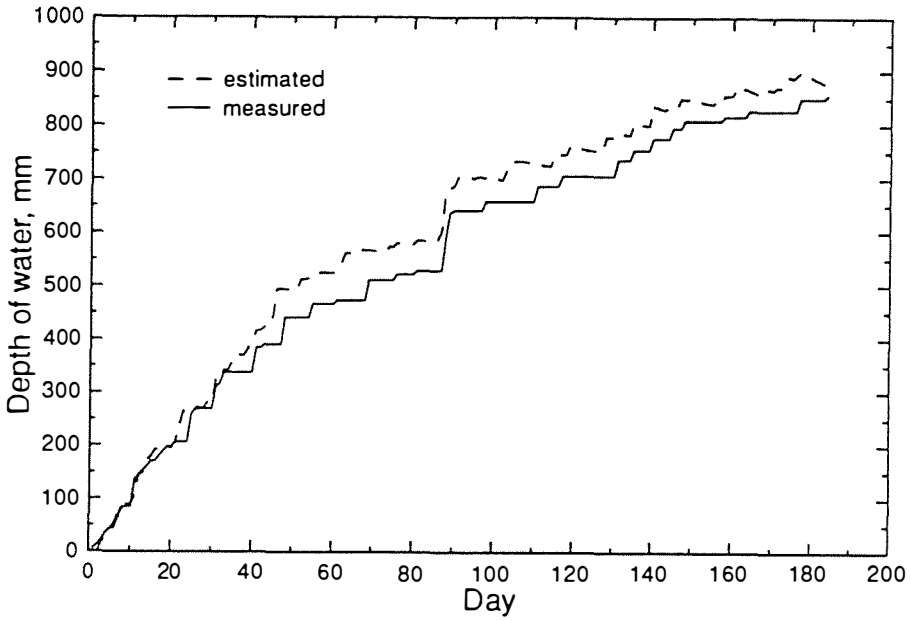

Figure 3.3 Measured and estimated drainage from the lysimeter in 1988 with enforced equality on day 85.

Although there appears to be a steadily widening gap between the measured and estimated drainage, there is a single large discrepancy on day 85 when there was a very large rainfall event. The reason for the difference on day 85 is likely to have been the inability of the lysimeter to accept all the incoming rainfall. It is likely that the combination of the large amount of rainfall at high intensity, resulted in runoff from the lysimeter. In Figure 3.3 the estimated drainage was recalculated simply with the estimated drainage amount on day 85 being that measured. The agreement was much better. Once this effect of day 85 is removed, the discrepancy between the measured and estimated drainage amounted to less than 5% of the total, and so is not significant.

As previewed in Chapter One, cumulative drainage was intended to be used as the independent variable, rather than time. For the lysimeter, measured drainage could

be the variable used. It has been shown that it is possible to estimate this drainage on the basis of the soil water balance. Now for the measurement sites, because the paddock was flat, there would have been no runoff. So in these cases, estimated drainage, using the appropriate irrigation input, can be used as the independent variable.

3.1.2 Porous Cup Samples and Lysimeter Outflow

Twenty measurement sites, with four depths sampled at each site, provided a formidable amount of data. These need to be presented in a form which allows the detail at individual sites and depths to be discerned but also allows the overall pattern across the field and the variability to be evident. To this end, only data from example *characteristic* sites will be individually presented in graphical form. This will allow depth-wise trends and mass balances to be discussed. Following this the data from each depth will be bulked and shown. Finally the lysimeter outflow data are presented.

Characteristic Sites

Four sites were chosen as example sites. Sites 12 and 14 were chosen for their 'ideal' behaviour. In this respect ideal behaviour means essentially that the solute peaks occur in the correct order with respect to the depths of the samplers. The variability of the data was such that any more rigorous criterion would essentially reject all sites. Other considerations, such as approximately equivalent amounts of solute mass recovered, or uni-modal peaks could not be included. Results from these two sites, along with the bizarre data from sites 16 and 19, are shown in Figure 3.4. It is interesting to note in passing that the well-behaved site 14 had the lowest irrigation input, while the unusual site 19 had the highest input. Given the high hydraulic conductivity of the soil, the magnitude of the average water input is unlikely to be the reason. High instantaneous input rates and the possible confounding effects of ponding and preferential flow could have been contributing factors.

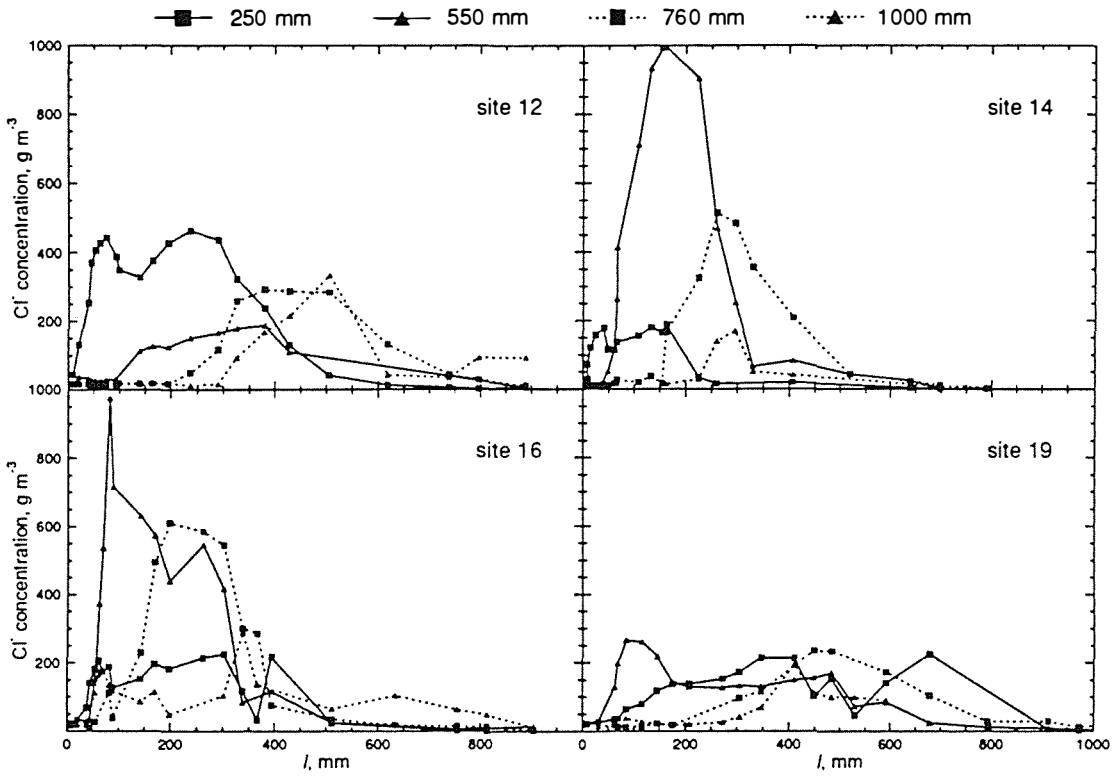

Figure 3.4 Porous cup concentrations measured at sites 12, 14, 16, and 19, in 1988.

Data collected at 250 mm depth at the otherwise ideal site 12 not only show a distinct bi-modal character not seen at any other depth, but also the spread in the data is greater at the shallower depth than deeper in the soil. At site 14, data from the 550 mm depth indicate that a large amount of solute has passed through, namely 194 g m^{-2}. Whereas the masses recovered for the 250 mm, 760 mm and 1000 mm depths were just 37, 107, and 27 g m^{-2} respectively. This could arise either from spatial variability in the application of the solute to the surface of the soil or from variable patterns of flow of water, and hence solute, in the soil. It is probable that both contributed.

With sites 12 and 14 the timing of initial rise in solute concentration, and usually the passage of the peak in solute concentration, corresponded to the order of sampler depth. This behaviour was not however universal, as evidenced here with the examples of sites 16 and 19. For example the solute appeared to arrive at the

550 mm sampler in site 19 before it reached the 250 mm sampler. There are a number of reasons why this may happen. Firstly, it should be remembered that the samplers at any one site are not directly underneath each other but are offset by distance of approximately 600 mm. This could be significant in terms of the highly variable solute transport processes. Secondly, imperfections in the installation of the samplers could possibly disrupt or enhance solute transport in the immediate vicinity of the sampler. This seemed unlikely as this type of behaviour would result from a gap between the sampler and the soil coinciding with ponded water. Where a gap had formed it was plugged. A more likely reason is that the variability of the irrigation within the 0.6 × 0.6 m was significant. For the above reasons it is not clear if the samplers at any one site should be considered more alike than samplers at adjacent sites. These points will be discussed further in Section 3.6.

Bulked Data

Solute transport was not only depth-wise variable at any one site, but was also extremely spatially variable at the same depth across the paddock. Figure 3.5 shows the bulked data for the four depths of measurement. As the irrigation input at each site was measured independently, the cumulative drainage, I, calculated for each site was different. Data at the shallower depths exhibit the positive skew typical of a pulse input of solute moving into a semi-infinite medium. This skew, which gives the impression of a lognormal distribution of solute transport, is not necessarily indicative of an underlying lognormal distribution of solute transport times. It can just be a consequence of this boundary condition, as noted in 1967 by Gardner. Jury and Roth (1990) pointed out that it is necessary to examine solute transport at a number of depths, or times, in order to discriminate between alternative distributions of solute transport times. At greater depths the spread of solute becomes less skewed, which is also typical of a pulse input.

At any particular depth and interval of I, the data also exhibit positive skew. This property of the data should be accounted for in any curve fitting procedure undertaken with the bulked data, so that the few outlying high-concentration data should not have undue influence on fitted values.

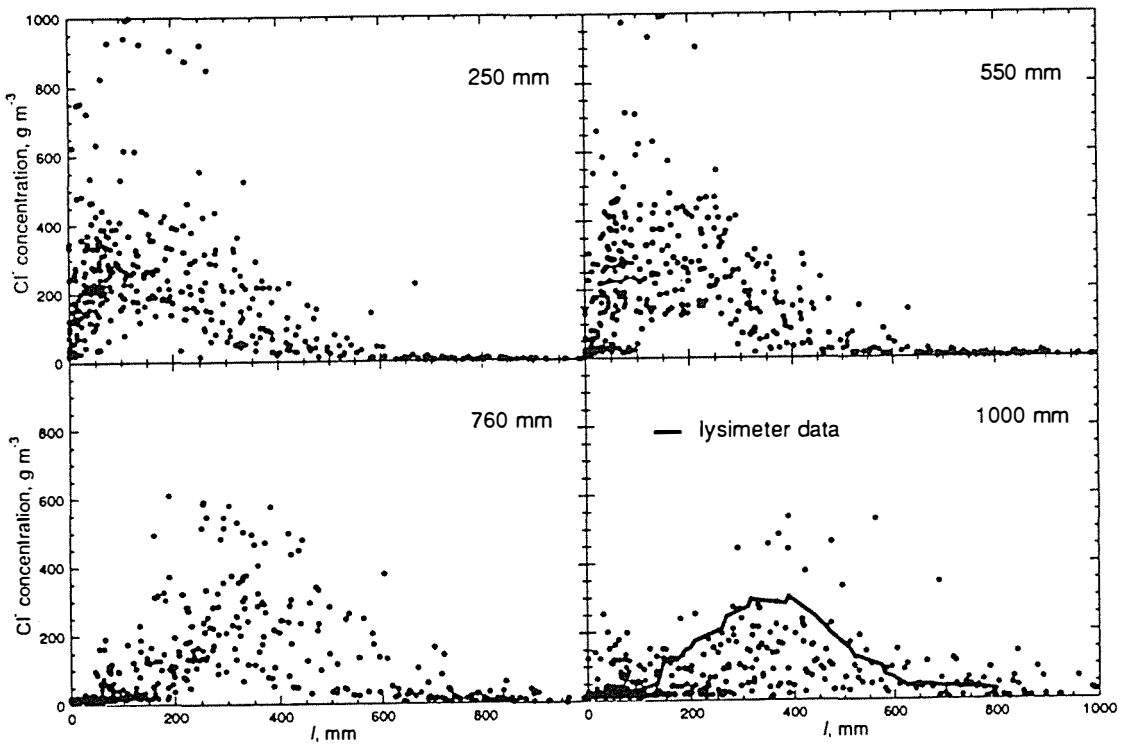

Figure 3.5 Porous cup concentrations for all sites and depths in 1988.

Lysimeter Data

The outflow from the lysimeter was at 1000 mm, and so its solute concentration was comparable, at least in a depth-wise sense, to that from the 1000 mm deep suction cups. There are however differences with respect to the horizontal extent of the sampled volume, the geometry of the streamlines during sample accumulation, and the tension at which the sample was collected. Nevertheless the BTC from the lysimeter does fall within the general scatter of the porous cup data (Figure 3.5). This comparison will be examined in more detail in Section 3.6 and so will not further be dwelt upon here.

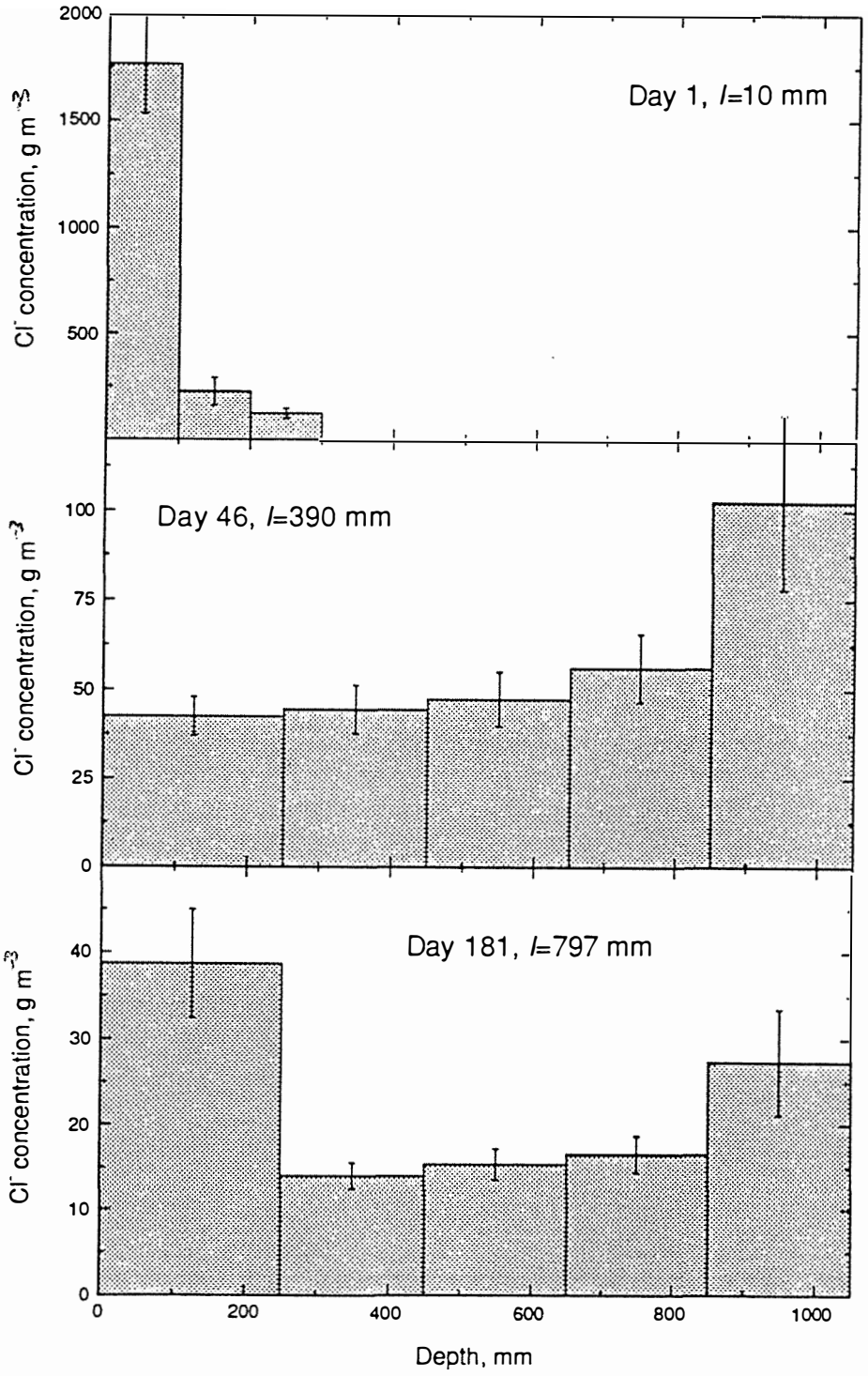

Figure 3.6 Solute concentration and se in the 1988 soil cores. Concentration is expressed per volume of soil solution.

3.1.3 Soil Cores

Soil coring during 1988 was limited to cores taken in the surface soil on the day that the solute was applied, day 46 after 390 mm of drainage, and those taken at the end of the experiment. These data are shown as depth-wise profiles in Figure 3.6. Note the differing scales on the vertical axis. At any particular depth, the spatial variability of the concentration data were better described by a lognormal distribution than a normal distribution and the statistics were calculated as described by Sichel (1952).

Of interest was the remaining high concentration in the uppermost soil cores taken on day 181. This is an indication that part of the solute had remained impervious to leaching, as might be expected (Tillman *et al.*, 1991) due to absorption of some solute-laden water into the soil matrix. Other possible reasons were that it could result from dung or urine, or possibly redeposition from decaying herbage. As an input of dung or urine should lead to an increased variability of concentration, this is unlikely to be the reason.

3.1.4 Chloride Mass Balance

The mass balance for chloride in the soil after a given amount of cumulative drainage, I, down to any given depth, z, may be expressed as,

$$\int_0^z \theta(z)\, c^r(z', I)\, dz' - \int_0^z \theta(z)\, c^r(z', 0)\, dz' - \int_0^I c^f(z, I')\, dI' + Rc_r + Pc_p - H + M = 0 \quad , \tag{3.2}$$

where $c^r(z,I)$ is the depth-wise profile of resident soil solution concentration of chloride at the 'time' of drainage I, and c^f is the flux-averaged concentration. Also c_r and c_p are the concentration of chloride in the irrigation water and rainfall respectively [M L^{-3}], H is the amount of chloride removed by the herbage [M L^{-2}], and M is the amount of chloride in the initial input of fertilizer KCl [M L^{-2}]. The prime refers to the dummy variable of integration.

Equation (3.2) states that the amount of solute stored above depth z, after some drainage I, minus the initial solute and that which has leached below z as well as that removed by the herbage equals the additions in the form of rainwater, irrigation, and fertiliser.

The amount of solute present to a certain depth in the soil was best determined using data from soil cores as these data are already depth-averaged and give the resident concentration, whereas the porous cup samples represent sparse, point-sampled data and are probably closer to the flux concentration. Unfortunately soil cores were not taken at the start of the experiment, however, porous cup samples indicated a low concentration of 19 g m^{-3}, close to the concentration of the irrigation water used to pre-wet the soil. This was uniform with depth. The concentration of chloride in the rainfall was negligible, with the concentration measured on several occasions less than 1 g m^{-3}. The average concentration and standard deviation of chloride in the irrigation water was 24 ± 2 g m^{-3}.

The mass balance results are presented in Table 3.1. At any particular depth the mass balance has been calculated according to equation (3.2), and so under perfect conditions should equal zero. For all depths excluding 1000 mm the balance was well within the one standard error of zero. The significant negative balance for the 1000 mm depth indicates that more solute was added than was recovered, and may result from insufficient measurements taken to characterise the extremely variable transport at this depth.

For the lysimeter no soil cores could be taken but the solute concentration in the outflow at the beginning of the experiment was 24 g m^{-3}, whereas at the end it was 30 g m^{-3}. Thus it was assumed that there was no net change in chloride store in the soil. Irrigation resulted in the addition of 19.2 g of chloride to the 190 g applied as fertiliser to the 2 m^2 lysimeter surface. As 206.8 g of chloride was recovered in the drainage, the balance was just 2.4 g. This excellent balance was probably a result of the closed lysimeter system which allowed better monitoring of additions and losses.

Table 3.1 Chloride mass balance for the 1988 experiment, showing the amount of solute present in the soil at the beginning and end of the experiment as well as the solute in drainage water, irrigation water and in the fertiliser.

Depth (mm)	Cl^- at start (from porous cups) ($g\ m^{-2}$) **a**	Cl^- at end (se) (from soil cores) ($g\ m^{-2}$) **b**	Cl^- in drainage (se) (from porous cups) ($g\ m^{-2}$) **c**	Solute balance (se) ($g\ m^{-2}$) **b-a+c-d-e**
0 - 250	2	2 (0.3)	112 (12)	10 (21)
0 - 550	4	3 (0.4)	111 (8)	8 (17)
0 - 760	5	4 (0.6)	105 (9)	2 (18)
0 - 1000	6	6 (1.0)	77 (10)	-25 (19)
	Cl^- in irrigation (se) (g) 10 (0.4) **d**		Cl^- in fertiliser (se) (g) 92 (8) **e**	

3.2 1989 DATA

Atypical weather, compounded by equipment failure, rendered the 1989 data essentially useless as far as formal solute transport modelling was concerned. However these data were used in a limited manner for other purposes, and are here presented in a format similar to that of the 1988 data.

3.2.1 Water Balance

In contrast to the water balance computed for the 1988 experiment, Figure 3.7 shows the measured drainage to exceed the estimated drainage. It should be noted that because changes in water content of the soil are not taken into account, the estimated drainage at times was seen to decrease with time. Although this was obviously incorrect for the lysimeter, this can happen in the field with upward flow of water. The margin between estimated and measured drainage was not great,

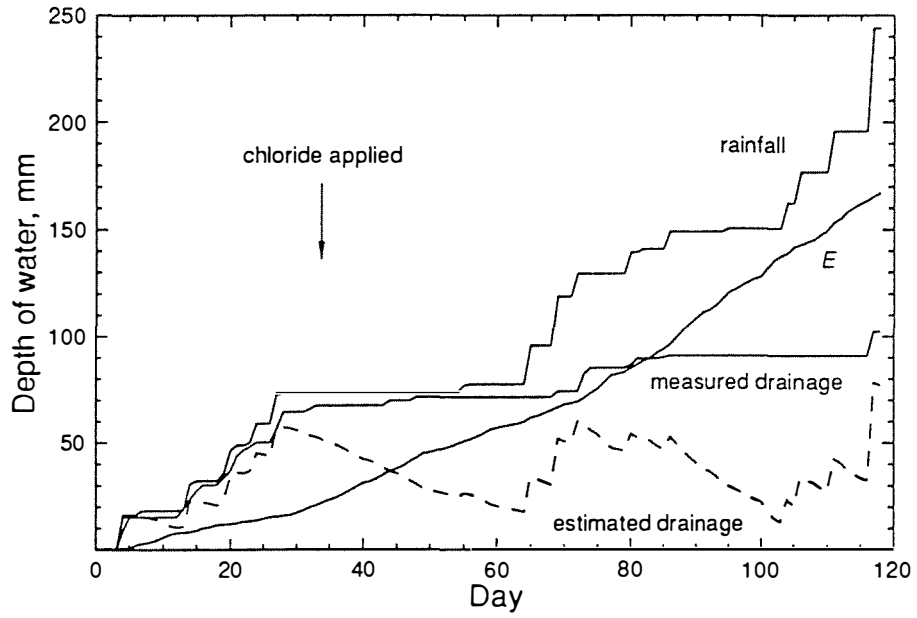

Figure 3.7 Water balance for the 1989 experiment, showing evapotranspiration and rainfall, as well as measured and estimated drainage for the lysimeter. Day 0 was 21 June 1989.

approximately 20 mm, but was both consistent and a reasonable proportion of the total cumulative drainage. Possible reasons were an under-catch of rainfall, or an over-estimation of evapotranspiration. The latter was quite likely as during the period of 30 to 60 days there was little rainfall and the pasture was unlikely to have been using water at the Priestley and Taylor rate. Given the small discrepancy, the estimated drainage is reasonable and in further analysis of the solute concentration data, the measured drainage will be used as the independent variable.

3.2.2 Porous Cup Samples and Lysimeter Outflow

Characteristic Sites

For comparison with the 1988 experiment, the same sites are now shown in Figure 3.8. Note that the chloride fertiliser was applied on day 34, or after 68 mm of drainage. All the 250 mm samplers now show a rise in chloride concentration at the

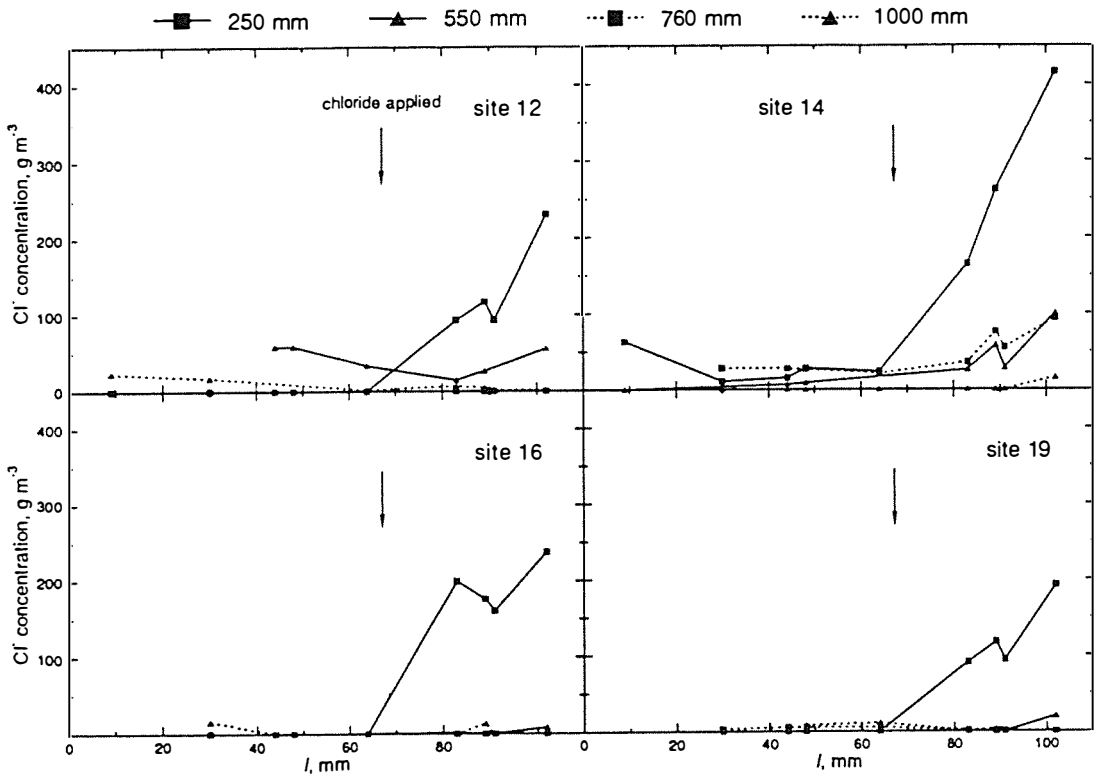

Figure 3.8 Porous cup concentrations for sites 12, 14, 16, and 19 in 1989.

first sampling after the fertiliser application. This was after 83 mm of drainage, or just 15 mm after the fertiliser application. Although there was only 15 mm of drainage between these two samplings, the added rainfall was 55 mm. This is an indication of the difficulty of using the cumulative drainage measured at 1 m as the independent variable for all depths under highly transient flow. Jury *et al.* (1982) noted a similar difficulty. Where the water balance is dominated by drainage this measure is however likely to be reasonably adequate. In order to analyse the data correctly, a more detailed model of water movement would be required to provide a more realistic estimate of the cumulative drainage at each depth.

It would appear that by the end of the experiment solute concentration was starting to rise in tandem at the 550mm and 760 mm samplers at site 14. Unfortunately more data were not obtained due to the combined effects to inclement weather and breakdown of the irrigation pump.

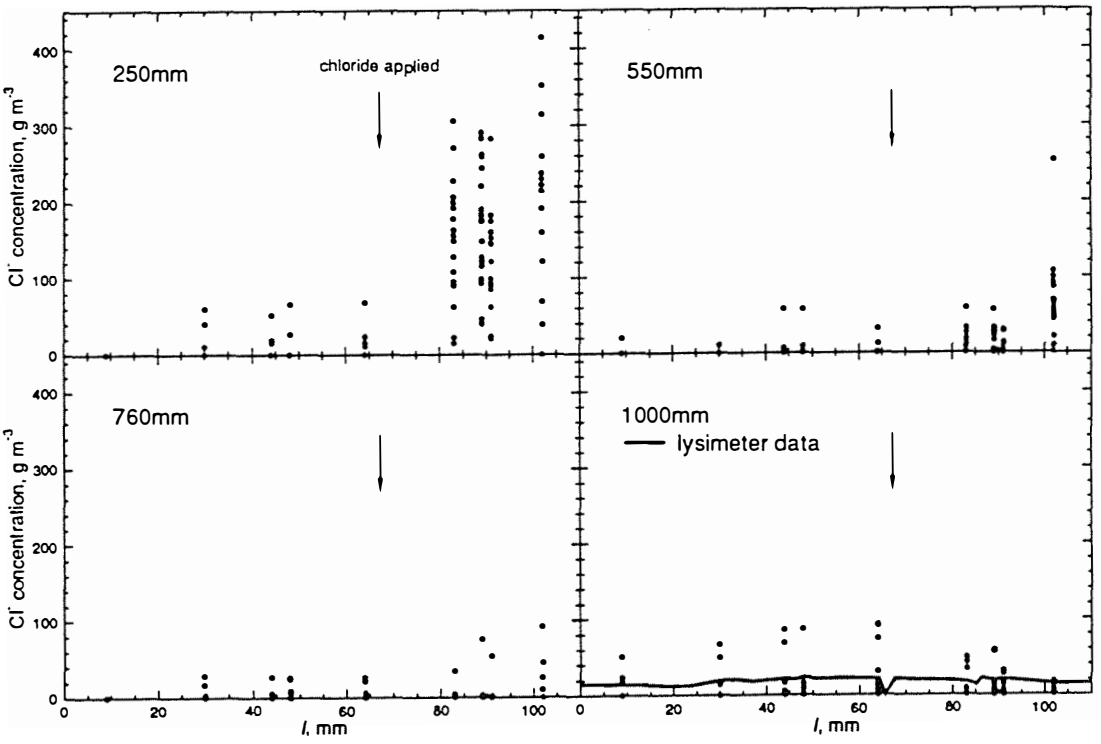

Figure 3.9 Porous cup concentrations for all sites and depths in 1989.

Bulked Data

The considerable variation in solute concentration across the paddock found in the 1988 experiment was again evident in the 1989 results (Figure 3.9). For the last

sampling, at the 250 mm depth the range of measured concentrations was from an undetectable level to a high of 400 g m^{-3}.

At 250 mm depth, approximately 20 mm of drainage led to the first rise of solute concentration, whereas for the samples taken at 550 mm depth some 40 mm of drainage was required. This was more-or-less as expected.

Lysimeter Data

Due to the lack of rainfall no rise in solute concentration was observed in the lysimeter. These data are shown in Figure 3.9

3.2.3 Soil Cores

In order to provide data to examine the relationship between flux- and volume-averaged, or resident, soil solution samples, and to give initial data for what were expected to be fairly discrete leaching events during the winter, significantly more soil samples were collected during the 1989 experiment than during the 1988 experiment. However, so little rain fell that on only a few occasions was it possible to collect core samples as well as samples from the porous cups. The data collected are shown in Figure 3.10.

The samples taken to a depth of 1 m were collected using a corer with an internal diameter of 50 mm, whereas the shallower samples were collected with a 20 mm diameter corer. Thus, the samples collected on days 33 and 96 had approximately 6 times the cross-sectional area of the samples collected on days 44, 49, 70, and 118. Conventional wisdom says that it is wise to collect large volume samples so that the variation in the sampled concentrations is not excessive (Hassan *et al.*, 1983), yet here, the variability in the sampled concentrations did not decrease with the larger sample. Either the smaller corer cross-sectional area of 314 mm^2 was sufficient to overcome the variability, or more likely, the variability was on a larger scale than either of the corers.

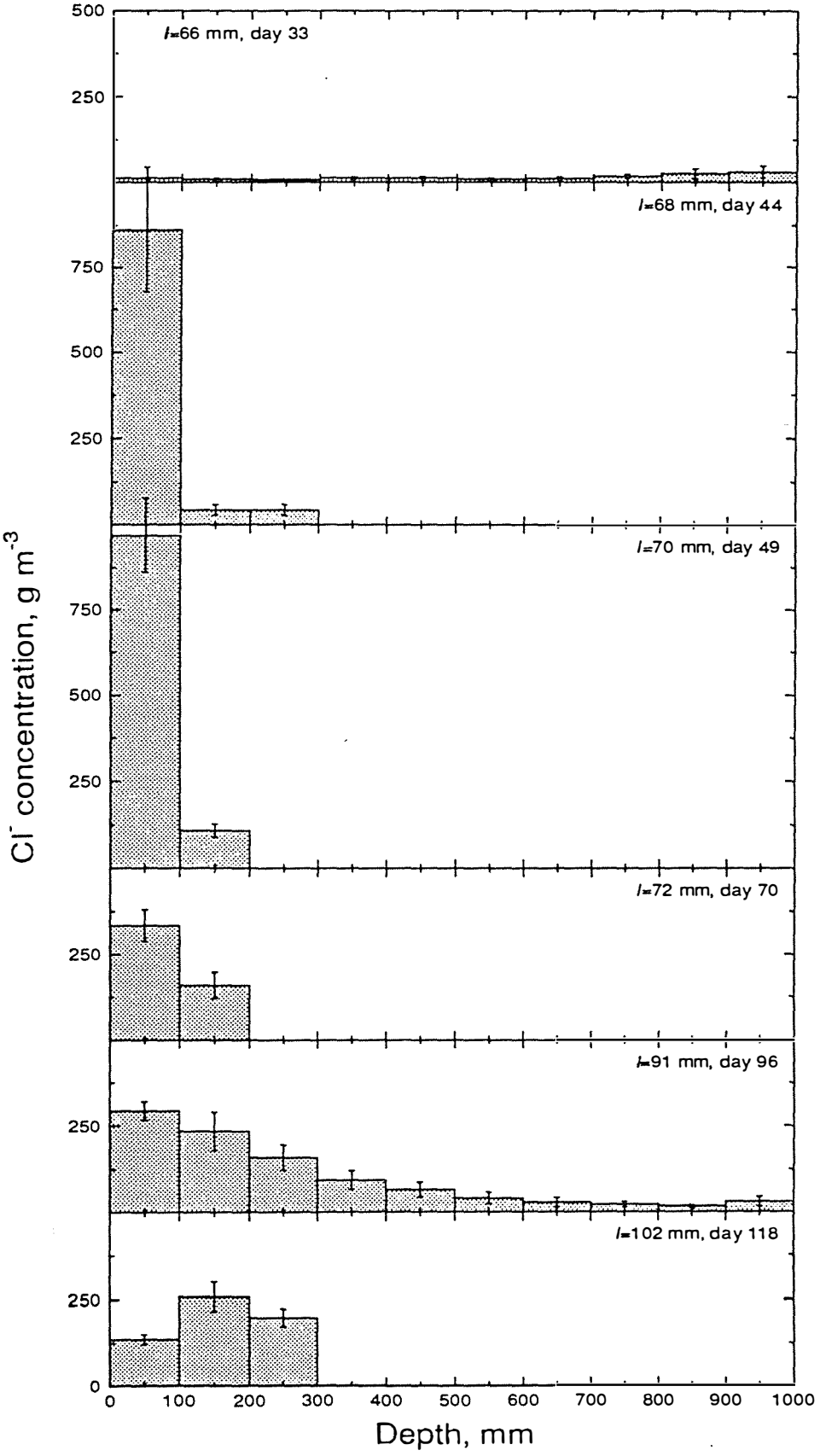

Figure 3.10 Soil solution concentration in the 1989 soil cores.

Although solute concentration between 100 mm and 300 mm depth remained constant between the samples collected on days 96 and 118, the surface concentration dropped by almost a half. This may indicate that the peak solute concentration was at the 100-200 mm depth, and by comparison of I with z that the transport porosity, θ_{st} [L^3 L^{-3}], was between 0.5 and 1. Both of these estimates were greater than the saturated water content but are consistent with the 1988 data. This matter will be discussed further in Chapter Four.

3.2.4 Chloride Mass Balance

For the 1989 experiment the data were such that meaningful calculations could not be made for depths exceeding 250 mm. Shown below are the components of the chloride mass balance for z=250 mm. The errors given on the figures are se's.

- Soil core samples revealed the amount of chloride stored in top 250 mm at the start of the experiment was 2.0±0.2 g m^{-2}.
- Solute remaining in the top 250 mm of soil at the end of the experiment was 11.0±1.3 g m^{-2}.
- The amount of chloride in the rainfall was assumed negligible.
- The porous cup data show that 4.4±0.5 g m^{-2} of chloride leached past the 250 mm depth.
- Plant uptake of chloride over the experimental period was found to be 11±4 g m^{-2}.
- The amount of fertiliser chloride applied was 25 g m^{-2} and soil core samples taken after the fertiliser addition revealed 23.5±4.3 g m^{-2} were stored in the top 100 mm of soil.

Applying equation (3.2) to these figures yields a net balance of chloride of -1±10 g m^{-2}. Considering the assumptions about the nature of the water flow through the soil, the balance was excellent.

3.3 1990 DATA

The results of the smaller-scale lysimeter-based experiment carried out in the winter of 1990 are now presented.

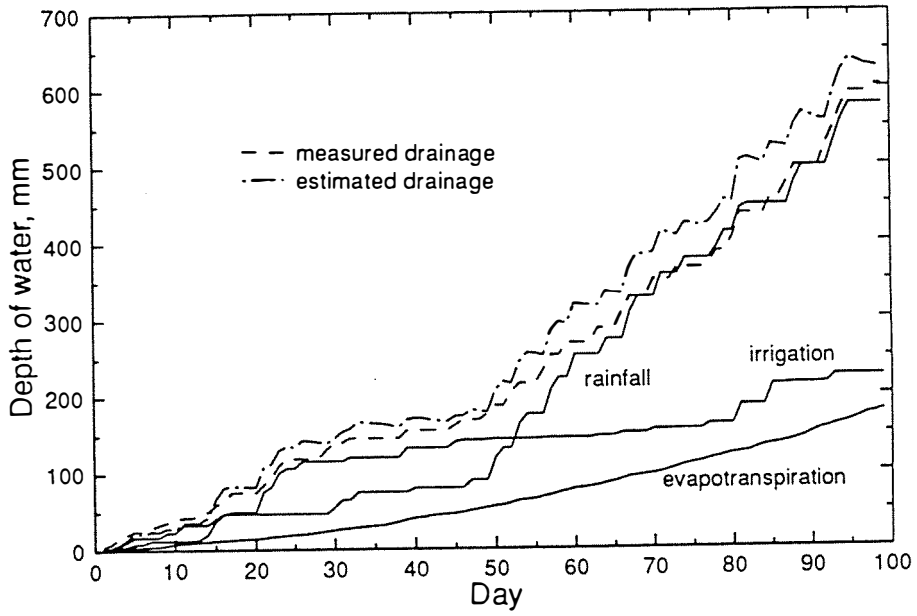

Figure 3.11 Water balance for the 1990 experiment showing evapotranspiration, rainfall, irrigation, as well as measured and estimated drainage. Day 0 was 23 July 1990.

3.3.1 Water Balance

As with the 1988 experiment, drainage was first estimated from irrigation, rainfall, and evapotranspiration and these are presented in Figure 3.11. Estimated drainage exceeded the measured drainage from the lysimeter, however here the discrepancy of 25 mm was insignificant compared to the total 600 mm of drainage.

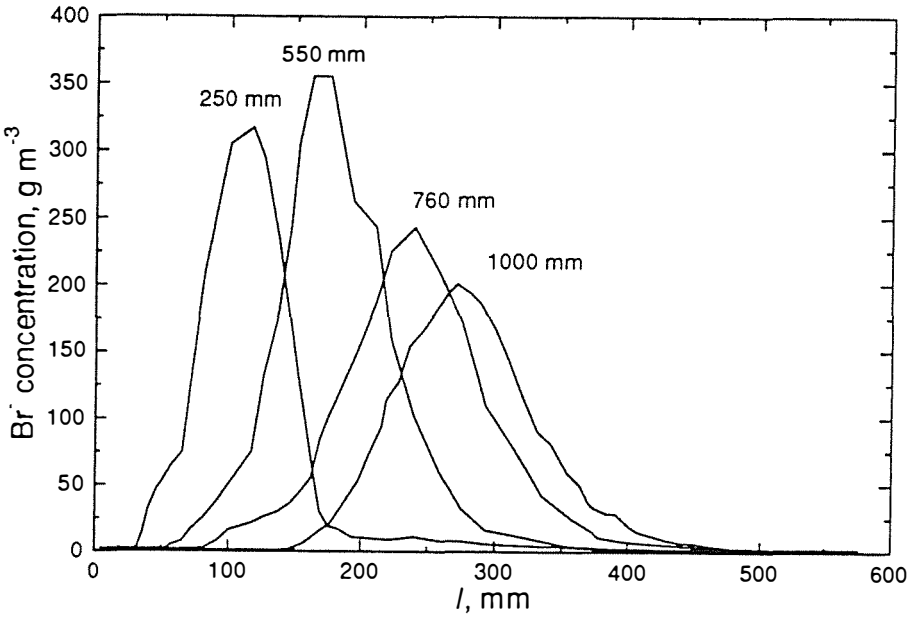

Figure 3.12 Porous cup and outflow concentrations measured in the lysimeter during the 1990 experiment.

3.3.2 Porous Cup and Lysimeter Data

The data from the single porous cups at 250 mm, 550 mm, and 760 mm, along with the outflow from the lysimeter at 1000 mm are shown in Figure 3.12. The coherence of the data was quite remarkable. This was especially so considering the small sample area for the top three breakthrough curves compared with the 2 m^2 area for the lysimeter outflow. These data thus represent a very useful data set upon which to examine solute transport. This will be done in Chapter Four, prior to considering the much more complex data derived from the field experiment in 1988.

3.3.3 Bromide Mass Balance

When calculating the mass balance for this 1990 lysimeter experiment, the plant uptake of bromide must be considered. Here there was no Br^- in the soil at either

the start or end of the experiment, and the concentration in the irrigation water and the rainfall was also zero. The fertiliser addition was 30 g Br^- m^{-2}, and the plant uptake was measured at 3.2 g m^{-2}. Mass balance figures for this experiment are presented in Table 3.2.

Table 3.2 Bromide mass balances, calculated from equation (3.2), as well as bromide recovered in the drainage water.

Depth (mm)	Br^- in drainage (g)	Balance (g)
250	25.9 *	0.9
550	34.7 *	-7.9
760	29.8 *	-3
1000	25.1 **	1.7
* from porous cup samples, ** from lysimeter leachate.		

The balance was quite remarkable, and is again most likely a result of the enclosed system and the even distribution of bromide and water on the lysimeter surface.

These last three sections have presented the data from the experiments as well as brief discussions of the patterns of solute leaching observed and the mass balance of solute in each of the experiments. The following four sections will bring together these data and examine in more detail some aspects relevant to solute transport.

3.4 Comparison of Cup and Core Samples

Soil solution samplers collect a sample by drawing water from the surrounding soil, in response to a lower pressure in the cup compared to that in the surrounding soil water. Because the sample is collected by a transport process, this sample then contains water weighted by its ability to move through the soil, as well as by its proximity to the sampler. A sample collected in such a manner is referred to as

being flux-averaged (Kreft and Zuber, 1978; Parker and Van Genuchten, 1984) and where this distinction is necessary it will be denoted by a superscript *f*.

Another method of obtaining soil solution concentration involves collecting all the water within a defined volume of soil. This would usually arise when a sample is obtained by collection of a soil core followed by complete extraction of the solute. A sample collected in this manner is weighted not by its ability to move to the sampler, rather by virtue of is position in the soil only. Because parcels of water are sampled in accordance with their relative abundance in the sampled soil volume the sampled collection is referred to as volume-averaged. This is often called the resident solute concentration, c^r.

That the two measurements are different from a sampling viewpoint, and so can be completely different in terms of c is not always appreciated. Early work concerned with soil solution samplers concentrated on the mechanics of sampler construction and on the chemical composition of the sample collected (eg. Wagner, 1962; Wood, 1973; Morrison, 1982; Riekerk and Morris, 1983). The nature of the sampling process was largely ignored. The exception was Warrick and Amoozegar-Fard (1977) who developed a numerical model of water movement to a sampler. Even here, however, the effect of the water movement to the sampler on the resultant concentration of solute was not addressed.

Resident and flux-averaged concentrations may be related using the law of mass conservation (Kreft and Zuber, 1978; Jury and Roth, 1990) so that,

$$Q \int_o^t c^f(z,t')\, dt' = \theta A \int_z^\infty c^r(z',t)\, dz' \quad , \tag{3.3}$$

here A refers to some cross-sectional area of soil [L^2] and Q is the water flow rate [$L^3\, T^{-1}$]. Assuming that there is no solute present initially, equation (3.3) states that the amount of solute which has flowed past some depth z until time t, multiplied by Q is equal to the cross-sectional porosity of the soil times the amount of solute within the soil between z and infinity. Although this is a simple statement of mass balance, it may not be so simple to measure the integral of c^r where the soil is deep.

The formulation given in equation (3.3) does not require any assumption to be made concerning the solute transport process, but does indicate a potential difficulty. This is the need to determine accurately the integrals in equation (3.3). An alternative formulation to obtain the relationship between c^r and c^f (Kreft and Zuber, 1978; Parker and van Genuchten, 1984) is based on the assumption of the applicability of the CDE to solute transport in the soil. By stating the total solute flux is equal to the sum of the convective flux and the dispersive flux then,

$$v c^f = v c^r - D \frac{\partial c^r}{\partial z} \quad , \tag{3.4}$$

where v is the mean pore water velocity ($Q/A\theta$) [L T^{-1}], and D is the dispersion coefficient [L^2 T^{-1}]. It is necessary to accept that the CDE adequately represents solute transport in order to use equation (3.4) with confidence. The presence of mobile and immobile water or preferential flow will destroy the relationship represented in equation (3.3). Nonetheless it is a useful framework with which to examine how various physical conditions might affect the relationship between c^r and c^f. From equation (3.4) it can be seen that the discrepancy between resident and flux concentration will be greatest in media with high dispersivity and where steep gradients in the resident concentration are present.

Arguing on simple physical grounds, where there is a high degree of preferential flow, for example in highly structured soil under high flow regimes, one can see that only a small proportion of the total soil water will be involved in the transport of solute. Thus there is potential for a large difference between the resident and the flux concentration.

There are essentially two methods of measuring the solute concentration in the soil, and it has also been determined that these two concentrations are different (Kreft and Zuber, 1978; Parker and van Genuchten, 1984). However few have examined whether this has any impact in the field. Using some of the data collected in 1988 and 1989, it was possible to compare these two concentrations.

Figure 3.13a shows the depth-wise profile in chloride concentration found in the water phase of soil sampled by coring on day 46 of the 1988 experiment. Shown

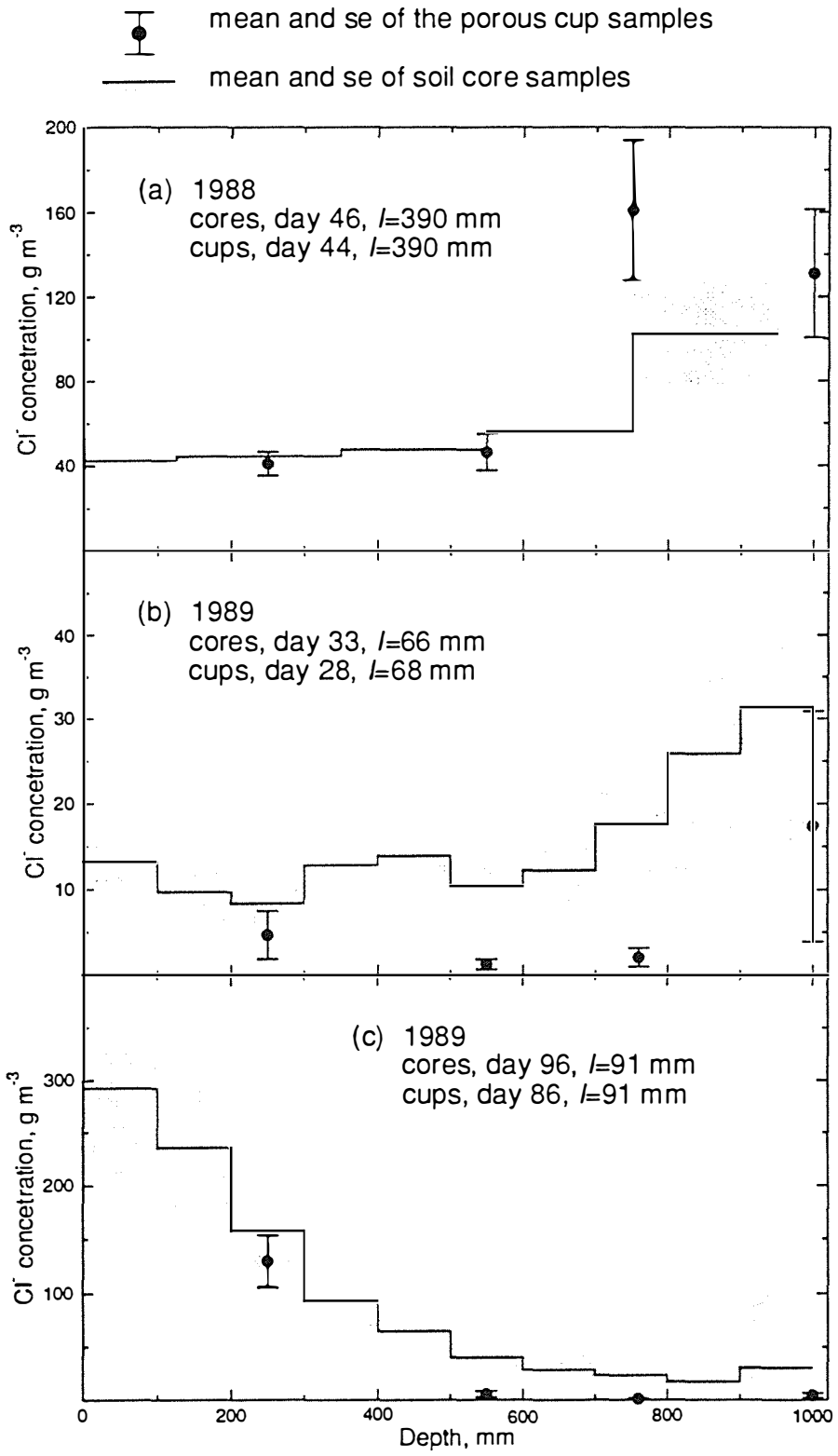

Figure 3.13 Comparison of solute concentration from soil core and porous cup samples. Note the changes of scale in the vertical axis.

along with the soil core data are the concentrations measured by the porous cup samplers. In both cases, in the following figures, the mean and the standard error of the mean (se) were assessed using the method of Sichel (1952).

Indeed, at none of the depths in this first comparison was the porous cup concentration statistically significantly different from the core concentration. However, the trend indicates that the differences between the two measures at 760 mm and 1000 mm are greater than elsewhere. This is also where the spatial gradient in c' is greatest, due to the location of the solute pulse at the time of sampling. Here, according to equation (3.4), there should be a greater discrepancy between c' and c^f.

In contrast to the data shown in Figure 3.13a, the data in Figure 3.13b show c^f to be less than c'. This however might have been anticipated given the history of the solute in the soil. Data shown in Figure 3.13b were collected before the 1989 chloride application took place, so the elevated chloride concentration at greater depths might have been the result of the chloride which had been applied in 1988, and had become resident by virtue of being incompletely leached from the soil profile. The solute would have been present in the soil for almost a year and during that time might have become more evenly redistributed throughout the soil. Given the length of time involved, diffusion could have been important in distributing the solute throughout the soil water. Next winter, water began to move downwards from the upper soil with low resident concentration, into soil with higher resident concentration. Under these conditions the flux concentration might well be expected to be lower than the resident concentration.

A further set of chloride data from 1989 are presented in Figure 3.13c. By day 96 in 1989 there had been 25 mm of drainage after the application of the chloride fertiliser. However during the approximately 2 months that had elapsed, substantial redistribution could have occurred. Locally then the solute may be expected to be relatively evenly distributed through the soil. This may account for the relative similarity of the flux and resident concentrations.

Unfortunately there were limited data with which to compare core and cup samples. However they do indicate that the solute was probably not evenly distributed throughout the soil water. Hence cores and porous cup samplers would yield differently-averaged samples. A matter of concern was whether cup data was averaged with the same flux-weighting as the lysimeter, or indeed the field as a whole. Comparison of the porous cup and lysimeter data in Section 3.6 will provide more information on this.

3.5 Computing the Field Average Solute Flux

A common goal in field studies of chemical transport is the calculation of the field-average solute flux (Richter and Jury, 1986). In this calculation it is usually assumed that the solute concentration in the drainage from a field is the average of the solute concentrations in individual samples. However it can be shown that this assumption is valid only if the solute flux and the drainage flux at the individual sites are uncorrelated.

Consider a set of N observations of the amount of drainage during some fixed interval of time, I_j, and the flux-averaged solute concentration, c_j in that drainage. Over the whole field the total loss by drainage is,

$$I^{\phi} = \sum_{j=1}^{N} I_j = N\bar{I} \quad , \tag{3.5}$$

where I^{ϕ} is then this drainage flux from the entire field, and $\bar{I}$ is the average drainage flux at all the sites. The solute loss from the whole field, J^{ϕ} will be,

$$J^{\phi} = \sum_{j=1}^{N} I_j c_j \quad . \tag{3.6}$$

Therefore the flux-averaged solute concentration for the whole field, c^{ϕ}, will be,

$$c^{\phi} = \frac{J^{\phi}}{I^{\phi}} = \frac{\sum_{j=1}^{N} c_j I_j}{\sum_{j=1}^{N} I_j} = \frac{\sum_{j=1}^{N} c_j I_j}{N\,\bar{I}_j} \quad . \tag{3.7}$$

Now the covariance, Cov, between the individual measurements of drainage flux and the solute concentration can be expressed as,

$$\begin{aligned} \mathrm{Cov}(I_j,c_j) &= \mathrm{E}(I_j c_j) - \mathrm{E}(I_j)\mathrm{E}(c_j) \quad , \\ &= \frac{\sum_{j=1}^{N} I_j c_j}{N} + \overline{I}_j\,\overline{c}_j \quad , \end{aligned} \tag{3.8}$$

where E is the expectation operator. Therefore,

$$\sum_{j=1}^{N} I_j c_j = N\,\mathrm{Cov}(I_j,c_j) + N\,\overline{I}_j\,\overline{c}_j \quad . \tag{3.9}$$

So it follows that,

$$c^{\phi} = \frac{\mathrm{Cov}(I_j,c_j)}{\overline{I}_j} + \overline{c}_j \quad . \tag{3.10}$$

Thus, by examining equation (3.10), it can be seen that if there is some covariance between the concentration measured at each site and the drainage flux, then the field average solute concentration will not equal the average concentration measured at each site. In this case the correct measure would be to weight the concentration by the drainage flux as shown in equation (3.7).

As an aside, it should be noted that implicit in the assumption that drainage flux does not affect the pattern of solute leaching, is that the covariance is zero.

A number of physical arguments can be sustained as to whether the drainage flux and solute concentration should, or should not, be related. Regardless of any argument, if these quantities are related then it is not valid to simply take the average of each quantity to characterise the field. In the 1988 experiment the amount of irrigation input to each site was measured so that the drainage could be estimated. These data then provide for a test of the hypothesis that there is no correlation between drainage flux and solute concentration at each site.

In the early stages of the leaching, positive correlations might be expected. At any particular depth, those sites which received the most irrigation water might also be expected to have the applied chloride pulse reach them first, thereby causing a rise in concentration. This would cause a positive correlation. Later these sites would be the first to experience decreasing solute concentrations as the solute peak passed the sampler depth and negative correlations might then be expected. These patterns would be preserved only as long as the irrigation application was consistently high or low at any one site.

In order to determine whether any relationship existed between the drainage flux and solute concentration, the change in the amount of cumulative drainage for each site was correlated by depth and day against the measured solute concentration for the 1988 field data. Naturally only the data arising from the period when the irrigation system was in operation was used. As the underlying population distributions of the two measures were not necessarily the same a Spearman or rank correlation, ρ_s, was applied. For each sampling date and depth of sample, the sites were ranked for both c and I and these ranks correlated. The results of this exercise are summarised in Table 3.3. As, in total, 56 correlation coefficients resulted, only those coefficients which were statistically significant are given.

Only eight of the total 56 correlation coefficients were significant. In retrospect, this might be expected even if there was a relationship between c and I. This is because the sign of the correlation is excepted to change part way through the leaching process and the time at which the change in sign is expected is not constant but itself related to the amount of irrigation received. It is of interest that the data from the 250 mm depth on day 1 were significant, indicating that those sites which received more irrigation on the first day were more likely to show increases in solute concentration. So from the above analysis it is not clear whether there was any underlying correlation between c and I.

This analysis could be carried a stage further if the J^{ϕ}, given by equation (3.6) is compared with the method more-commonly used,

$$J^{\phi} = I^{\phi} c^{\phi} \quad . \tag{3.11}$$

Table 3.3 Statistically significant correlation coefficients between c and I. Here ρ_s is the Spearman correlation.

day	depth (mm)	N	ρ_s
1	250	18	0.394 *
4	760	19	0.412 *
7	1000	18	-0.550 **
9	760	19	-0.407 *
14	760	20	0.449 **
16	550	20	-0.591 ***
22	250	20	0.427 *
37	250	16	-0.430 *
* significant at 5%, ** 1%, *** 0.1%			

This analysis is essentially the same as that carried out by Richter and Jury (1986). However in that study the irrigation system was of higher uniformity. In order for any difference to become evident, considerable variation in I is required. Calculations are for the 250 mm data only, as it was here that the measured cumulative net water input was most appropriate.

The field-average solute flux was calculated both from the individual measurements of c and I, as in equation (3.6), and also using equation (3.11). Where J^{ϕ} was calculated from equation (3.6) it will be referred to as the average flux. When calculated from equation (3.11) it will be called the estimated flux as it excludes the covariance effect. The results of this calculation are shown in Figure 3.14. Although the average of the individuals was consistently higher than the averaged flux, the difference was not statistically significant.

As the analysis was carried out in the period that the irrigation system was operated, these results are indicative only of the early stage of solute leaching. The hint of a small negative covariance was an indication that some of the solute might have

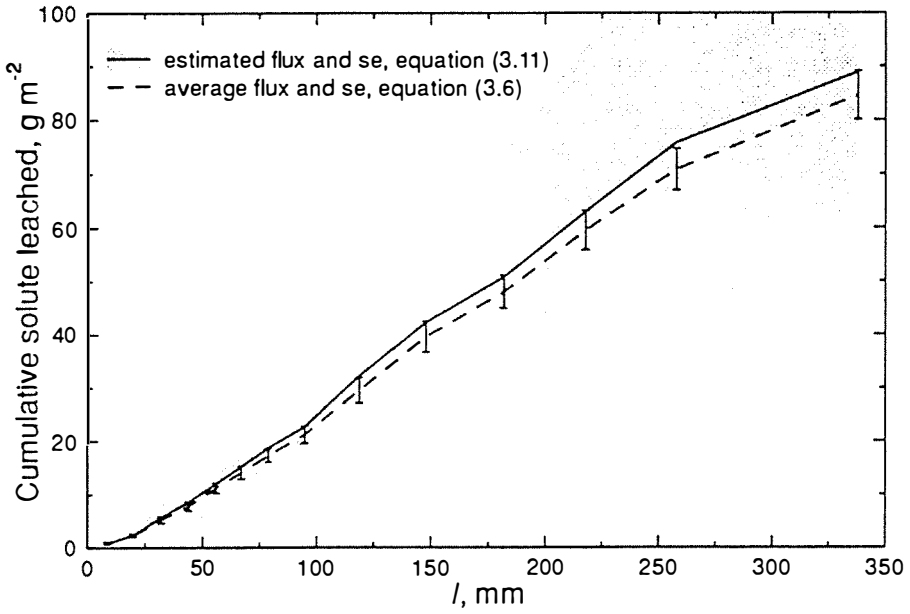

Figure 3.14 Comparison of field-average solute flux given by equations (3.6) and (3.11).

been relatively impervious to the leaching effect of the draining water. This covariance is opposite in sign to that calculated by Richter and Jury (1986) where an application of solid KBr was immediately followed by irrigation. A similar effect to that in the current study was noted by Tillman (1991) and Tillman *et al.* (1991) when comparing timing of irrigation in relation to solute application.

The main difference between the two measures was the accompanying standard error. It should be noted that as the soil water content approaches saturation, the covariance between c and I will in all probability increase in magnitude. However, it would appear that the two measures of J^{ϕ} are sufficiently similar to render acceptable the computationally-simpler, estimated J^{ϕ}, at least in this study.

3.6 Spatial Variability

As the study of solute movement has moved towards field-based experimentation, the topic of spatial variability of solute transport has become more important. However little work has been done in this area due to the paucity of data. A good deal more work, theoretically at least, has been done regarding the variability of flow of water and solute in aquifers. But, as pointed out by Dyson *et al.* (1990), soils differ from aquifers in a sufficient number of important details that the assumptions and conclusions developed for the latter may be invalid. For example in aquifers much of the stratification is parallel to the water flow, whereas in soils it is usually normal to the flow.

Solute transport properties of soil vary in both the transverse and depth-wise directions. Considering the distinct change in soil physical properties in the vertical, this variability may, *a priori* be thought to be of greater magnitude than variability in the horizontal or transverse plane. Longitudinal variability has already been addressed earlier in this chapter and will be considered further in Chapter Four. Therefore in this section only the transverse spatial variability which will be considered.

There are many questions concerning spatial variability of relevance in the current study. Some of these are now presented and discussed.

- Are the porous cup samplers within a measurement site dependent or independent of one another?
- Are the porous cup samplers at the same depth but at different measurement sites independent of each other?
- Given the variability inherent in the field, what is the best representation of the field-average BTC?
- Is the lysimeter outflow representative of field-average solute transport?

The essence of the first question is best explained by example. Does the BTC measured at a particular site, at say the 550 mm depth, include some of the signal of the 250 mm BTC sampled at the same measurement site? If this cannot be

assumed then it will not be possible to analyse separately solute transport at each site. Instead the data from all sites at a particular depth must be bulked.

Van Wesenbeeck and Kachanoski (1991) measured BTC's at 0.4 m deep at 0.2 m intervals along two transects in the same soil, under both cultivation and forest. Solute BTC's were remarkably similar at the two sites. They found the range of spatial variability, or the horizontal distance over which solute transport was dependent, to be between 1.0 and 2.8 m in the forested site and 3.5 to 4.0 m in the cultivated site. As an aside it is interesting to note that deforestation and 50 years of cultivation of that soil produced little effect on solute transport, other than in the distance over which solute transport was correlated.

If the results of Van Wesenbeeck and Kachanoski (1991) are representative of soils in general, then this would indicate that the samplers within a measurement site, which is less than one metre across, are likely to be more closely related to each other than to samplers at another site. That this is not universally true was clearly demonstrated by those data collected at site 19 where solute arrived at 550 mm depth before it arrived at 250 mm! (See Figure 3.4) This phenomenon had been noted by Roth *et al.* (1991) and can be attributed to the fact that samplers at different depths sample different flow regions. Other sites, for example numbers 12 and 14, plus the data collected in the lysimeter during the 1990 experiment, are quite adequately explained by the assumption that the samplers are dependent on each other.

An alternative worthy of consideration here is concerned with the variability of the irrigation water application. If the pattern of variability of water application was such that the single measurement per site was not appropriate then anomalies such as site 19 may be explained. Given the comparison of the data from the lysimeter from 1988 and 1990 (discussed in Section 3.7), the water application is probably significant in affecting variability.

Given that the measurement sites here were 10 m apart, in relation to the range of variability found by Van Wesenbeeck and Kachanoski (1991), it would appear reasonable to assume that the measured BTC's from different sites were

independent of each other. Therefore it is also reasonable to assume that the variance determined from the data bulked from these sites reflects the field-average variance.

Regarding the third question, there are two methods of determining the moments of the field average BTC. Either all the concentration versus cumulative drainage data can be bulked together, or the moments of each BTC can be found and averaged. The former approach is more common and has been employed by several authors, including Butters *et al.* (1989). Dyson *et al.* (1990) pointed out that the field average variance for travel could be calculated from the expected value of the local variances and the variance of the local expectations. Expressed mathematically this is,

$$\mathrm{Var}_f = \mathrm{E}_f(\mathrm{Var}_l) + \mathrm{Var}_f(\mathrm{E}_l) \quad , \tag{3.12}$$

where E and Var refer to the expectation and variance operators respectively. The subscripts l and f indicate that the quantity should be measured at either the local or field scale.

Dyson *et al.* (1990) tabulated the results of applying equation (3.12) to four field studies of solute transport with varying field sizes. As might be expected the field variance became dominated by the variance of the local expectations, the second term on the RHS of equation (3.12), as the size of the field increased and more variability was encountered. It would also be reasonable to expect this term to dominate as the water content of the soil approaches that of saturation, and solute transport becomes more variable. Unfortunately it is not possible to test this theory as no trials were of the same spatial scale yet with different water contents.

An analysis such as that suggested by Dyson *et al.* (1990) will now be carried out on the data collected during the 1988 experiment. In calculating the moments of the BTC's a lognormal distribution was assumed,

$$c(I) = \frac{\exp\left\{\dfrac{-(\ln I - \mu)^2}{2\sigma^2}\right\}}{\sqrt{2\pi}\,\sigma I} \quad , \tag{3.13}$$

where μ and σ are the mean and standard deviation of the log-transformed distribution respectively. This assumption does not encompass any assumptions as to the underlying structure of the solute transport process. Here μ and σ were found by fitting equation (3.13) to the individual BTC's using the NAG routine E04FDF. These results are given in Table 3.4. The quantities μ_{field} and σ_{field} were calculated as the average of the individual μ and σ values. Also shown in Table 3.4 are the parameters fitted to the bulked data.

As these are population estimates rather than sample statistics the expectation and variance may be calculated as,

$$E = \exp\left(\mu + \frac{\sigma^2}{2}\right) , \tag{3.14}$$

and

$$Var = \exp^2\left(\mu + \frac{\sigma^2}{2}\right)(\exp(\sigma^2) - 1) , \tag{3.15}$$

(Sichel, 1952; Parkin *et al.*, 1988). The results of these calculations are given in Table 3.5.

Table 3.5 shows that the two measures of E_{field} are in reasonable agreement. The greatest discrepancy was in the highly variable 250 mm data. However the same cannot be said of Var_{field}. At the 250 mm depth, the bulked data variance was 40% higher than that from the individual data. The opposite holds for the greater depths where the bulked estimates are approximately half that of the individual estimates.

Calculation of the parameters of the lognormal distribution appropriate for the entire field is possible using equations (3.14) and (3.15) in conjunction with E_{field} and Var_{field} calculated from the parameters resulting from the distribution fits at each site. These parameters, denoted μ_{field} and σ_{field} were given in Table 3.4 and the effect of these estimates as compared with the parameters resulting from the bulked data are shown in Figure 3.15. Although in all cases the curves resulting from the individual data show greater spread than those from the bulked data, either curve could be regarded visually as a good fit to the highly variable data. The difference between the two measures is probably a result of the difficulty of fitting

Table 3.4 Lognormal distribution parameters for the 1988 BTC's calculated by either fitting equation (3.13) to the individual site data and then averaging or by fitting to the bulked data.

Depth (mm)	individual data						bulked data	
	μ (se)		σ (se)		μ_{field}	σ_{field}	μ	σ
250	5.3	(0.09)	0.86	(0.05)	5.2	1.00	5.3	1.02
550	5.4	(0.06)	0.76	(0.06)	5.1	1.07	5.4	0.81
760	5.9	(0.05)	0.40	(0.04)	5.9	0.54	5.9	0.43
1000	6.1	(0.07)	0.46	(0.06)	6.0	0.64	6.1	0.49

Table 3.5 Expectation, and variance, calculated from equations (3.14) and (3.15), of the solute BTC's from either the individual site or the bulked data.

Depth (mm)	individual data					bulked data	
	E_{field}	$Var_f(E_i)$	$E_f(Var_i)$	Var_{field}	$E_f(Var_i)/Var_{field}$	E_{field}	Var_{field}
250	305	12840	147378	160218	0.92	349	225595
550	315	14733	197626	212359	0.93	317	93578
760	415	10565	48620	59185	0.82	402	31983
1000	494	12068	110654	122722	0.90	503	67718

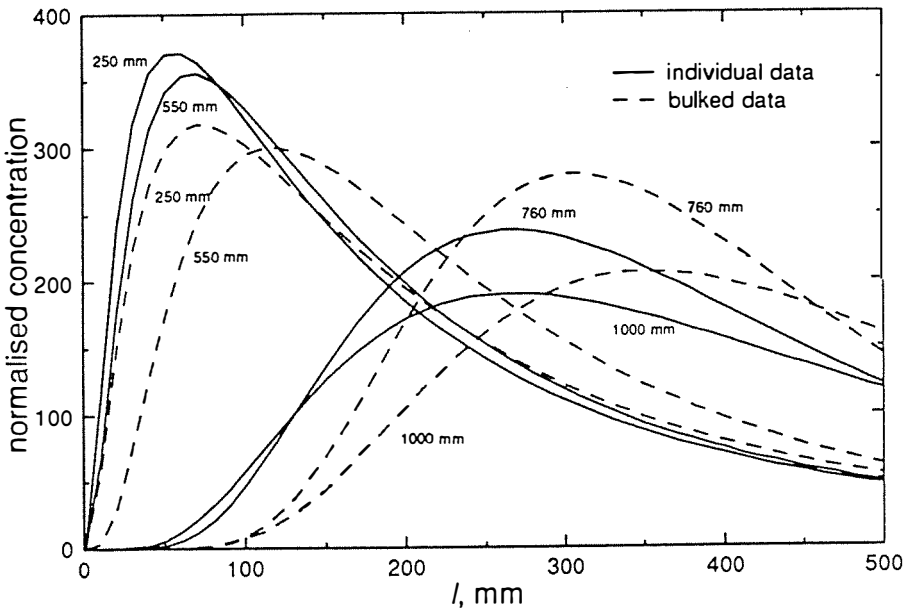

Figure 3.15 Field-average BTC's derived by calculation from parameters of individual data and from fitting to the bulked data.

an equation such as (3.13) to scattered data, especially where the parameters are correlated. Fitting the distribution to the individual data should however be regarded as the more correct method of obtaining the field-scale parameters.

The last question posed at the beginning of this section concerned the degree to which the outflow from the lysimeter could be regarded as representative of the field-average solute flux. Figure 3.16 shows the lysimeter outflow in 1988 as well as the mean and standard error (se) of all the 1000 mm porous cup data. In some sections of the BTC the lysimeter data fell beyond one se of the mean of the porous

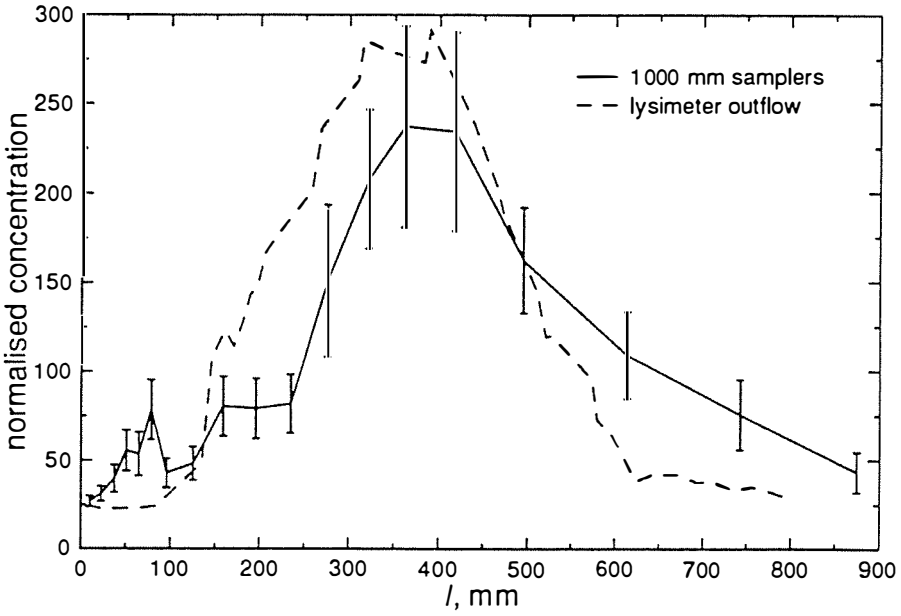

Figure 3.16 Solute BTC at 1000 mm for 1988 determined from the lysimeter outflow as well as the porous cup samples.

cup data, but the peak concentrations of the two BTC's nearly coincide. The lysimeter has exhibited a slightly earlier arrival of solute to 1000 mm than the porous cup data and is also less dispersed than the cup data.

Dyson *et al.*, (1990) have shown that spatial variability of the water input will increase both the expected value and variance of a BTC. Although the water input to the lysimeter was undoubtedly spatially variable, it was unlikely that the 2 m^2 lysimeter experienced anything near the large variability in water input rates experienced by the rest of the field. This could account for the observed differences between the lysimeter and field data. Notwithstanding this, it would seem that the lysimeter is a reasonable representation of the field.

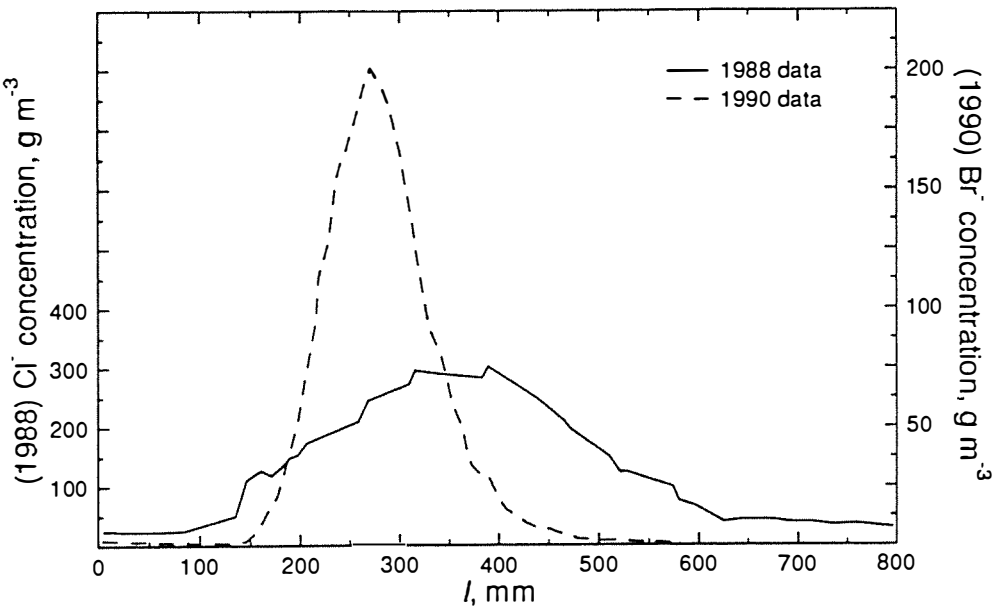

Figure 3.17 Solute BTC from the lysimeter in both 1988 and 1990.

3.7 Comparison of Lysimeter Drainage in 1988 and 1990

The lysimeter BTC's of chloride in 1988 and of bromide in 1990 were quite different, as can be seen in Figure 3.17. Here the scales of the two vertical axes have been chosen so as to give approximately the same area under each curve. The BTC resulting from the 1988 experiment is both delayed and considerably more dispersed than that measured in 1990. Some statistics from these BTC's are given in Table 3.6.

The two major differences between the 1988 and 1990 experiments as far as the lysimeter was concerned were the relative timing of the initial solute and water input and, to a lesser extent, the spatial and temporal variability of the water input. Also the high solute input in 1988 resulted in an earthworm kill which was not seen in 1990, although it may simply have been that there were fewer earthworms in 1990. Worm counts were not taken. However the main effect was not simply the kill of earthworms, but the combination of this kill with the grazing of the plot during very wet conditions with cattle. This latter effect is less important in the

Table 3.6 Mean, standard deviation, and median for the BTC's from the lysimeter outflow in 1988 and 1990.

Year	Mean (mm)	Standard Deviation (mm)	Median (mm)
1988	374	149	365
1990	281	60	277

lysimeter as the cattle avoided trampling it.

A single irrigation gauge was used to assess the irrigation input to the 2 m^2 surface of the lysimeter. Within this area the variability of water input was likely to have been considerable. An attempt to measure the smaller scale irrigation variability during 1989 was foiled by mechanical breakdown. As discussed in the previous section, this spatially variable water input will increase the mean and spread of the BTC (Dyson *et al.*, 1990). As the water input during 1990 was much more spatially uniform the effect there would not be as great as during 1989.

Thus it can been seen from the above that the detail of the inputs, of both solute and water, are likely to be very important for the result of the BTC from the soil. Indeed these effects may be more important than soil type and other macro-variables.

3.8 Summary

In the above sections the data collected during the three years of field experimentation have been presented and some aspects of the data discussed. There were four major topics addressed and these are summarised below.

- Soil cores and porous cups probably collected differently averaged samples. It is however not clear if the porous cup data was averaged with the same flux-weighting as the lysimeter or field.

- It was unclear if there was any covariance between c and I, however if calculation of the field-average solute flux is desired then the computationally-simpler equation (3.11) is adequate.
- Porous cup samplers within a site are likely to experience different flow regimes due to the spatially variable water input.
- The field-average BTC should be determined from the individual BTC's rather than by bulking the data.
- Solute outflow from the lysimeter in 1988 was delayed and dispersed compared with that measured in 1990. The difference was probably due to a combination of the antecedent condition of the soil surface and the spatially variable water input in 1988.

These points lead to the subsequent Chapter Four, in which predictive modelling of the data will be carried out.

Chapter Four

CONVECTIVE-DISPERSIVE MODELLING OF SOLUTE TRANSPORT

4.1 INTRODUCTION

Process-based modelling combined with field-experimentation occupied one sector in the diagram summarising the research philosophy presented in the first chapter. That sector of the diagram will be addressed here.

Given the history of process-based modelling, the choice to use of the convection-dispersion equation model (CDE) was not difficult. So, in this chapter the data collected from the field during the 1988 experiment and from the lysimeter during the 1990 experiment are investigated using the CDE. As the data resulting from the lysimeter outflow in 1988 represent only a single depth, there was little to gain from their use. Rather than use analytical solutions to the CDE in a direct way, the Transfer Function Model of Jury (1982; Jury *et al.*, 1986) with a Fickian probability density function will be employed for it is the direct equivalent of the CDE.

Section 4.2 presents the theory relevant to the modelling that will be undertaken within this chapter. This is followed by details of data manipulation and how the modelling was carried out. Sections 4.4 and 4.5 deal with modelling the 1990 and 1988 experiments respectively. A section summarising the mixed success of the modelling concludes this chapter.

4.2 THEORY

Convection-dispersion modelling of solute transport holds a commanding position in past work. Therefore it is appropriate that this model first be used to investigate the data collected through field-experimentation. The convection-dispersion equation (CDE) is first introduced and its development reviewed. Then a non-mechanistic model, the Transfer Function Model (TFM), will be scrutinised and the reason why this non-mechanistic model is included in a chapter about process-based modelling given.

4.2.1 The Convection-Dispersion Equation and its Application to Field-Scale Transport

Much of the current work on solute transport in soil has as its basis Taylor's (1953) model of solute transport in a capillary tube. The convection dispersion equation (CDE) and its more-sophisticated variants, such as the mobile-immobile CDE of Coats and Smith (1956) and van Genuchten and Wierenga (1976), have been used, albeit with varying degrees of success to data from repacked and intact column experiments (e.g. Smiles *et al.*, 1978; Elrick *et al.*, 1979; Kahn and Jury, 1990), as well as field data (e.g. Biggar and Nielsen, 1976; Jury *et al.*, 1976; Roth *et al.*, 1990). This approach has been used to describe and predict solute transport more often than any other model.

For one-dimensional steady-state water flow in a soil of uniform and constant water content,

$$\frac{\partial c}{\partial t} = -v\frac{\partial c}{\partial z} + D\frac{\partial^2 c}{\partial z^2} \quad , \tag{4.1}$$

where c is solute concentration in the soil solution [M L^{-3}], t is time [T], v is the pore-water velocity [L T^{-1}], z is depth [L], and D is the dispersion coefficient [L^2 T^{-1}]. The CDE describes solute movement as the sum of convection with the moving water and dispersion about the convected front. The dispersion term is considered to include the effects of molecular diffusion, tortuosity, velocity-diffusion interactions, and as well as spatial and temporal variations in the local value of v. In field-scale transport however it is probably spatial variation of v from the assumed steady state which accounts for much of the observed smearing of solute (Jury and Fluhler, 1992).

Most early work using the CDE involved testing against leaching experiments carried out in columns of repacked soil. The success of the CDE was such that discussion could then centre upon the secondary effects of anion exclusion (e.g. Cassel *et al.*, 1975), velocity-diffusion interactions (e.g. Smiles and Philip, 1983; Bond and Smiles, 1983) and other relatively small-scale phenomena. Little attention

was directed towards consideration of whether the CDE was itself an appropriate exposition of solute transport in soil.

However when applied to solute transport in undisturbed columns of soil or to results from field experiments, the CDE equation was often found deficient. One such inadequacy resulted from the common observation of asymmetric solute breakthrough curves (BTC's) following a pulse input which showed an early appearance of the solute as well as a long asymptotic tail back to the original level (e.g. Kissel *et al.*, 1973; Tyler and Thomas, 1981; White *et al.*, 1984). This effect was usually attributed to violation of the assumption that an average v could be used to describe adequately the true range of velocities that occurred in structured field soils. Repacking homogenised the soil and eliminated this structure. An alternative explanation was that part of the soil water did not contribute to the active transport process but provided a reservoir for solute which would later diffuse only slowly into the actively-moving soil water. This was the basis of the mobile-immobile CDE model of van Genuchten and Wierenga (1976), which took as its starting point the model of Coats and Smith (1964).

Further work, with aquifers rather than in soils, focused on the spatial and temporal scale dependence of solute transport (e.g. Freyberg, 1986; Dagan and Bresler, 1983; Dagan, 1984). As the scale of observation in the transverse plane increased, there was a concomitant increase in the magnitude of the observed dispersion coefficient. This was attributed to additional measurements encountering ever greater variations in the transport properties of the medium. This further violated the assumption of an undeviating D.

Most work on solute transport had simply monitored transport at a single depth or time. As data became available from measurements taken at multiple depths and times, it became apparent that the dispersion coefficient often increased with time (Warrick *et al.*, 1971; Freyberg, 1986). Taylor's (1953) theory was based on the assumption that there was adequate time for mixing of solute in the direction transverse to the main flow. The success in repacked soils may have been due to the homogenisation process, whereas in the field continuous longitudinal flow-paths may exist.

It would appear that there are two extremes of dispersive behaviour in solute transport. At 'short' time, solute parcels move in essentially isolated paths, or stream tubes, between which there is little or no mixing. Here the CDE, by definition, cannot describe the dispersive properties of transport. Smith and Schwartz (1980), and also Simmons (1982), described a stochastic-convective model where solute transport was modelled as taking place in isolated stream tubes at varying velocity. During stochastic-convective transport the spreading, or the variance if one regards the BTC as a probability density function of travel times, increased with the square of the time or distance of observation (Simmons, 1982; Jury and Roth, 1990; Dyson *et al.*, 1990). Here dispersivity, λ [L], grows linearly with depth or time. Jury and Fluhler (1992) have called this "zero-time" behaviour.

At larger times, or at "infinite-time" as noted by Jury and Fluhler (1992), the other extreme holds. Here parcels of solute in stream tubes are not isolated, but either through diffusion or intermingling, parcels of solute can move between stream tubes and thereby experience a range of velocities. Because a parcel of solute does not remain exclusively in a fast or slow stream tube, the variance of the BTC increases only linearly with time, as opposed to with the square of time in the "zero-time" behaviour, so that λ is constant. It is at this stage, when the longitudinal scale is much greater than the transverse mixing scale, that it is appropriate to use the CDE.

Currently models exist to describe both zero-time (Jury, 1982; Simmons, 1982) and infinite-time behaviour. Dagan (1984) has proposed a model to describe the transition between the zero- and infinite-time models. In practice there are few data with which to verify these models, and it is not clear *a priori* which model should be used given a certain distance or time. Freyberg (1986) found that even after 90 m of travel in an aquifer infinite-time behaviour was not realised, whereas Garabedian *et al.* (1991) found infinite-time behaviour after just 26 m of travel.

In a sandy loam soil, Butters *et al.* (1989) found zero-time behaviour to a depth of approximately 3 m. Below this depth there appeared to be a check in the growth of the variance of the BTC. After this interruption the variance continued to grow with zero-time behaviour until at least 15 m, and perhaps even 25 m. The

temporary change in the growth of the variance was attributed to the presence of sand lenses in the soil profile at the appropriate depth. This was predicated by the theory of Matheron and De Marsily (1980) which anticipated that stratification transverse to flow would simulate infinite-time behaviour. Conversely, stratification longitudinal to flow should preserve the zero-time behaviour.

Which model, zero- or infinite-time, ought to be applied to field soils is not clear. Jury *et al.* (1982) and Butters *et al.* (1989) found the zero-time model appropriate in the upper several meters of a sandy soil. Whilst ignoring preferential flow, Roth *et al.* (1990) however found that infinite-time behaviour adequately described solute transport in the top 2.4 m of a structured clay soil. What is clear is that it is essential to examine solute transport at more than one depth and time in order to determine which, if any, model of transport is appropriate (Jury *et al.*, 1990).

4.2.2 The Transfer Function Model

In what, at first, appeared to be a significant break with the largely mechanistic modelling of solute transport, Jury (1982) and then Jury *et al.* (1986) proposed that a transfer function model (TFM) be used to describe and predict solute transport in soil. The central concept of the TFM is the probability density function (pdf) of the lengths of time taken for a 'parcel' of solute to travel through some depth of soil (Jury *et al.*, 1986; Jury and Roth, 1990).

In its most general sense this travel time pdf would include the antecedent distribution of the solute in the soil, the convoluted travel pathways the solute passes through, and the effects of sorption/desorption, as well as production/ consumption, and decay. These factors, if linear or linearised, could all conceptually be included in the model. However the type of data that is generally available, and the fact that many of the processes are transient, limit the applicability of the model to the distribution of travel times taken for solute to travel from the upper to lower boundary of the soil (Jury *et al.*, 1986). Jury and Roth (1990) and Heng (1991) both give examples of how processes other than 'simple' mass flow transport might be included in a TFM.

Jury *et al.*, (1986) described the TFM for a volume of soil with both entrance and exit surfaces. Such surfaces are not always particularly well defined. In a lysimeter or soil core these would be the proximal and distal ends of the core or lysimeter. However for the field, where the solute concentrations would be measured using either soil cores or suction cups, the meaning of such surfaces is less clear. Usually they would be some plane of nominal areal extent at the depth of the sample. In a multidimensional transport system some consideration of the geometry of the process would be needed.

The basic TFM equation considers that the flux of solute exiting from the soil transport volume is the result of the convolution integral of the input solute flux and the solute travel time pdf. Mathematically this is,

$$Q_{out}(t) = \int_0^t g(t-\tau_{in} \mid \tau_{in})\, Q_{in}(\tau_{in})\, d\tau_{in} \quad , \tag{4.2}$$

where Q_{out}, and Q_{in} [M T^{-1}] are the output and input solute fluxes respectively, and g is the solute life-time pdf [T^{-1}]. Note that in the formulation given here in equation (4.2), g is conditional on the time at which the solute was applied to the soil. In the case where water flow is steady the input time is usually assumed not to affect solute travel and may be removed from the equation. Further, if the solute is unreactive, then the solute life-time pdf is replaced by the solute travel-time pdf, f [T^{-1}]. Additionally, if the input and exit surfaces have, or are assumed to have, equal areas then the solute flux, Q [M L^{-2}], can be replaced with the solute concentration, c [M L^{-3}], which is a function of both depth of measurement, z [L], and time, t. Equation (4.2) now becomes

$$c(z,t) = \int_0^t c(z,t')\, f(z,t-t')\, dt' \quad . \tag{4.3}$$

A cumulative-drainage form of the equation can also be derived by using the relationship,

$$I = J_w t \quad , \tag{4.4}$$

where I [L^3 L^{-2}] is the cumulative drainage, so that now,

$$c(z,I) = \int_0^I c(0,I')\, f(z,I-I')\, dI' \quad . \tag{4.5}$$

The use of I rather then t as an independent variable when describing non-steady transport has previously been employed (Gardner, 1965; Jury *et al.*, 1982; Roth *et al.*, 1990). Indeed both White *et al.*, (1984) and Heng (1991) suggested that this form was the most appropriate when analysing solute transport resulting from transient water flow. However that is only correct when it is appropriate to assume that solute transport, or f, is independent of the water flux.

Equation (4.5) can be solved analytically for a limited number of idealised input functions. The simplest of these is the Dirac delta, or impulse, function. In this case, the pdf simply becomes the output solute concentration normalised to an integral of one,

$$f(z,I) = \frac{c(z,I)}{\int_0^\infty c(z,I')dI'} = \frac{c(z,I)}{M} \quad , \tag{4.6}$$

where M [M L^{-2}] is the total mass density of solute which has leached past z as I approaches infinity. Analytical solutions to the TFM are available for other input functions, such as the step function. But for more-complex inputs, analytical solutions might not exist.

Despite the fact that equation (4.5) is formulated without an explicit time dependence, it is not necessarily suitable for use with transient flow. As well as the assumption that solute transport is unaffected by water flux, as previously discussed, it is also necessary to assume either that, with respect to depth,

$$\int_0^t J_w(0)dt = \int_0^t J_w(z)dt \quad , \tag{4.7}$$

or to correct for the initial water content of the soil (Jury and Roth, 1990).

Any function with the appropriate properties of a pdf may be used as the transfer function, f, in the TFM. This could come from some observations or be a mathematical function. This was aptly demonstrated by Sposito *et al.*, (1986) when

they reformulated the mobile-immobile CDE model of van Genuchten and Wierenga (1976) into a TFM. More recent work (D.R. Scotter, pers. comm., 1992) involves re-analysing Burn's (1975) model within a TFM framework. Thus the TFM has particular utility as a framework for the comparison of different models of solute transport.

Sposito *et al.* (1986), and later Jury and Roth (1990), showed that the Fickian pdf,

$$f(z,t) = \frac{z}{\sqrt{4\pi D t^3}} \exp\left(-\frac{(z - vt)^2}{4Dt}\right) , \qquad (4.8)$$

where D [L^2 T^{-1}] is the dispersion coefficient, and v [L T^{-1}] is the pore water velocity, was, within a TFM, was a solution of the CDE given in equation (4.1). As this is essentially the one-dimensional steady-date CDE expressed as a TFM, equation (4.8) will model behaviour appropriate to "infinite-time" behaviour. Jury and Roth (1990) called this particular form of the model a convective-dispersive TFM.

Another form of the TFM which has received much attention is one which will represent the "zero-time" behaviour of the stochastic-convective models. In this formulation the lognormal pdf,

$$f(z,t) = \frac{1}{\sqrt{2\pi}\,\sigma t} \exp\left(-\frac{(\ln(t) - \mu)^2}{2\sigma^2}\right) , \qquad (4.9)$$

where μ and σ are the mean and standard deviation of the distribution respectively, is commonly used for its ability to represent BTC's well. This pdf has no explicit depth dependency within it, but is combined with the assumption that,

$$f_z(z,t) = \frac{Z}{z} f_Z\left(\frac{Zt}{z}, t\right) , \qquad (4.10)$$

where Z is the prediction depth [L], and z the calibration depth [L]. This is mathematically equivalent to saying that the probability of a parcel of solute reaching a depth z in time t is equal to the probability of the solute reaching depth $2z$ in time $2t$ (Jury, 1982). This is also consistent with the stochastic-convective

model, where parcels of solute are envisaged as behaving as if they were in isolated stream tubes. The combination of equations (4.9) and (4.10) leads to

$$f(z,t) = \frac{1}{\sqrt{2\pi}\,\sigma\,(Zt/z)} \exp\left(-\frac{(\ln(Zt/z) - \mu)^2}{2\sigma^2}\right) , \qquad (4.11)$$

and the parameters μ and σ are determined from the lognormal pdf at the calibration depth, Z.

The convective-dispersive TFM described above provides a convenient method with which to apply the CDE to data. This will be done, initially to the 1990 and then to the 1988 data, below. First, however, there is a section describing data manipulation and curve fitting.

4.3 METHODOLOGY

The CDE is conventionally written with time as the independent variable, yet the data within this thesis are clearly most easily analysed with respect to cumulative drainage. Roth *et al.* (1990) presented a form of the CDE dependent on cumulative drainage. They applied this to unsteady flow in a field soil. Here, a simpler, though perhaps less elegant, technique is employed. For every 10 mm of drainage, a day will be assumed to have passed. This is equivalent to saying,

$$t = \frac{I}{J_w} , \qquad (4.12)$$

and the drainage flux density, J_w, will be prescribed as being 10 mm day^{-1}. Thus t in this chapter is not related to elapsed time, rather is the number of intervals of 10 mm of drainage. Note that neither this operation, or the manipulation of the CDE performed by Roth *et al.* (1990) take into account the possibility that the drainage flux will affect solute transport, except in so far as its effect on the cumulative drainage.

The curve fitting required here was carried out using the NAG routine E04FDF. This routine uses the iterative Newton-Raphson scheme to find the parameters which result in the best least-squares fit of a function to supplied data. As E04FDF uses numerical approximations to the derivative of the sum-of-squares function, analytical differentiation of the function is not required. Where an integration was required to evaluate the value of the function, the trapezoidal rule was used.

4.4 APPLICATION OF THE CDE TO THE 1990 LYSIMETER DATA

As pointed out above, data at multiple depths or times are required to ascertain if a model of solute transport is appropriate. Therefore, during 1990 the lysimeter was instrumented with single porous cups each at depths of 250 mm, 550 mm, and 760 mm, so providing three BTC's, in addition to that determined from the outflow of the lysimeter at 1000 mm. Details of the experiment have already been provided in Chapter Two and the results have been presented in Chapter Three. These data provide a useful starting point from which to investigate solute transport in this soil.

Where solute transport has been measured at more than one depth or time, the traditional method of modelling has been to calibrate an appropriate equation, considering the input boundary condition relevant to the soil surface, and the measured solute concentrations at a particular depth. Attempts are then made to predict solute concentrations at other depths or times. This method will first be applied to the data collected during the 1990 experiment on the lysimeter.

In the first instance the convective-dispersive TFM, the equivalent to the CDE given in equation (4.1), is applied. The data were transformed to obtain time as the independent variable, as suggested in Section 4.3.

The coefficients of the CDE so fitted using a Dirac delta function input are given in Table 4.1.

For the CDE fitted to the BTC measured at 250 mm, the resultant v was 21 mm day^{-1}. However the data have been transformed such that the drainage flux density

Table 4.1 Coefficients of the CDE fitted to the 1990 lysimeter data with a Dirac delta function input at the surface as the input data. Dispersivity is also given.

z (mm)	D (mm^2 day^{-1})	v (mm day^{-1})	λ (mm)
250	220	21	10
550	370	28	13
760	460	28	16
1000	470	31	15

was 10 mm day^{-1}. Thus a transport porosity, θ_{st} [L^3 L^{-3}], of 0.48 appeared to result. In this layer of soil, the volumetric water content was measured on several occasions, both before and after irrigation, and on average was observed to be 0.36. The saturated water content of the soil has been found to be as high as 0.43. Thus the porosity through which the solute would appear to have been transported is significantly greater than the water content of the soil could possibly have been. This apparently anomalous result has been previously observed (e.g. Starr *et al.*, 1978; Butters *et al.*, 1989; Tillman *et al.* 1991) and is attributable to preferential flow.

The immediate perception of preferential flow is usually that it leads to early arrival of solute at some depth, whereas piston displacement would predict it to be still located somewhere above the depth at which it has been found. This is what happens when the solute is within that part of the soil's porosity where water is moving preferentially. However if the solute had moved into the part of the porosity which is being bypassed by the infiltrating water, preferential flow will lead to the solute arriving at a depth somewhat later than otherwise would be predicted.

As J_w was arbitrarily prescribed, rather than reflecting the actual drainage, the absolute value of the coefficients presented in Table 4.1 are not meaningful but are relevant only within this particular experiment.

Further down Table 4.1 are the D and v values found when the convective-dispersive TFM was calibrated using the data collected at greater depths. As depth increases, both D and v also increased. This increase in v could then be interpreted as a decrease in θ_{st} to 0.36 at both 550 mm and 760 mm, and a further decrease to 0.30 at 1000 mm depth. This would be despite θ being reasonably constant with depth, thus suggesting that there is no linkage between θ and θ_{st}.

Now for the pattern of the calibrated D parameters. Here there was also an increase with increasing depth. The dispersion increased more quickly than the velocity, so that the net effect upon the dispersivity is a rise from 10 mm, to 13 mm, 16 mm, and 15 mm at the respective measurement depths.

Obviously then, given these changes, good predictions of solute transport to depths greater than 250 mm will not arise from the CDE calibrated at 250 mm. Just how poor these predictions are is shown in Figure 4.1a. The centre of mass of the BTC's at the greater depths are over predicted.

From the dispersivity values obtained via the calibrated D and v parameters, it would appear that the soil is not transporting solute in a convective-dispersive manner, for this would require the dispersivity to remain constant. It would now be reasonable to investigate if the layering of the soil had affected solute transport, and also the possibility that the data are representative of stochastic-convective transport. However the varying v coefficient indicates that the centre of mass of the solute BTC is not progressing smoothly down the soil profile with increasing amounts of drainage. This excludes the possibility that a simple zero-time model ignoring layering could successfully predict the BTC's. Nor is it likely that the solute transport has remained constant within a layer, but varied in the different layers, as it is clear that the soil between the surface and 250 mm has quite different transport properties than the soil between the surface and 550 mm. Sandy loam soil is found between the surface and 500 mm deep, so the measurements at 550 mm are influenced only by 50 mm of fine sand soil, yet the parameters found to fit the 550 mm data are quite different to those fitting the 250 mm data. It would appear that solute transport is rather slow between the surface and 250 mm. However,

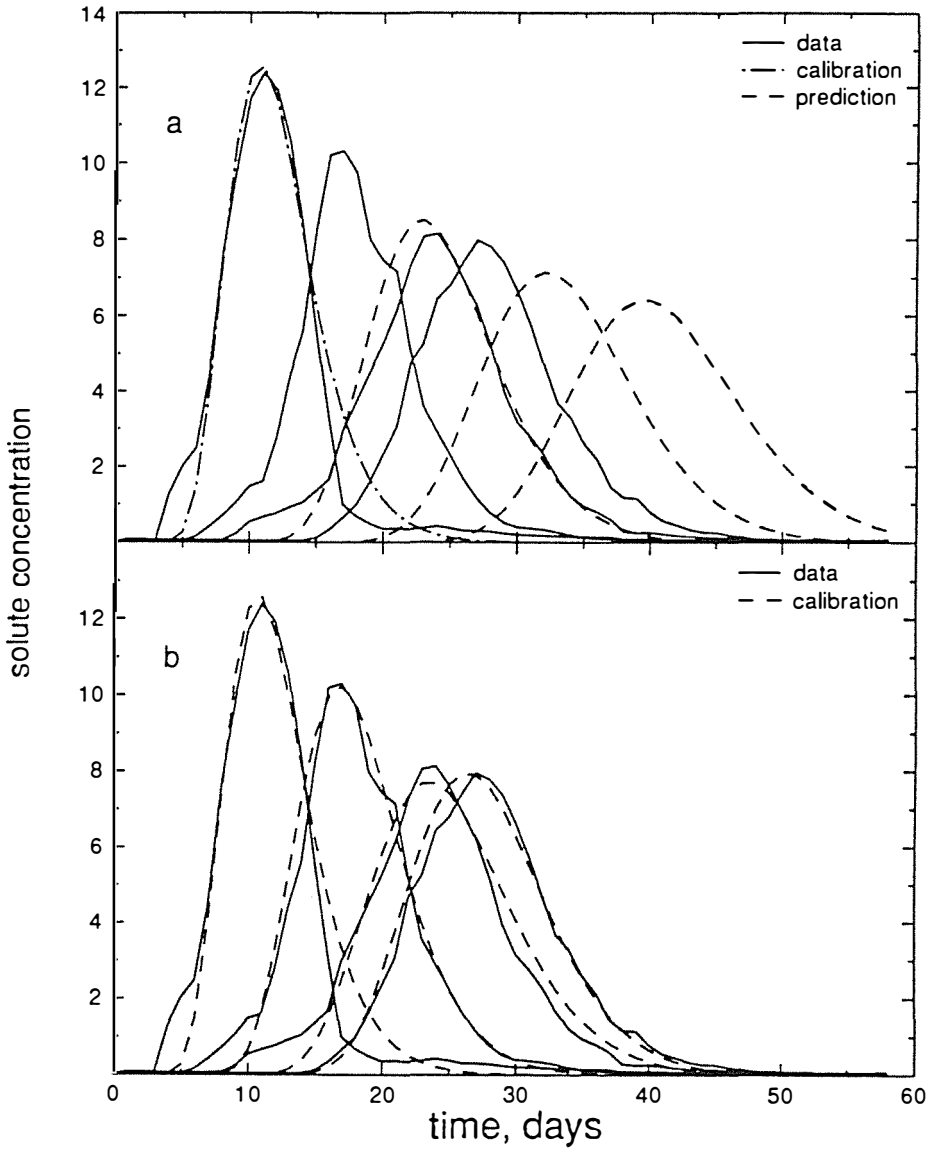

Figure 4.1 Data from the lysimeter and, a) a CDE calibrated to the 250 mm data and predicted at 550 mm, 760 mm, and 1000 mm, and b) a CDE calibrated at each depth.

below 250 mm the applied water seemed to become more effective at moving solute downward.

Consider both the structure of the surface soil and the water and solute input regime. Firstly, the structure of the soil was most highly developed in the top 250 mm, it was this zone through which the majority of pasture plant roots traverse.

Soil fauna will also be more active in the surface soil. Secondly, the intermittent water input will be at its most variable in the upper part of the soil. As depth increased the extremes in the water application regime will be smoothed by transit through the soil. If there is any place in this soil where the assumption that the transient water input cannot be successfully substituted for by an equivalent steady input, it would most likely be in this surface layer. Also this is where the soil might be considered to be most prone to preferential flow.

Additionally, it is not clear if the pulse input of solid fertiliser to the soil surface resulted in a pulse input to the mobile soil water. If some of the solute dissolved directly into the immobile water within soil aggregates, then slow diffusion into the mobile water would cause the slow and dispersed BTC seen at the 250 mm depth.

For these reasons solute transport may be different in the surface soil than in the rest of the soil. Therefore it may be inappropriate to include this part of the soil profile in a calibration intended to predict solute transport to greater depths in the soil.

It would thus appear that solute transport through the soil near the surface might be inappropriate for CDE calibration. Alternatively then the transfer function CDE could use the solute concentration data from 250 mm as the input data function. This is in place of the Dirac delta function that was assumed to apply at the soil surface. The data collected at 550 mm can then provide the solute concentrations necessary to calibrate the TFM form of the CDE.

For an analytical solution of the transfer function equation to be found, the input function must be one of a restricted group of functions. It was unlikely that the solute concentrations measured at 250 mm would conform closely to one of these functions and misrepresentation of the input data would add considerable error to the calibration. To obviate the requirement of the input function, the transfer function equation was fitted to the data in its integral form,

$$c(250+z,t) = \int_0^t c(250,t')\, f(z,t-t')\, dt' \quad . \qquad (4.13)$$

This allowed the data collected at 250 mm to be inserted directly into the equation.

Again the parameter fitting was carried out using the NAG routine E04FDF as described in Section 4.3. The necessary integrations were carried out numerically using the trapezoidal rule. Parameters of the Fickian pdf transfer function using the data measured at 250 mm as the input, and 500 mm, 760 mm or 1000 mm as the output concentrations are given in Table 4.2.

Table 4.2 Calibrated CDE parameters of the Fickian transfer function, and the dispersivity. These result from using the data measured at 250 mm in the lysimeter as the input function.

z (mm)	D ($mm^2\ day^{-1}$)	v ($mm\ day^{-1}$)	λ (mm)
550	720	37	19
760	850	38	22
1000	630	36	18

In contrast to the parameters of the Fickian pdf assuming a Dirac delta function at the surface (Table 4.1), here the D and v are remarkably constant with increasing depth. This is an indication that the soil may indeed be acting in a convective-dispersive manner, at least below the 250 mm depth.

It remained unclear what happened in the top 250 mm of soil, except that it was substantially different from what happened in the lower soil. This is the most 'disturbed' and biologically active zone, thus such failure is not surprising. However of note, is that the simple, but distinct, layering of the soil would appear to have no measurable effect on solute transport.

The average velocity was 37 mm day^{-1}. Then, using the assumed J_w of 10 mm day^{-1}, this yields an effective solute transport porosity, θ_{st} of 0.27. Measurements of average water content in the lysimeter to the depths of 200 mm and 500 mm, revealed that the water content between these two depths to be 0.39. Thus, the immobile water content, θ_{im} [L^3 L^{-3}], may be calculated from the CDE as 0.12.

An alternative method (Dyson *et al.*, 1990) of determining θ_{st} is to compute the mean I of the BTC each at 250 mm and 550 mm, and divide the difference between these two measures by the increment in depth, ie. 300 mm. This produced an estimate of θ_{st} of 0.17 and therefore of θ_{im} of 0.22. It was not at all clear why these two estimates of θ_{im} are so different. It was likely that the long tail of the 250 mm data, which is not seen a greater depths for the simple reason that measurements continued longer after the peak passed the 250 mm depth than at any other depth, has affected the calculation of the mean for 250 mm but not the means for the greater depths.

Excluding the tail of the 250 mm data from the calculation of the mean resulted in an estimate of 0.22 for θ_{st} and θ_{im} of 0.17. This highlighted the errors involved in any calculation, and indicated the care needed before submitting data to analysis.

When solute is not all contained within the moving phase of the soil water, then the use of the above methods to obtain θ_{im} are inappropriate. However, in the surface of the Manawatu fine sandy loam Tillman *et al.* (1991) estimated the immobile water content to be 0.18, and Clothier *et al.* (1992), using a direct measurement technique found, θ_{im} to be 0.20. Thus, assuming the estimates calculated from the mean to be the most reliable, these significant θ_{im} values corroborate our results. The slow transport seen here in the top 250 mm would appear to be a result of the solute moving from the immobile to the mobile water in the soil. There were two mechanisms by which solute could be moved to the immobile water upon application of the solid fertiliser. First the fertiliser granules may dissolve directly into the aggregates once in contact with the soil surface. This would be particularly true of the small crystals of laboratory-grade KBr used. Additionally the early small water applications could have encouraged solute to move into the aggregates via a

combination of mass flow and diffusion. Once within the aggregates this solute would become amenable to leaching only once it moved back into the mobile water.

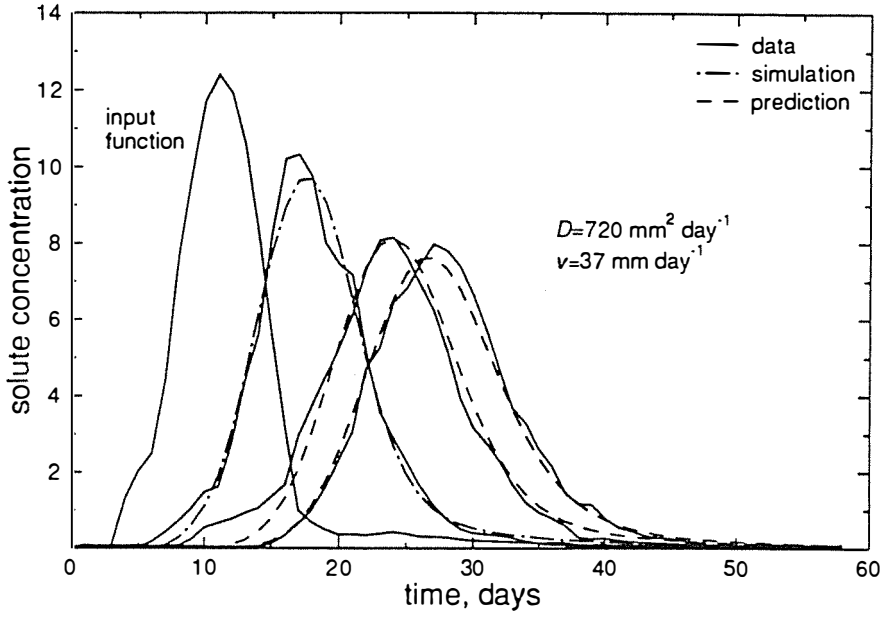

Figure 4.2 1990 lysimeter data and a CDE calibrated with the 250 mm data as the input and the 550 mm data as the output, as well as predictions to 760 mm and 1000 mm.

Predictions of solute transport to the greater depths of 760 mm and 1000 mm, but still using the 250 mm data as the input, may be made using the parameters determined from the fit obtained between the 250 mm and 550 mm data. These predictions are shown in Figure 4.2. Not surprisingly, an excellent rendition of the data is obtained. All indications are then that the soil in the lysimeter, under the boundary conditions imposed during the 1990 experiment, transported solute in accordance with the convection-dispersion equation.

Now, having found a scheme to predict successfully solute transport in the lysimeter, this will be applied to the data collected in the field during 1988.

4.5 APPLICATION OF THE CDE TO THE 1988 FIELD DATA

The successful CDE analysis applied to data of solute transport from the 1990 lysimeter experiment will now be applied to the data collected during the 1988 field experiment.

Table 4.3 contains data analogous to that in Tables 4.1 and 4.2, but here presented for the 1988 data. The second and third columns give fitted D and v using a Dirac delta function as the input, while the last two columns are for the fitted equation using the 250 mm data as the input. In both cases the equation (4.8) has been fitted individually to the BTC's and the parameters reported are the averages.

Table 4.3 CDE parameters fitted to the 1988 field data with either a Dirac delta function at the soil surface or the data measured at 250 mm as the input function.

Output depth, (mm)	Input, Dirac delta function at z=0 mm.				Input, data measured at 250 mm.			
	D (se) (mm^2 day^{-1})		v (se) (mm day^{-1})		D (se) (mm^2 day^{-1})		v (se) (mm day^{-1})	
250	1090	(170)	8	(0.5)				
550	2130	(310)	18	(1)	2170	(1540)	83	(14)
760	900	(100)	18	(1)	1050	(340)	26	(3)
1000	1380	(220)	18	(1)	2050	(840)	26	(3)

Table 4.3 reveals a different pattern in the 1988 field data to that seen in the 1990 lysimeter experiment. Examining first the v coefficients resulting from the Dirac delta function input, it is again the data collected at 250 mm that are anomalous. The v coefficient is uniformly 18 mm day^{-1} except at 250 mm where it is less than half that at the greater depths. It cannot be simply that the 250 mm samplers were not adequately sampling the actively moving solute, as the mass balance of solute was correct. By examination of the v resulting from the Dirac delta input it was also clear that these data could not be explained by solute moving initially into some immobile porosity then moving slowly back into the mobile water. Improved

understanding of the solute input and the nature of the samples collected by porous cups, and how they might be affected by soil structure and the water regime, may aid the interpretation of this data. From Table 4.3 it is however clear that calibration of the CDE assuming a Dirac delta input at the soil surface to the 550 mm data would lead to good predictions of the centre of mass of the 760 mm and 1000 mm data.

Whereas in the lysimeter data calibration of the CDE using the 250 mm data as the input function resulted in D remaining constant with depth, the estimates of the field data show no such trends. If velocity is constant with depth then there is no mechanistic explanation of a decrease in the dispersion coefficient. The large uncertainty on all the estimates of D, is such that a constant D with depth would not be inappropriate.

Given current understanding, from the above it would appear that these field data can not be modelled using the CDE model. Nor probably will any other model succeed as there are currently no models which would deal with decreasing D. Indeed it is unlikely that these data are a true reflection of the spreading of solute in the field soil. Probably solute transport is itself so variable that 20 samples at a given depth are inadequate. Spatial variability of the irrigation probably also was important.

4.6 CONCLUSIONS

The convection-dispersion model was applied first to the data collected in the lysimeter during 1990, then to the field data collected in 1988.

Modelling the lysimeter data was successful provided that the surface soil was not included in the calibration. Solute transport process in the surface soil appeared different to that below. This may result from either the nature of the solute input or from the water flow regime. The changes in soil texture and structure with depth, apart from the surface soil, appeared to have no effect on solute transport.

The modelling strategy developed to deal with the lysimeter data was not successful when applied to the field data. With the exception of the 250 mm data, the v parameters made sense within our current understanding of solute transport. The pattern of the fitted D parameter was however inexplicable. The most likely reason for this was the highly variable nature of solute transport and water application in this soil.

Although the application of a process-based model to the data has increased our understanding of the factors affecting solute transport in the lysimeter, it has left many questions regarding the field data unanswered. In an effort to discover more of solute transport in the field, next a non-mechanistic model will be used. This model, presented in Chapter Five, subdivides θ_{st} into convective and dispersive components, and also into non-interacting flow paths. Such delineation of θ_{st} may reveal more of solute transport and perhaps the nature of solute transport variability.

Chapter Five

THE AGGREGATED MIXING ZONE MODEL

5.1 INTRODUCTION

One could imagine that the flow of chemical through soil may mimic solute transport through a network of tanks. This was the basis of Beven and Young's (1988) Aggregated Mixing Zone (AMZ) model which described the transport properties of soil as analogous to a network of delayed-input, continuously-stirred tanks. Beven and Young (1988), and later Hornberger *et al.* (1990) examined the model only under calibration conditions, which established the model's descriptive ability. The data described in Chapter Three are sufficient to test further the model's performance as a predictive, as well as descriptive, tool.

The Beven and Young (1988) model arose from earlier work on solute transport in streams by Beer and Young (1983). Beven and Young (1988) used data from soil cores leached in the laboratory under steady flow to parameterise the AMZ model. Although Beven and Young (1988) used the AMZ model in a descriptive manner only, it was able to represent solute transport regimes which resulted in breakthrough curves (BTC's) with high, early peaks and long tails, as well as multi-modal curves. Solute leaching patterns such as these are not readily modelled using the traditional convection-dispersion equation approach.

Hornberger *et al.* (1990) further tested the AMZ model, applying it to data from undisturbed lysimeters in a forested catchment. In this experiment, three lysimeters were leached of pulse applications of bromide under steady water flux at three different intensities of water input. As in the paper by Beven and Young (1988) however, Hornberger *et al.* (1990) used the AMZ in a descriptive manner only, as already indicated. Beer and Young (1983) also based their model on steady flow (in a stream rather than in a soil), however the model was used predictively.

In this chapter the concept of solute flow through a network of tanks as a model for solute transport in soil is developed in some detail. Unsteady water flow is considered, and the model is used both descriptively and predictively. First, in Section 5.2.1, the theory of solute transport through a single tank is presented and

the governing equation is then manipulated into a particular form. Following this is a sub-section describing the extension of solute transport through a single tank to that through a network of tanks. Next, in Section 5.2.3, the rather unusual method that is used to parameterise the AMZ model is elaborated. That sub-section is followed by the method by which predictions of solute transport at depths greater than the calibration are made. Prior to investigation of the utility of the AMZ model using the data both from the field and the lysimeter (Section 5.5), is a section outlining the effect of changing the parameters of the AMZ model on simulated output solute concentration. Although those with a chemical engineering background are likely to be *au fait* with the concepts described, to most soil scientists they will be quite novel. A summary indicating the strengths and weaknesses of the model and a promising direction for the model concludes the chapter.

The significant advances to the pre-existing AMZ model theory which are presented in this chapter are:

- Reformulation of the model to express solute transport with respect to cumulative drainage rather than time.
- Inclusion of the possibility that water may flow preferentially through one of a number of pathways.
- The factorisation of the auto-regressive moving-average equation to form the AMZ model is described in some detail and the conditions where this factorisation is not possible derived.
- Tanks allowing convective transport only are included in the model.

5.2 THE AMZ MODEL

5.2.1 Solute transport through a single tank

A continuously-stirred tank is considered a vessel with some fixed volume, V_m [L^3]. It has both input and output flows (see Figure 5.1). Solute entering V_m through the input flow is assumed to become instantaneously and completely mixed with the liquid in the tank. For this reason, V_m will be referred to as the mixed volume.

Consequently, the concentration of solute measured in the output flow is equal to the solute concentration in the mixed volume.

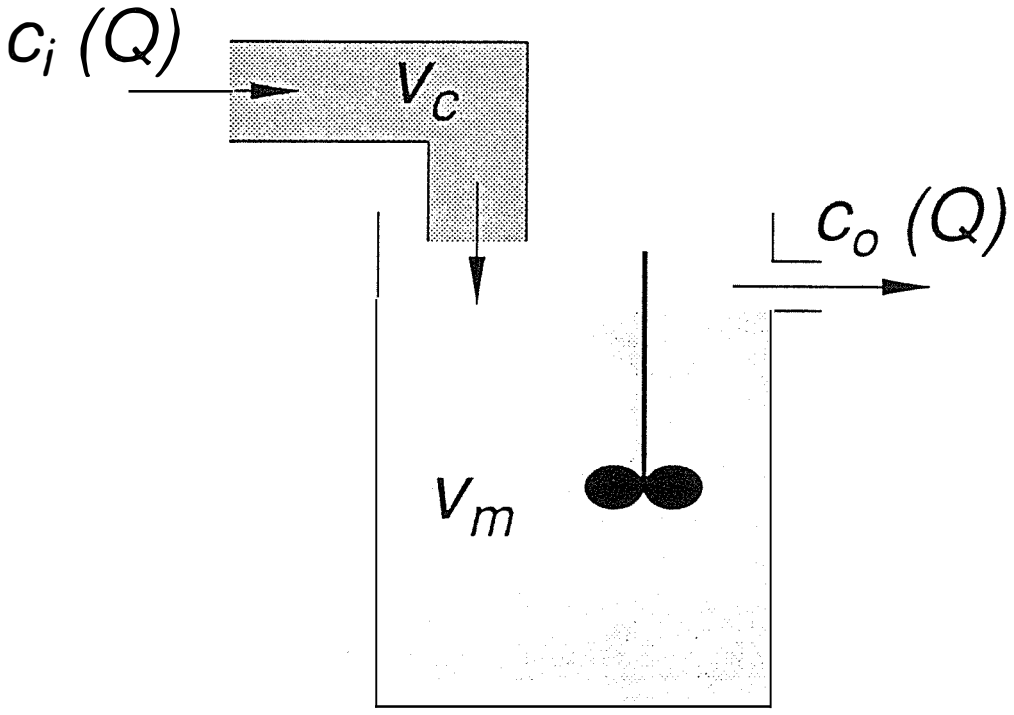

Figure 5.1 A continuously-stirred tank, showing the convective volume, V_c, and the mixed volume, V_m.

In the current application, the input and output flow-rates are not necessarily constant in time. However the requirement of fixed volume necessitates that cumulative output of liquid equals cumulative input. The output, or drainage, may be considered as resulting from an overflow pipe, as is represented in Figure 5.1.

Solute added to a tank does not immediately appear in the mixed volume, but must first travel through some entrance volume, V_c [L^3]. Within this entrance volume, dispersion-free transport (or plug flow) is assumed to occur, so V_c is referred to as the convective volume.

The average length of time, or amount of drainage, required to transport a 'parcel' of solute from the input point to the output is determined by the total volume of the tank. But dispersion of solute from a single tank is caused by the mixed volume only. The total volume of the tank, V_t [L^3], is the sum of V_c and V_m.

In contrast to the model presented by Beven and Young (1988), here the independent variable for solute transport through the tank is Q [L^3], namely the cumulative amount of drainage from the tank. Thus the first step in deriving an equation for solute transport through such a tank is to describe the mass balance of solute.

Within a drainage interval ΔQ, the mass balance of solute in the tank demands that the change in the mass of solute in the tank be equal to the mass of solute added in the input stream minus the mass of solute removed from the tank in the output,

$$\Delta \left(V_m c_o(Q) \right) = \Delta Q \left(\overline{c_i}(Q - V_c) - \overline{c_o}(Q) \right) \quad . \tag{5.1}$$

Here c_o and c_i [$M\ L^{-3}$] are the output and input solute concentrations respectively. Solute entering the tank must first be subjected to a drainage of volume V_c in order for the solute to enter V_m, and so appear instantaneously in the output stream. Thus, c_i is subject to a delay of V_c in the mass balance equation. The overbars on the solute concentration symbols represent the fact that the average concentration during ΔQ should be taken. When equation (5.1) is divided by ΔQ, and in the limit taken as $\Delta Q \rightarrow 0$, a differential equation describing the mass balance in the tank is formulated such that,

$$V_m \frac{d\, c_o(Q)}{d\, Q} = c_i(Q - V_c) - c_o(Q) \quad . \tag{5.2}$$

Equation (5.2) may now be solved (see Appendix A), resulting in,

$$c_o(Q) = c_o(0)\, e^{-\frac{Q}{V_m}} + \frac{1}{V_m} e^{-\frac{Q}{V_m}} \int_0^Q e^{\frac{Q'}{V_m}} c_i(Q' - V_c)\, dQ' \quad . \tag{5.3}$$

The prime on the variable Q indicates a dummy variable of integration.

Qualitatively it may be seen that in response to an impulse solute input, the output solute concentration, c_o, will rise sharply after a drainage delay of V_c. For a given amount of solute added in the pulse, both the magnitude of the rise in c_o and the rate at which c_o will fall to the antecedent level is determined by V_m.

At this point, Beven and Young (1988) reformulated equation (5.3) into a discrete form. They argued that in doing so advantage could be taken of the methods developed for model identification and calibration for time-series models. This discretisation may be carried out if the input concentration is assumed constant over each cumulative drainage interval, ΔQ, and equation (5.3) is applied over the interval $j\Delta Q \leq Q < (j+1)\Delta Q$, where j is here the number of intervals of ΔQ. With these assumptions it is possible to represent the solution of equation (5.3) in the following discrete form,

$$c_o([j+1]\,\Delta Q) = c_o(j\,\Delta Q)\, e^{-\frac{\Delta Q}{V_m}} + \left(1 - e^{-\frac{\Delta Q}{V_m}}\right) c_i([j+1]\,\Delta Q - V_c) \quad . \tag{5.4}$$

The derivation of equation (5.4) from equation (5.3) is given in Appendix B.

If j is re-defined as $\langle [j+1]\Delta Q \rangle$, and k as $\langle V_c / \Delta Q \rangle$, where $\langle\rangle$ stands for the nearest integer, then equation (5.4) may be written as

$$c_o(j) = e^{-\frac{\Delta Q}{V_m}} c_o(j-1) + \left(1 - e^{-\frac{\Delta Q}{V_m}}\right) c_i(j-k) \quad . \tag{5.5}$$

Employing the backward difference, or delay, operator, q^{-1}, defined by,

$$q^{-1} c_o(j) = c_o(j-1) \quad , \tag{5.6}$$

equation (5.5) may be rewritten as discrete transfer function equation,

$$c_o(j) = \frac{1 - e^{-\frac{\Delta Q}{V_m}}}{1 - \left(e^{-\frac{\Delta Q}{V_m}} q^{-1}\right)} c_i(j-k) \quad , \tag{5.7}$$

or,

$$c_o(j) = \frac{\left(1 - e^{-\frac{\Delta Q}{V_m}}\right) q^{-k}}{1 - \left(e^{-\frac{\Delta Q}{V_m}} q^{-1}\right)} \; c_i(j) \quad . \tag{5.8}$$

Equation (5.8) is analogous to equation 6 of Beven and Young (1988), except that it is here expressed with Q, rather than time, as the independent variable. Now the output solute concentration resulting from any form of solute input can be described.

5.2.2 Solute transport through a network of tanks

The equation developed for solute transport through a single tank must now be extended to encompass the network of tanks required for the AMZ model. Certain restrictions must be placed on the spatial arrangement of the tanks within the network. The tanks may be arranged either in series, or in parallel. A series of tanks will be referred to as a pathway. Thus a network with two parallel series of tanks would have two solute transport pathways which act concurrently.

Water is separated into the solute transport pathways at the proximal end of the network. Subsequently it cannot cross between pathways. In Figure 5.2 a diagrammatic representation of this is given for a network with two pathways; one series with 2 tanks and the second with 1 tank. The meaning of the symbols will shortly be explained. Each tank is represented as a rectangle, with the dashed lines indicating the boundaries across which water may move. A solid line represents a barrier to water flow.

Within a given pathway, the output of solute and water from one tank becomes the input to the next. So the equation for a single series of n tanks is,

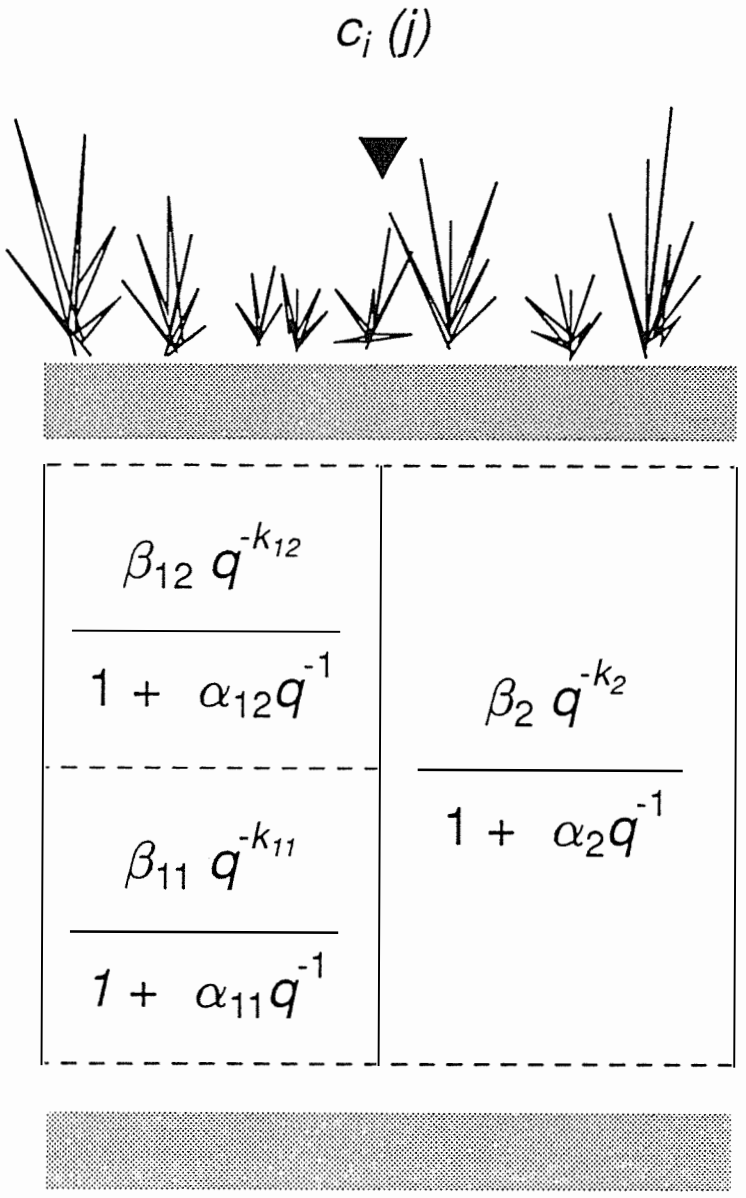

$$c_o(j) = \left[\left(\frac{\beta_{11}\, q^{-k_{11}}}{1 + \alpha_{11}\, q^{-1}}\right) \times \left(\frac{\beta_{12}\, q^{-k_{12}}}{1 + \alpha_{12}\, q^{-1}}\right) + \left(\frac{\beta_2\, q^{-k_2}}{1 + \alpha_2\, q^{-1}}\right)\right] c_i(j)$$

Figure 5.2 A diagrammatic representation of the AMZ model for two solute transport pathways, one pathway with two tanks, the other with one tank.

$$c_o(j) = c_i(j) \left[\prod_{l=1}^{n} \left(\frac{\left(1 - e^{-\frac{\Delta Q}{V_{m_l}}}\right) q^{-\left\langle \frac{V_{c_l}}{\Delta Q} \right\rangle}}{1 - \left(e^{-\frac{\Delta Q}{V_{m_l}}} q^{-1}\right)} \right) \right] . \quad (5.9)$$

The symbol Π stands for the multiplicative product of the terms for the single tanks, and l is a dummy variable of multiplication. Solute output from the pathways is combined upon exit from the distal end of the network. Thus the general equation for the AMZ model at the distal end of the network may be found by summing across all pathways. Equation (5.9) is now extended to encompass x parallel pathways, where each pathway itself comprises n tanks in each pathway,

$$c_o(j) = c_i(j) \sum_{i=1}^{x} \left[\prod_{l=1}^{n} \left(\frac{\left(x_i \prod_{l=1}^{n} \left(1 - e^{-\frac{x_i \Delta Q}{V_{m_{li}}}}\right)\right)^{\frac{1}{n_i}} q^{-\left\langle \frac{V_{c_{li}}}{x_i \Delta Q} \right\rangle}}{1 - e^{-\frac{x_i \Delta Q}{V_{m_{li}}}} q^{-1}} \right) \right] . \quad (5.10)$$

Here i is the dummy variable of summation and x_i is the proportion of water flowing down the i^{th} pathway. This may be written more concisely as,

$$c_o(j) = c_i(j) \sum_{i=1}^{x} \left[\prod_{l=1}^{n} \left(\frac{\beta_{li} q^{-k_{li}}}{1 + \alpha_{li} q^{-1}} \right) \right] , \quad (5.11)$$

by defining

$$\alpha_{li} = -e^{-\frac{x_i \Delta Q}{V_{m_{li}}}} , \quad (5.12)$$

$$\beta_{li} = \left(x_i \prod_{l=1}^{n} (1 + \alpha_{li}) \right)^{\frac{1}{n_i}} , \quad (5.13)$$

and,

$$k_{li} = \left\langle \frac{V_{c_{li}}}{x_i \Delta Q} \right\rangle \quad . \tag{5.14}$$

Note that

$$\sum_{i=1}^{x} x_i = 1 \quad . \tag{5.15}$$

The differences between equations (5.9) and (5.10) are simply those necessary to enforce mass balance in a multi-pathway network.

5.2.3 Model structure identification and parameterisation

The AMZ described thus far is not radically different from existing models of solute transport. For example, there is a similarity between the layer models described by Addiscott and Wagenet (1985) and the concept of using a series of tanks to describe solute movement in soils. There are even greater similarities between the AMZ model and the Transfer Function Model. But there is a unique method by which the AMZ model structure, and the values of the parameters, are determined.

In common with the models developed for solute transport in streams (eg. Beer and Young, 1983; Wallis *et al.*, 1989), Beven and Young (1988) use an auto-regressive, moving-average (ARMA) equation to determine the AMZ model. It is this ARMA equation that is fitted to the data, rather than fitting equation (5.10) directly.

The structure of the AMZ model is determined by the values of n_1 to n_x. The determination of this structure is to a certain extent separated from the process of finding values of the α and k parameters. It is these parameters that eventually give rise to the more physically-meaningful volume parameters. Both however are derived from an ARMA equation identified from measured input and output solute concentrations at some calibration depth. Note from equation (5.13) the value of the β parameters are determined completely by the α's.

The equation fitted to the data has the general form of an ARMA,

$$Ac_o(j) = B c_i(j-n_k) + e(j) \quad , \tag{5.16}$$

where

$$A = 1 + a_1 q^{-1} + \ldots + a_{n_a} q^{-n_a} \quad , \tag{5.17}$$

$$B = b_1 + b_2 q^{-1} + \ldots + b_{n_b} q^{-n_b+1} \quad , \tag{5.18}$$

and where n_k is the delay from the input to the output, and e is a term representing the combined effects of modelling error, plus other stochastic and non-linear phenomena.

Equation (5.16) is fitted to data, thereby testing various combinations of n_a, n_b, and n_k. Once the ARMA equation structure which best describes the observed solute transport behaviour has been determined, equation (5.16) is factorised to find the values of the parameters of the AMZ model in equation (5.11). An example of this process is now given.

If equation (5.16) was fitted to the data with the structure n_a=3, n_b=3, and n_k=4, the resulting ARMA equation would be of the form,

$$c_o(j) = \frac{b_1 + b_2 q^{-1} + b_3 q^{-2}}{1 + a_1 q^{-1} + a_2 q^{-2} + a_3 q^{-3}} \; c_i(j-4) \quad . \tag{5.19}$$

From here for brevity, the error term will be omitted from the equation. If the values x=2, k_{11}=1, k_{12}=3, k_2=4, n_1=2, and n_2=1 (corresponding to the structure shown in Figure 5.2) are inserted into equation (5.11) the resulting equation is,

$$c_o(j) = \left[\left(\frac{\beta_{11} q^{-k_{11}}}{1 + \alpha_{11} q^{-1}} \right) \left(\frac{\beta_{12} q^{-k_{12}}}{1 + \alpha_{12} q^{-1}} \right) + \left(\frac{\beta_2 q^{-k_2}}{1 + \alpha_2 q^{-1}} \right) \right] c_i(j) \tag{5.20}$$

This particular AMZ model may be rearranged so that,

$$c_o(j) = \left[\frac{(\beta_{11}\beta_{12}+\beta_2)+(\alpha_2\beta_{11}\beta_{12}+(\alpha_{11}+\alpha_{12})\beta_2)q^{-1}+(\alpha_{11}\alpha_{12}\beta_2)q^{-2}}{1+(\alpha_{11}+\alpha_{12}\alpha_2)q^{-1}+((\alpha_{11}\alpha_{12})+\alpha_2(\alpha_{11}+\alpha_{12}))q^{-2}+(\alpha_{11}\alpha_{12}\alpha_2)q^{-3}} \right] c_i(j-4) \quad . \tag{5.21}$$

By comparing the ARMA of equation (5.19) with the AMZ model in equation (5.21), it may be deduced that, $a_1=\alpha_{11}+\alpha_{12}+\alpha_2$, $a_2=(\alpha_{11}\alpha_{12})+(\alpha_2(\alpha_{11}+\alpha_{12}))$, $a_3=\alpha_{11}\alpha_{12}\alpha_2$, $b_1=\beta_{11}\beta_{12}+\beta_2$, $b_2=\alpha_2\beta_{11}\beta_{12}+\beta_2(\alpha_{11}+\alpha_{12})$, and $b_3=\alpha_{11}\alpha_{12}\beta_2$. Appropriate equations are chosen from those above in order that the values of α_{11}, α_{12}, α_2, β_{11}, β_{12}, and β_2 may be found.

At this point the relationship between the α's and β's needs to be checked to confirm that equation (5.13) is satisfied. If this relationship does not hold, even approximately, then alternative AMZ structures should be considered. For example, an AMZ model structure of three pathways each of a single tank would also form an ARMA equation equivalent in order to that in equation (5.19).

Continuing to use the above example to demonstrate the general procedure, the structure of the AMZ model has now been revealed. In this case two parallel series, the first with two tanks, and the second with one. Of more interest to soil scientists will be the various volumes associated with the α and k parameters. If the structure concerned had that of a single pathway, then $x_1=1$. The parameters, V_c and V_m, would then be easily obtained from equations (5.12) and (5.14). For a multi-pathway structure, determination of these volumes is more difficult.

Again using the example in equation (5.20), there are eight parameters to be determined, V_c and V_m for each of the three tanks, as well as x_i for each of the two pathways, so eight equations are required. Six equations are provided by the application of equations (5.12) and (5.14) to each of the tanks. A further equation parameter may be determined by equation (5.15). The last equation can be extracted from the matching of the parameters from equation (5.19) to equation (5.21). In this example, the a_3 parameter is probably the simplest to use. Here

$$a_3 = \alpha_{11}\alpha_{12}\alpha_2 \quad ,$$

$$= \left(-e^{-\frac{x_1\Delta Q}{V_{m11}}}\right)\left(-e^{-\frac{x_1\Delta Q}{V_{m12}}}\right)\left(-e^{-\frac{2x_2\Delta Q}{V_{m2}}}\right) \quad , \qquad (5.22)$$

$$\text{so,} \quad \ln(-a_3) = \frac{-x_1\Delta Q}{V_{m_{11}}} - \frac{x_1\Delta Q}{V_{m_{12}}} - \frac{x_2\Delta Q}{V_{m_2}} \quad .$$

Thus there are eight equations which once solved will determine the convective and mixed volumes of each pathway, as well as the proportional diversion of the water.

It should however be noted that not every ARMA equation can be factorised. For an ARMA equation to be fully factorisable two conditions must be met. Firstly the relationship between n_a and n_b must be such that the ARMA equation (5.16) can be rearranged into a form which can be matched to the AMZ model equation (5.11). If this requirement is met then the model is be said to be structurally factorisable.

Next, if the V_c, V_m, and x_i parameters can be determined, and are revealed to be physically sensible, that is both real and positive, then the model will be said to be algebraically factorisable.

The structure of the ARMA equation provides some information about the structure of the network of tanks. If $n_b=1$ then there can be only one pathway; the number of tanks in the single series is equal to n_a.

If $n_b>1$ then the situation becomes somewhat more complex. However, certain relationships can be gleaned from the order of the ARMA equation. If for all tanks $V_m>0$ then the total number of tanks is again equal to n_a. From here however the tanks could be arranged in several ways.

Appendix C shows that, if the ARMA can be structurally factorised then,

$$n_b \geq n_a + 1 - \min[n_i] \quad , \tag{5.23}$$

where $\min[n_i]$ is the smallest number of tanks in any pathway of the AMZ model. The relationship in inequality (5.23) is a direct algebraic consequence of the addition of the fractions in equation (5.11). From inequality (5.23), it follows that if n_b is greater than 1, for the ARMA to be structurally factorisable,

$$n_b \geq \frac{2n_a + 3}{3} \quad . \tag{5.24}$$

The derivation of inequality (5.24) is also given in Appendix C.

If a solute transport pathway exists where solute is transported by plug flow only, then for that tank $V_m=0$. In the above discussion it was stated that the total number of tanks in the AMZ model would equal n_a. Strictly this should have been stated as n_a equalling the total number of tanks with $V_m>0$. In this case, the relationships detailed in inequalities (5.23) and (5.24) are still valid. Thus the possibility of dispersion-free pathways should be considered when factorising ARMA equations. Indeed ARMA equations of the order $n_b>n_a$ can only be factorised with the inclusion of (n_b-n_a) parallel, dispersion-free tanks.

If inequality (5.24) is not satisfied then the ARMA cannot be factorised. Therefore no AMZ model can be formulated from that ARMA equation. It is the AMZ model which provides information about the transport volume, and as will be described in the following section, it provides a basis upon which to make predictions about solute transport. The ARMA equation can of course be used to simulate outflow solute concentrations at the calibration depth resulting from input functions different to that of the calibration.

If inequality (5.24) is fulfilled, then the smallest number of tanks in any pathway may be found using inequality (5.23). Provided $V_m>0$, the total number of tanks is given by n_a, therefore variants on the possible arrangements of the remaining tanks are limited.

For example, consider an ARMA equation with $n_a=7$ and $n_b=5$. This model satisfies inequalities (5.24), and (5.23) reveals the minimum number of tanks in any series to be three. Thus there are four tanks remaining. As the minimum number of tanks in a series must be three, these remaining four tanks can only be arranged in a single series of four. Therefore the AMZ model would have a structure involving two pathways, one with three tanks and another with four tanks. The possibility of a further tank with $V_m=0$ can be ruled out as this structure, although leaving $n_a=7$, would raise n_b to a value of at least six.

At this point, if the ARMA has been revealed to be structurally factorisable, it then remains to evaluate the parameters in the AMZ equation. This parameter estimation involves the solution of a set of simultaneous equations which will usually be over-determined. (See for example the paragraph after equation 5.21) If a model is algebraically factorisable then these equations can simply be solved for the unique estimates of each of the parameters in equation (5.11).

Models which are structurally, but not algebraically factorisable will yield estimates of the α parameters which either are significantly different, or yield parameter estimates which are physically impossible. These might for example include values outside the range $-1 \leq \alpha \leq 0$ which would result in negative volume estimates, or imaginary numbers. This point will be addressed further in Section 5.5.

Often more than one AMZ model structure could be conceived that would match a particular ARMA equation. In this case the success of the algebraic factorisation should be considered a test of the appropriate AMZ model structure for the ARMA equation under test.

Figure 5.3 summarises the steps necessary to find an AMZ model.

5.2.4 Prediction of solute transport through a network of tanks

Predictions of solute transport to network distances other than the calibration distance can be made by scaling the number of tanks in each series appropriately.

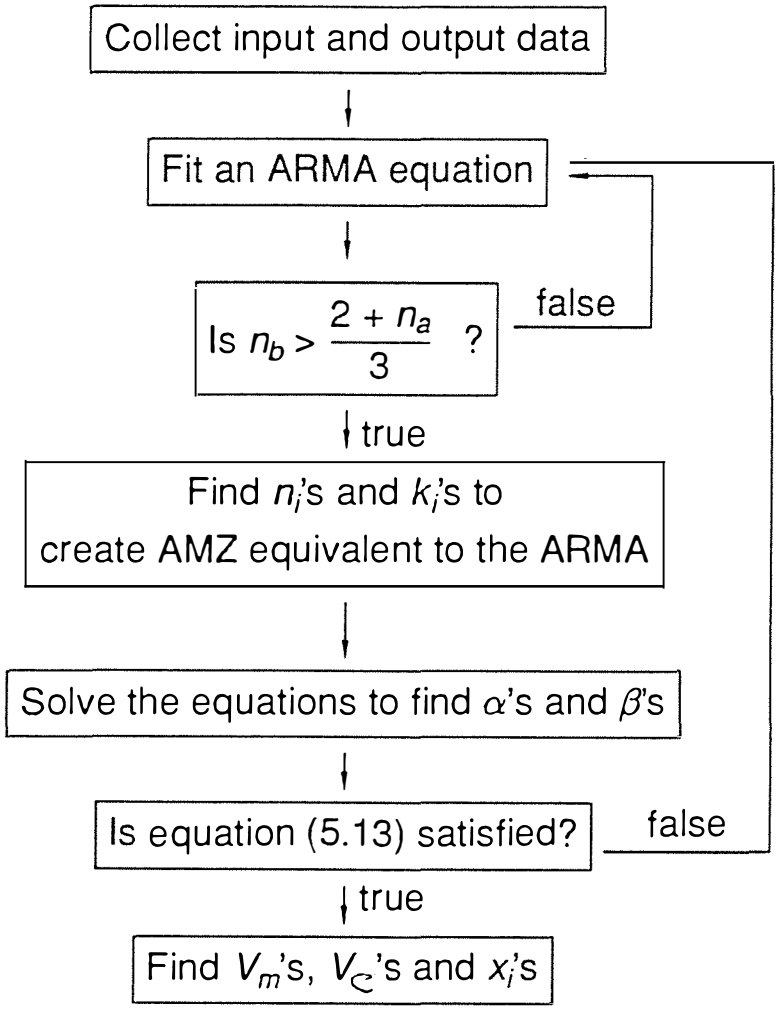

Figure 5.3 Flow chart showing the AMZ modelling process.

Let n_i^z be the number of elements in the i^{th} series in the prediction to distance z. It is given by,

$$n_i^z = \left\langle \frac{z}{Z} n_i \right\rangle \quad , \tag{5.25}$$

where Z is the calibration depth and z is the prediction depth. The number of elements, n_i^z, is rounded to the nearest integer because part-tanks cannot be considered.

A further consideration to that presented in equation (5.25) is that where tanks within a pathway are not all the same, the prediction must reflect the same mix of tanks as was in the calibration. This will usually mean that predictions can only be made at multiples of the distance between the input and output data. If however tanks within a series are equal, predictions can be made wherever equation (5.25) is appropriate.

5.3 AMZ MODEL PARAMETERISATION

All data manipulation, model fitting, simulation, and prediction was carried out using the software package MATLAB's System Identification Toolbox. Equation (5.16) was fitted to the data using the routine PEM. The general form of the equation fitted by PEM is,

$$A\, c_o(j) \;=\; \frac{B}{F}\, c_i(j-n_k) \;+\; \frac{C}{D}\, e(j) \quad , \tag{5.26}$$

where F, C, and D are defined in a similar manner to A (see equation 5.17). If n_c, n_d, and n_f are set equal to 0, then C, D, and F become 1 and equation (5.26) reduces to equation (5.16).

The model required data be supplied at constant intervals of the independent variable; in this case, Q. The data presented in Chapter Three were however collected at irregular intervals of Q. To overcome this all data were linearly interpolated at constant intervals of Q. The routine PEM was supplied with two matrices; one contained interpolated output and input solute concentration data, and the second contained various combinations of the orders of the polynomials A, B, C, D, and F, and the value of n_k. This defined the order of the ARMA equation to be tested against the data.

The output from PEM was also in the form of a matrix. This matrix contains encoded information about the form of the model fitted to the data, the parameters and their standard deviations, as well as a measure of the goodness-of-fit. The measure of goodness-of-fit supplied by the PEM routine is the sums-of-squares

based Akaike's Final Prediction Error (AFPE, see Ljung, 1988). In common with the Error Variance Norm (EVN) used by Beven and Young (1988) and Hornberger *et al.* (1990), the AFPE contains an adjustment prejudicing against models with a large number of parameters.

In order to create simulated output from an input and an AMZ model, the following procedure was carried out. The AMZ model was multiplied out to form its equivalent ARMA equation. The ARMA equation a and b parameters were entered into two matrices, and then the routine POLY2TH used to create an encoded matrix of the same form as the output from PEM. When the routine IDSIM was supplied with that encoded matrix and input solute concentration data, simulated output solute concentrations were created.

When supplied with calibration data, the result of IDSIM will be referred to as a *simulation*. When the input supplied is different to that used to parameterise the model then the results will be referred to as a *prediction*.

Detailed descriptions of the above mentioned routines may be obtained from Ljung (1987) and Ljung (1988).

5.4 SIMULATING THE EFFECT OF VARYING MODEL STRUCTURE AND PARAMETERS

Demonstrated in the following sections will be the effect of the different transport parameters of the AMZ model on the output concentration of solute. Although these sections may not provide much enlightenment for those with an engineering background, for soil scientists to whom stirred tank theory may be new, these sections will be useful. For a standard text on the subject, refer to Coulson and Richardson (1978).

Examples in this section will be only with equal tanks within a pathway. Inclusion of unequal tanks would considerably add to the notational complexity, but add little

the understanding. Where the possibility of unequal tanks in a pathway would significantly change the observed patterns in these examples, this will be noted.

Here the AMZ models will be identified by a code comprising either three or six numbers. The first three numbers will identify n, V_c, and V_m for the first solute transport pathway. If there is a second solute transport pathway then a further three numbers will be supplied. This may be regarded as an expanded form of the description given in the previous section. Taking as an example the third line in Figure 5.7, the particular model is specified as (1 0.02 0.03, 2 0.03 0.015). This particular line was created using an AMZ model with two solute transport pathways. The first pathway consisted of one tank with convective and mixed volumes of 0.02 m^3 and 0.03 m^3, while the second pathway had two tanks with convective and mixed volumes of 0.03 m^3 and 0.015 m^3 respectively.

Unless otherwise stated, the input function for all the models demonstrated in the following sections was a pulse input of 100 g m^{-3} of solute in 0.01 m^3 of water.

5.4.1 Effect of varying V_c and V_m in a single tank

First let us examine the effect of varying the convective and mixed volumes of a single tank on outflow solute concentration.

The solid line in Figure 5.4 shows the output solute concentration resulting from an impulse input of solute to a single tank with V_c of 0.02 m^3 and V_m of 0.03 m^3. The dashed line shows a similar model but with a higher convective volume of 0.04 m^3. The effect of the increase in V_c is simply to increase the amount of water which must pass through the system before the solute is first observed in the output stream. The solute concentration at the peak, and the rate of decline from the peak are identical in both cases.

A change in the mixed volume of a tank will however influence both the maximum solute concentration, and the rate and shape of fall from the peak. The effect of increasing V_m can be seen in Figure 5.4 by comparing the solid and the dotted lines.

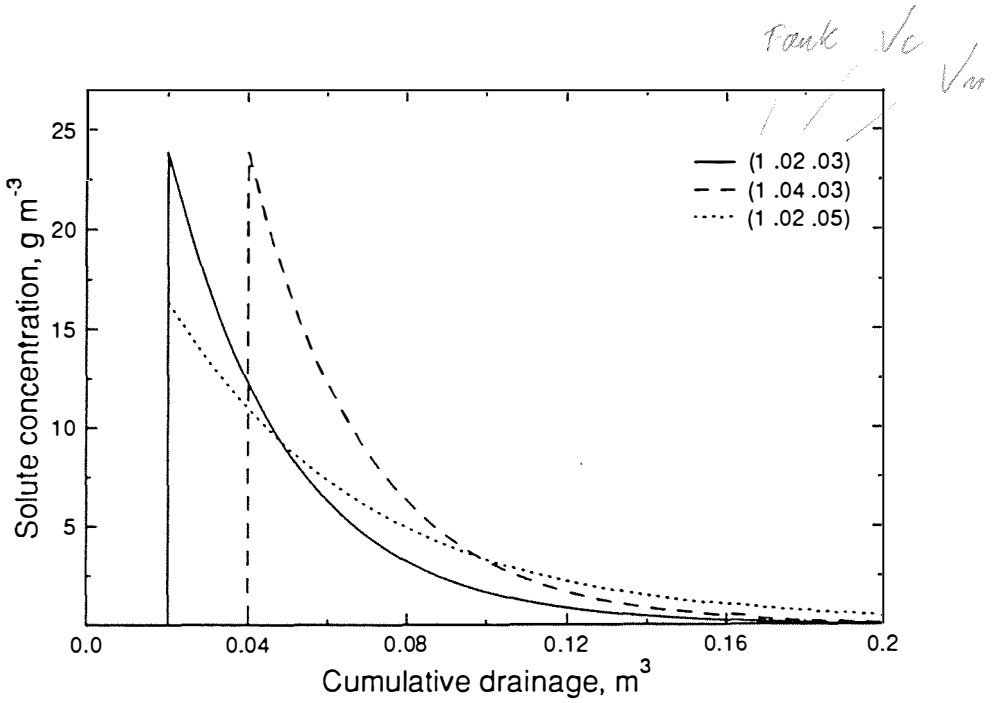

Figure 5.4 The effect of varying V_c and V_m on output solute concentration.

Both models have the same V_c, but the dotted line shows the output resulting from a 66% increase in the mixed volume. As the mixed volume increases, the peak solute concentration decreases. The rate at which the solute concentration falls to the antecedent level of solute concentration also decreases. In conventional solute transport terms, the solute becomes more dispersed as the mixed volume within a tank increases the buffering of the input.

Note that both the dashed line and the dotted line represent models with identical total transport volumes. However a change in the manner in which the volume is split between the convective and mixed volumes greatly influences the shape of the output solute concentration. As the mean amount of drainage required to transport solute through the system is equal to the sum of the convective and mixed volumes, the means are equal.

5.4.2 Effect of varying n, the number of tanks

With a single tank in a pathway, output solute concentration can only have a step increase to the peak solute concentration at $Q=V_c$. However with the addition of further tanks in series, c_o will become smoothed in shape, more like the traditional CDE output.

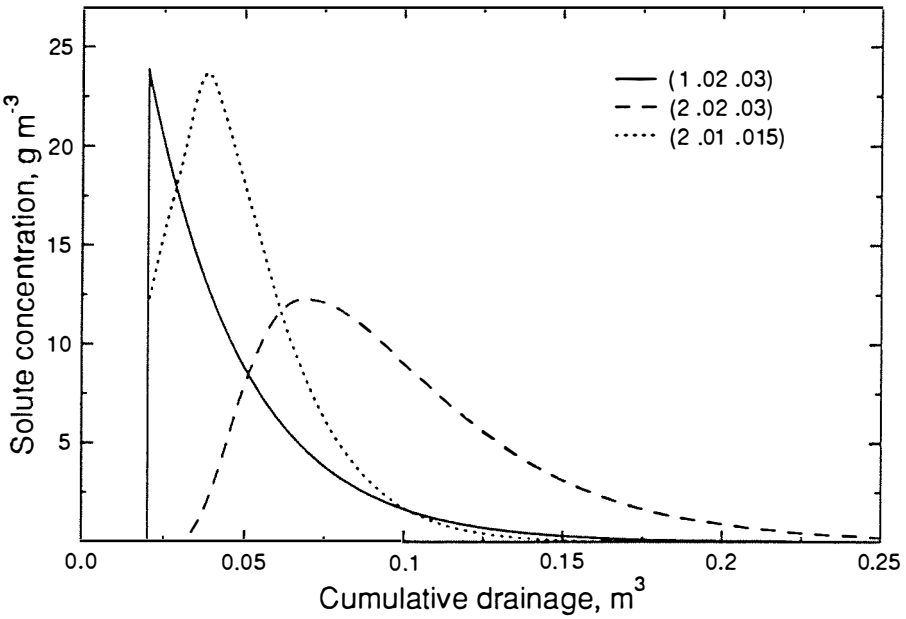

Figure 5.5 The effect of varying n on solute output.

Figure 5.5 shows the way in which changing the number of tanks in a single pathway can affect solute output. Comparison of the solid line, (1 0.02 0.03), with the dashed line, (2 0.02 0.03), shows the result of increasing the number of tanks in a series. The tanks in both examples are the same. In this case the total volume of the network doubles as the number of tanks doubles, thereby increasing the amount of drainage required to move solute through the network. Also the output solute is more dispersed than in a series with a smaller number of tanks.

This may then be contrasted with the case where the total volume remains constant but the number of tanks is doubled. Such a model is also shown in Figure 5.5 with the dotted line. When compared with the solid line it can be seen that the rate at which the solute concentration falls to the antecedent level is greater in the two tank series than in the single tank. Because the total volume is unchanged the amount of drainage required to produce the mean of the breakthrough curve is also unchanged. If the total volume is held constant, and the number of tanks in a pathway increases to infinity, the solute output concentration merely becomes a delayed version of the input solute concentration. The system becomes completely dispersion-free, plug flow.

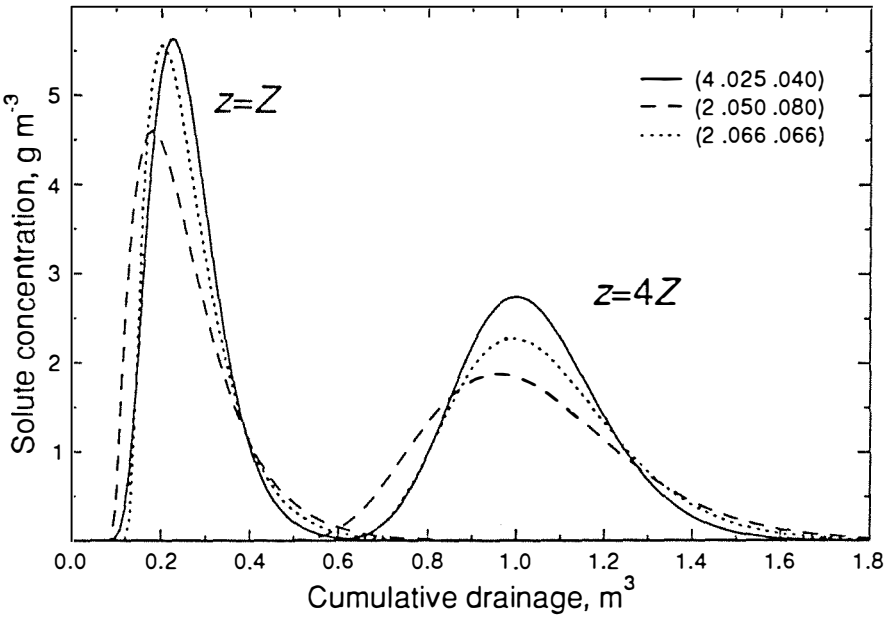

Figure 5.6 The effect of varying both n and depth on output solute concentration.

Thus, it is not possible to take the total convective or mixed volume of a series of tanks and simply redistribute it amongst a different number of tanks. This is demonstrated in Figure 5.6. The solid and dashed lines represent output solute concentration from systems having the same total convective (0.1 m^3) and mixed (0.16 m^3) volumes. For the solid line the volumes are distributed between four

tanks, while for the dashed line the volumes are distributed between only two tanks. Also shown is the output extrapolated to a depth two times greater than the original depth. As depth increases the two curves diverge further. The dotted line in Figure 5.6 is the result of a 'best fit' to the solid line. There is however a restriction that the fitted model must consist of only one pathway with a series of two tanks. This model had a ratio of mixed to total volume of approximately 0.5, whereas the original model of four tanks had a ratio of about 0.65. As the output solute concentration is extrapolated to greater depths, the fit between the two models deteriorates as a consequence of failure to pick correctly model structure. At a given depth the dotted line results from solute which has passed though a smaller number of tanks than the solid line model. As a consequence the solute is more dispersed in the two-tank model.

5.4.3 Effect of varying x, the number of pathways

Aggregated Mixing Zone models with multiple transport pathways are to some extent analogous to the mobile-immobile CDE (Van Genuchten and Wierenga, 1976; de Smedt and Wierenga, 1979) or its variants (see Nielsen *et al.*, 1986) in that the soil is not treated as if it were a homogenous medium. However this approach has more in common with the dual-density model of Rao *et al.* (1976) where the soil matrix was split into two regions and treated as behaving as two CDE-like soils in parallel. White *et al.* (1986) suggested that the mole-tile drained Evesham clay appeared to behave as if there were two distinct flow domains. This type of problem might be investigated using the AMZ model with two transport pathways.

The solute output concentration from a two-pathway model is not simply the average of the superimposed concentrations of the output from two equivalent single-pathway models. This is demonstrated in Figure 5.7. The solid and the dashed lines show the results of two, single-pathway models. The dotted line is the output from the double-pathway model each consisting of the single-pathway models. The solute output from the double-pathway model has much lower solute concentrations than either of the two single-pathway models. It also has a greater delay than the single-pathway models. The increased delay is of course a result of

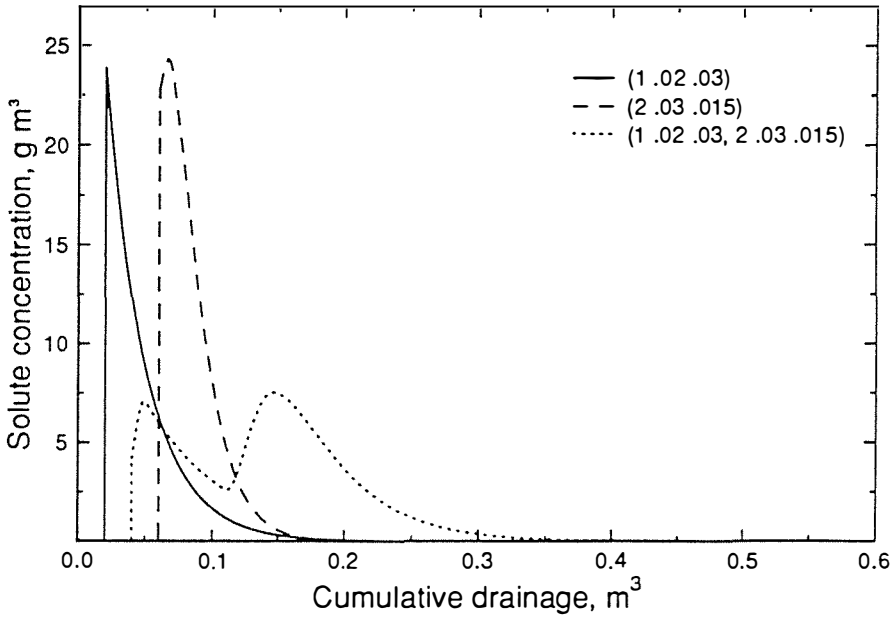

Figure 5.7 The effect of more than one solute transport pathway on output concentration.

the increased volume in the double-pathway model. When there is more than one solute transport pathway the water passing through the system needs to be apportioned between the two pathways, in this case it was done equally. As there is less water going through any one pathway, a greater amount of drainage is require to shift a given quantity of solute.

Double-pathway models can result in distinctly bi-modal solute transport as demonstrated in Figure 5.7. However, this need not necessarily be the case. In models where the convective and mixed volumes of the two pathways are not as dissimilar as in Figure 5.7, the model can produce a single peak with the early-rise, long-tail phenomenon that has been noted in many well-structured soils.

5.5 PRELIMINARY INVESTIGATION OF THE AMZ MODEL

It is now appropriate to discuss the problems involved in the application of the AMZ model to data from soils. First, solute concentration data in soil are collected at specific depths, whereas a network of tanks has no intrinsic depth. How this is dealt with has already been suggested in Section 5.2.4. Essentially the calibration, which will eventually result in n_i tanks in each series, is carried out using data collected with distance Z between the input and output sampling depths. Therefore these n_i tanks each have a notional depth of Z/n_i associated with them.

A further issue is the concept of volumes associated with data derived from suction cup samplers. The cups collect samples from some poorly-defined volume of soil around the sampler, and probably also with a weighting function which is non-uniform, both spatially and temporally. The latter is an intrinsic problem associated with sampling of the soil solution by this method. The former is dealt with by assuming that the sample is representative of solute concentration at the sampler depth and assigning a unit areal extent, namely 1 m^2, to the data.

Finally, the matter of the number of parameters in the AMZ model needs to be addressed. As discussed earlier, in Section 5.2.3, even relatively simple AMZ models require large numbers of parameters. The example given was of a three tank model that would require the identification of eight parameters. Although it would be possible to find the appropriate values for them, normally the data would not support this numbers of parameters. Therefore an initial attempt to factorise an ARMA equation will be made using the assumption that tanks within a pathway are equal. If this assumption results in a poor fit to the data, then the unequal tanks case will be investigated. This equal tank assumption makes more sense than the simple pragmatic one of reducing the number of parameters to a more manageable level.

Often the motivating aim for a solute transport experiment is to predict solute transport to a depth greater than that of the calibration. An essential assumption of any prediction is that solute transport to the prediction depth obeys the same rules as produced the calibration data. Given this, it is also then reasonable to

assume that transport to some depth less than the calibration also reflects the calibration. As discussed in Section 5.2.4, an equal tank assumption will also provide more flexibility in the depths to which predictions can be made. One circumstance where this assumption may be inappropriate is for layered soils. Here, if the layering has affected solute transport, one can see that equal tanks would be inappropriate and unequal tanks should be considered.

Where an assumption of equal tanks is used, the effect of this assumption on the measure of goodness-of-fit also needs consideration. As described in Section 5.3, the AFPE and the EVN used by Beven and Young (1988) and Hornberger *et al.* (1990), include adjustment for the number of parameters in the ARMA equation. The purpose of this adjustment is to guard against over-parameterised equations. In more-usual circumstances this type of adjustment would be quite satisfactory, however its use with the AMZ model it is inappropriate. This is because the number of parameters in the ARMA equation is not related to the number of parameters in the AMZ model.

Table 5.1 Example ARMA equations and associated AMZ models.

ARMA equation			AMZ model	
n_a	n_b	# parameters	structure	# parameters
5	4	9	(2,3)	5
8	1	9	(8)	2
1	1	2	(1)	2

For example, see Table 5.1 which contains three different ARMA equations and associated AMZ models. Here the structure of an AMZ model has been described by a series of one or more numbers in parentheses. Each number refers to the number of tanks in a series. For example, the notation of (2,1) refers to an AMZ model as depicted in Figure 5.1. Obviously both the AFPE and the EVN statistics, because they consider the number of parameters in the ARMA equation rather than in the AMZ model, are appropriate in this case. In this study the goodness-of-fit

statistic used was the mean of the squared deviations of the model estimates from the data.

In the following sections several aspects and uses of the AMZ model will be investigated. Firstly aspects of the ARMA equation are discussed. Then in Sections 5.2.3 and 5.2.4 the utility of the AMZ model for describing, predicting, and revealing solute transport in both the lysimeter and the field data is examined. Finally, the factorisation process is scrutinised.

5.5.1 ARMA equation structure differentiation

Ideally, one particular ARMA structure will stand out as fitting calibration data significantly better than any other. This should be especially true in the use of the ARMA equation considering the rather lengthy algebraic manipulation that must be carried out when examining each equation.

Here the data collected at site 12 during the 1988 field leaching experiment will be used to demonstrate the degree of certainty with which one particular ARMA equation structure can describe data. If a particular structure is a good one, then changing the equation structure slightly should significantly decrease the goodness-of-fit.

The ARMA equation found to describe best solute transport between 250 mm and 550 mm at site 12 was a model with n_a=6, n_b=5, and n_k=5. This particular model produced a mean square error (mse) of 0.025, and exhibited good fit. The effect of varying the model structure may be examined by holding two of the three parameters constant, whilst varying the third. In each case the mse associated with the set of parameter values was found. The results of this exercise can be seen in Figure 5.8. In each case the parameters n_a, n_b, or n_k were varied by one and two orders from their best fit values of 6, 5, and 5 respectively. The result for the structure with n_a=4 is not shown as the mse was 8.4 x 10^9!

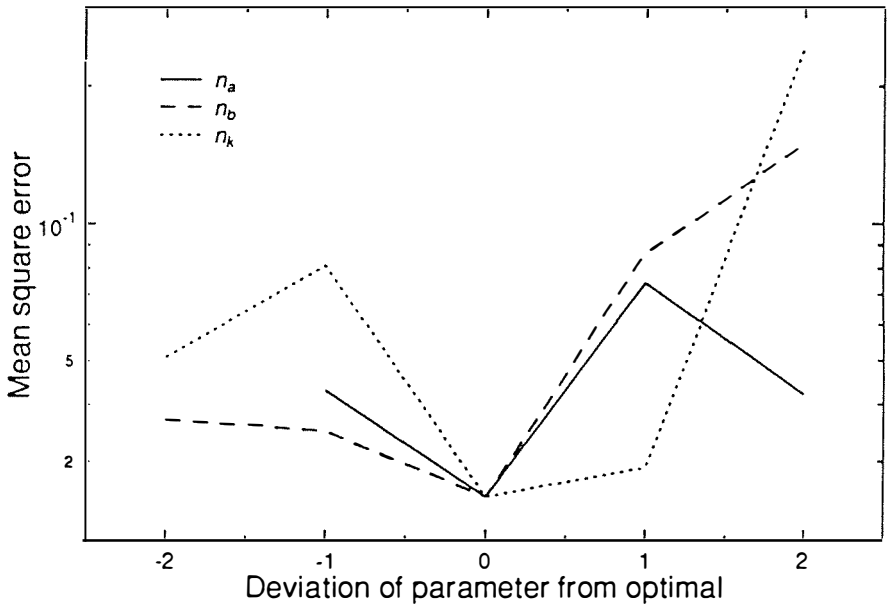

Figure 5.8 The effect of changing the ARMA equation structure on the calibration mse.

As can be seen from Figure 5.8 the optimal values of n_a and n_b represent a well-defined minimum. The figure indicates that the optimal value for n_k may be somewhere between 5 and 6. Although non-integer parameter values are not possible within this discrete model, it is possible to attempt to fit the ARMA equation to the data using a smaller value of ΔQ, thus decreasing the effect of the unit interval on the convective volume.

Generally it was observed that the orders of the ARMA equation found to represent best the data were not closely related to each other. To show this, results from the ARMA equation fitted to the data from site 12 between the depths of 250 mm and 550 mm will again be used. Table 5.2 shows the ARMA equations, and any corresponding AMZ model structures. The best ten such equations are shown. Neither the ARMA equations, nor their corresponding AMZ models, show great similarity. As increasing n_b and n_k will also increase the delay on the input data, their values may be expected to be inversely related. Thus the resultant AMZ models may be quite different. As a motivating factor for the use of the AMZ

Table 5.2 Site 12 ARMA and AMZ model structures.

Mse Rank of ARMA equation	ARMA equation structure			MSE	Possible AMZ model structure
	n_a	n_b	n_k		
1	6	5	5	0.025	(2,4) or (2,2,2)
2	7	1	2	0.031	(7)
3	8	4	5	0.033	none
4	8	1	3	0.035	(8)
5	6	6	2	0.035	several
6	6	4	5	0.035	(3,3)
7	3	3	5	0.035	(1,2)
8	6	2	2	0.035	none
9	5	1	2	0.036	(5)
10	8	2	5	0.037	none

model was its potential for subdividing the water-filled porosity of the soil into different flow paths, this is of some concern.

5.5.2 Application of the AMZ model to the 1990 lysimeter data

The ARMA equation structure found to fit best the 550 mm lysimeter data, using the 250 mm data as the input, was an equation with n_a, n_b, and n_k equal to 2, 1, and 4, respectively. This structure satisfies the requirements for structural factorisability, and an AMZ model consisting of one solute transport pathway of two tanks may be formed.

First a model of two equal tanks will be investigated. The ARMA parameter values, and the calculated AMZ parameters, are given in Table 5.3. As there is only one pathway, the α parameter can be calculated separately from each of the ARMA equation parameters. The α parameter calculated from the 3 different ARMA equation parameters varies only in the second decimal place and AMZ simulation

Table 5.3 ARMA and AMZ model parameter values for solute transport between 250 mm and 550 mm in the lysimeter.

ARMA parameter	ARMA parameter value (standard deviation)		α	V_m (m^3)
b_1	0.178	(0.110)	-0.579	0.018
a_1	-1.172	(0.093)	-0.586	0.019
a_2	0.354	(0.026)	-0.595	0.019

produced from the three α values results in outputs which are not visibly different from each other. The mse of the ARMA equation was 0.137, and was 0.101 for the AMZ model with α=-0.5904, being the average α calculated from the a_1 and a_2 ARMA parameters. The data and the simulations from the ARMA equation and AMZ model can be seen in Figure 5.9. As the estimation of α from the various ARMA parameters has resulted in values so close to each other, for this model the equal-tank assumption is adequate. Unequal tanks need not be further investigated.

From this calculated α parameter, the mixed volume for each tank can be calculated as 0.019 m^3, while the n_k parameter of 4 revealed a convective volume of 0.020 m^3 for each tank. This gives a total volume of 0.039 m^3 for each tank. The calibration distance, Z, was 300 mm, and this was represented by two tanks. Thus, the depth represented by each tank is 150 mm. So over a soil surface area of 1 m^2, the soil volume represented by each tank is therefore 0.150 m^3. Comparison of the soil volume and the volume of the two tanks reveals a transport porosity, θ_{st}, of 0.26. This compared with θ of 0.39, indicating that a substantial part of the water-filled porosity was not active in transporting solute.

Convection-dispersion analysis of the same data (Section 4.4) yielded an estimate of 0.27 for θ_{st}. Thus the ability of the AMZ to satisfactorily represent solute transport is in this instance demonstrated.

Predictions of solute transport at depths of 760 mm and 1000 mm may be made using equations (5.11) and (5.25). These predictions are shown in Figure 5.10. Predictions can be made only to depths which are multiples of tank 'depth'. Using

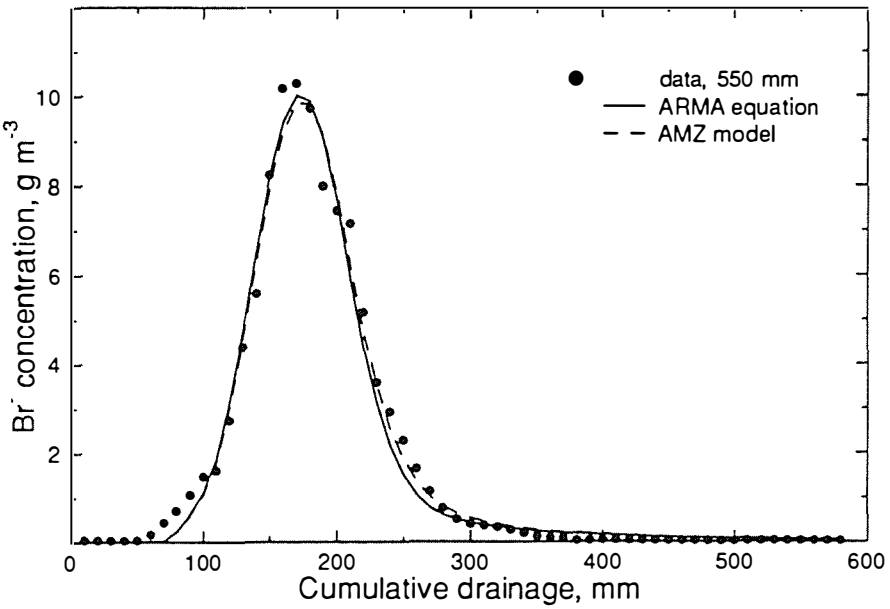

Figure 5.9 AMZ model calibration between 250 mm and 550 mm for the 1990 lysimeter data.

the 250 mm solute concentration measurements as input, and the tank depth of 150 mm, predictions with $n=3$ and $n=4$ correspond to depths of 700 mm and 850 mm respectively. Solute concentration was however measured at 760 mm, being approximately one third of the way between these two depths. Predictions at 700 mm and 850 mm and the data measured at 760 mm are shown in Figure 5.10a. It can be seen that although the data lie between the two predictions, it lies much closer to the 850 mm prediction than would be expected simply by the relative depths of measurement and prediction.

By serendipity the data collected at 1000 mm coincides with a 'distance' of 5 tanks from the 250 mm data. The prediction for the 5 tank model is shown in Figure 5.9b. The data and the prediction virtually coincide. Again this is somewhat surprising considering the difference in the texture of the soil through which the solute has travelled after calibration. To reach the 1000 mm samplers the solute will have travelled through 250 mm of A horizon, 400 mm of 1C horizon, 10 mm

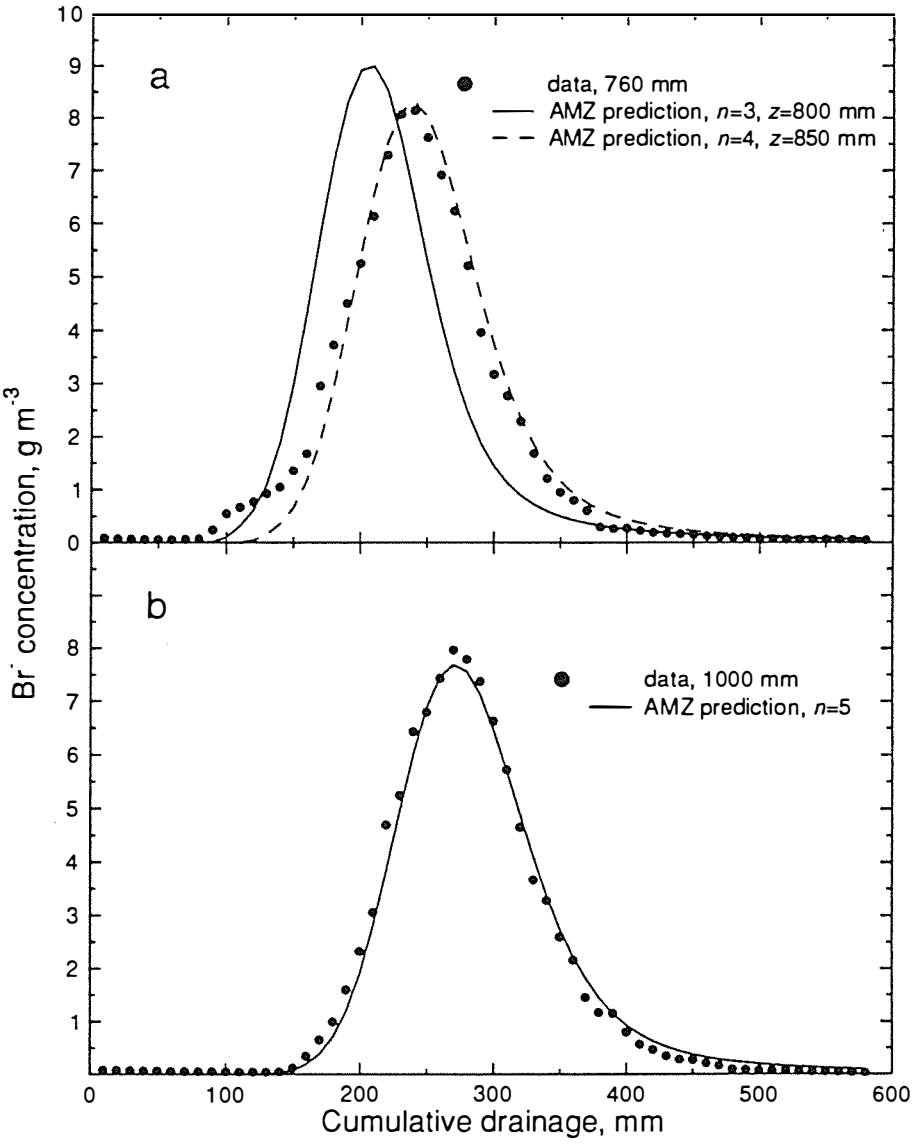

Figure 5.10 AMZ model predictions for solute concentration at, (a) 760 mm, and (b) 1000 mm for the 1990 lysimeter data.

of 2C horizon, as well as traversing the additional interface to the underlying 2C gravel.

It is interesting to note that for the 1000 mm data, solute travels approximately one third through the A horizon and two thirds through the underlying C horizon of fine sand. Despite the fact that the calibration was carried out on data representative of travel primarily through the A horizon of fine sandy loam, an excellent prediction still results. Because of its essentially structureless nature, there is good reason to

expect that the C horizon will utilise a greater proportion of its porosity during solute transport. Furthermore, generally, it will have a lower water content than the A horizon. These factors may thus compensate for each other.

As the purpose of this section is simply to carry out a preliminary evaluation of the model, the model predictions will not be dwelt upon further. It is simply noted that the initial results are encouraging.

5.5.3 Application of the AMZ model to the Aggregated 1988 field data

In order to provide data representative of solute transport leaching through the field, yet still provide the form of data required by MATLAB to fit the ARMA equation, the 1988 field data were bulked in the following manner. At each depth, the data were divided into 50 mm increments of drainage. Within each of these increments, mean drainage and solute concentration were found. In finding a mean, a log-normal distribution in both variables was assumed.

The ARMA equation found to describe most closely solute transport between 250 mm and 550 mm was one with $n_a=2$, $n_b=1$, and $n_k=2$. There is similarity of structure between this equation and that found to describe best the solute transport through the same depth of soil in the lysimeter where the same value of n_a and n_b were found, however n_k was found equal to 4. This ARMA equation can also be factorised into an AMZ mode consisting of one solute transport pathway of two tanks in series. The parameter n_k is however smaller than that found in the lysimeter. This indicates that the convective volume revealed by the aggregated data is smaller than that found in the lysimeter.

As with the lysimeter data, the more simple option of equal tanks within the pathway was initially investigated. The α parameter, as calculated from the different ARMA equation parameters, is given in Table 5.4. In contrast to that found in the lysimeter, it can be seen that there is now quite a range in the different estimates of α. The resulting V_m parameter also varies significantly, with the highest estimate being twice that of the lowest. Obviously then here the assumption of equal tanks

Table 5.4 ARMA equation and AMZ parameter values for solute transport between 250 mm and 550 mm in the aggregated field data.

ARMA parameter	ARMA parameter value (standard deviation)		α	V_m (m^3)
b_1	0.108	(0.054)	-0.671	0.025
a_1	-1.555	(0.108)	-0.777	0.040
a_2	0.669	(0.083)	-0.818	0.050

within pathway is inadequate. The more complex, unequal tank model must therefore be tested. Graphical examination of the A polynomial reveals that all roots are complex. Thus no satisfactory AMZ model can be formed from the ARMA equation found to fit best the aggregated field data.

This result occurs because of no direct link between the ARMA equation and the AMZ model. Therefore there is nothing to force these parameter estimates to be consistent. As the best AMZ model that could be formed was that shown in Table 5.4, this model will now be further investigated.

The variability in the estimates of α makes difficult the selection of which α to use. The mse between the data and the ARMA equation was 0.102. Of the various possible averaging combinations, the lowest mse (0.146), resulted from the b_1 parameter alone. The next lowest mse (0.261) was formed by using the average of all three parameters. Figure 5.11 shows the 550 mm field data, with the errors bars indicating ± 1 standard error on the data. Also given there are the ARMA equation output, and the two AMZ model simulations. It can be seen that the AMZ model differs significantly from both the data and the ARMA equation.

Whilst this is not entirely satisfactory, the AMZ model may still be used to predict the solute concentrations that might be expected at greater depths. Predictions were made assuming an α of -0.671 as this value resulted in the lowest mse for the calibration data. The results for these predictions are shown in Figure 5.12a for 760 mm, and 5.12b for the 1000 mm data. As noted for the lysimeter, the 760 mm predictions again preceded the measured data, but here to an even greater extent.

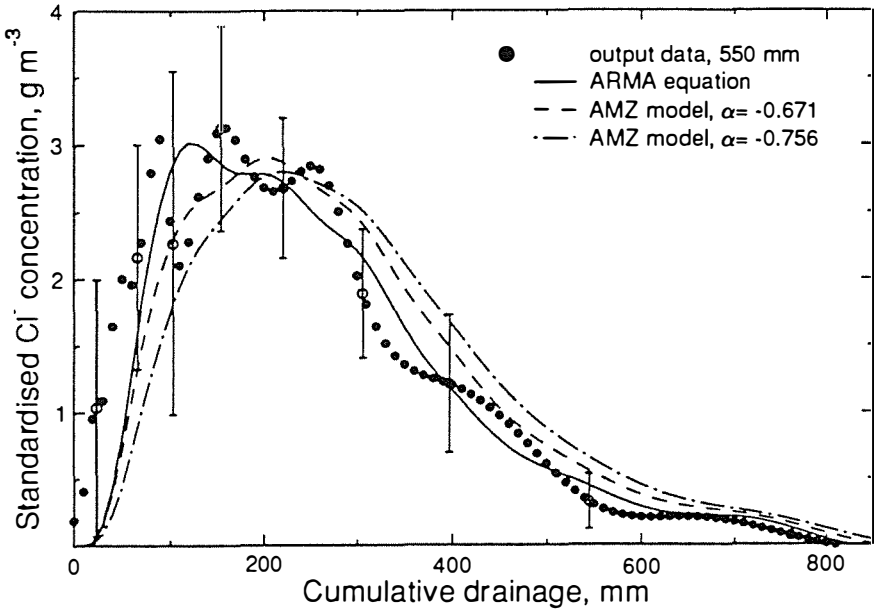

Figure 5.11 Calibrated ARMA equation and AMZ model output for the aggregated field data. The error bars show ±1 se for the data.

The fit to the data at 1000 mm is somewhat better than at 760 mm. This was also noted in the lysimeter data, however here the prediction again precedes the data.

Using the aggregated data was not a particularly satisfactory method with which to test this AMZ, or any, model. There may be consistent trends in the AMZ model parameter between sites that would be obscured. For example, it might be that all the sites have the same AMZ model structure with the same V_m, but that V_c varies between sites. Aggregating the data would result in some intermediate value of V_c but would result in a high value for V_m.

The factorisation of the ARMA equation that is required to form an AMZ model is not a simple matter. This will now be investigated in more detail.

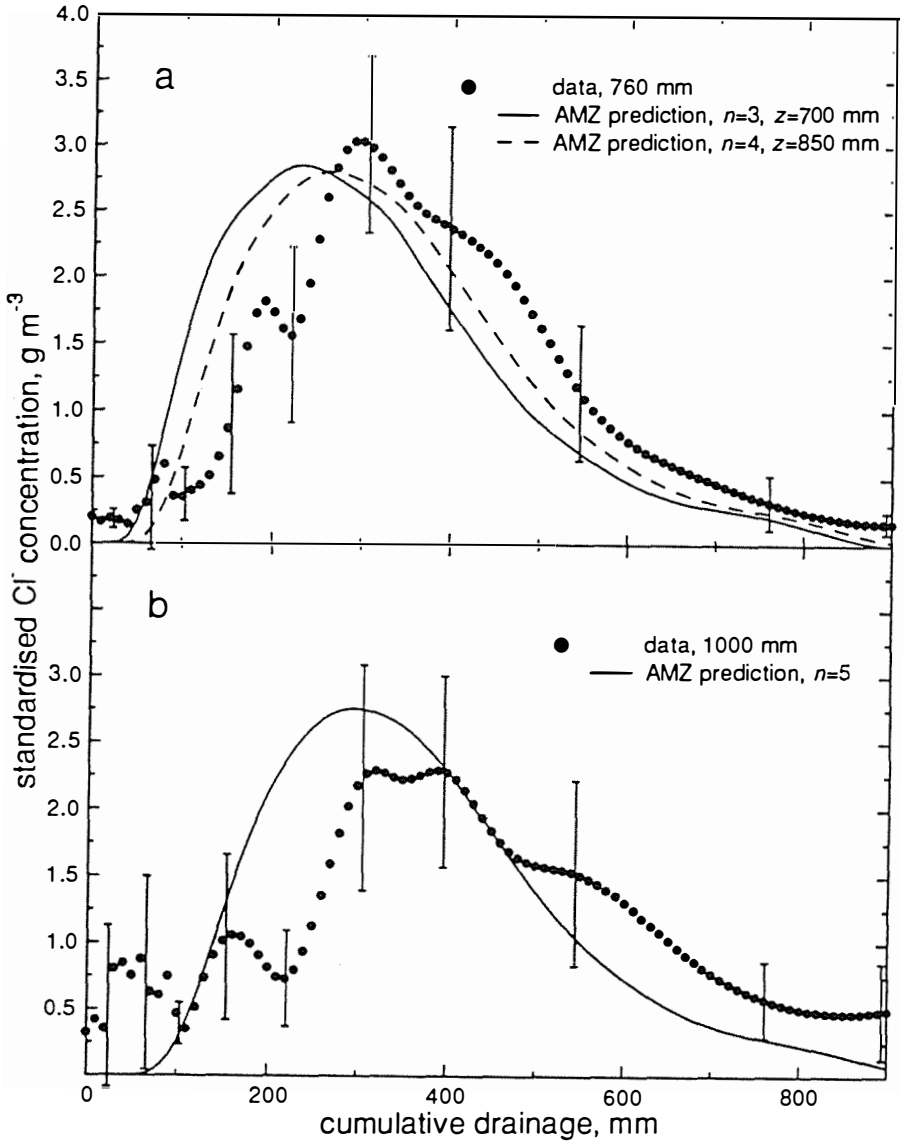

Figure 5.12 AMZ model predictions for the aggregated field data at, (a) 760 mm, and, (b) 1000 mm.

5.5.4 ARMA Equation Factorisability

As indicated in Section 5.2.2, not all ARMA equations of good fit to the data can be factorised successfully into an AMZ model. This arises because there is no direct link between the ARMA equation and the AMZ model. This characteristic can be regarded as either a strength or weakness. That the ARMA equation is not forced to match to an AMZ model may be considered a strength when the 'best' ARMA equation to describe solute transport is sought. However, if the primary

aim is to provide some insight into the transport process, or to generate a model which can predict solute transport to a depth greater than that of the calibration, then an ARMA equation which cannot be factorised into an AMZ model is a serious weakness.

On its own an ARMA equation does not provide any structural information about solute transport through the soil. Consequently the predictive utility of the ARMA equation is less than that of the AMZ model. Additionally, the ARMA equation provides little insight to the solute transport process. Solute transport could be predicted only through a depth of soil equivalent to that of the calibration. This could be the same physical depth as the calibration, but with a different input function. Predictions could also be made for depths which are multiples of the calibration depth. This may limit the utility of prediction, especially if a large calibration distance had been used.

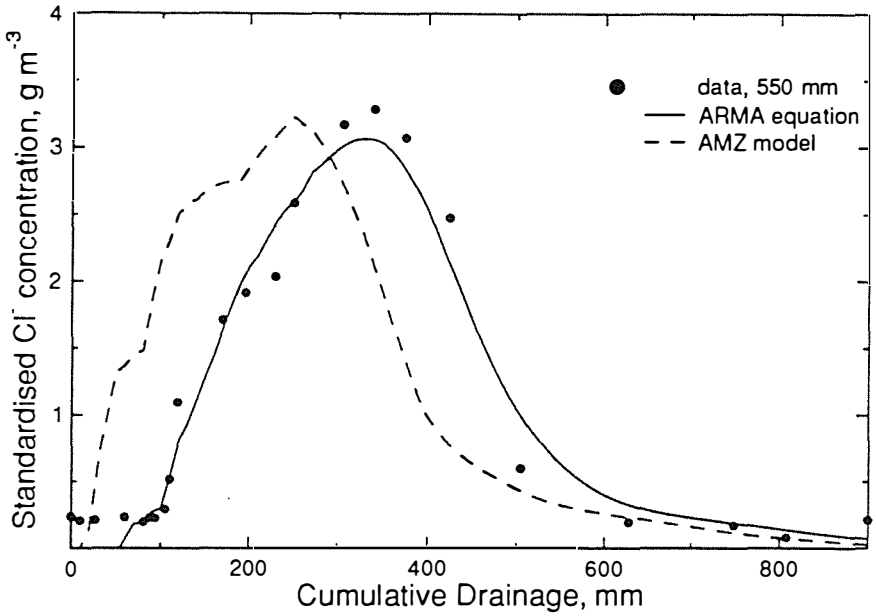

Figure 5.13 ARMA equation and AMZ model calibration for solute transport between 250 mm and 500 mm at site 10.

In this section the factorisation of the ARMA equation to form the AMZ model will be examined in some detail. The format will be that of a case study. The data from site 10 will be used as the example.

Table 5.5 Site 10 ARMA equation and AMZ model structures.

Mse Rank of ARMA equation	ARMA equation structure			MSE	Example AMZ model structure
	n_a	n_b	n_k		
1	8	2	1	0.025	none
2	8	3	1	0.027	none
3	3	6	5	0.027	(2,1,1)
4	7	4	3	0.027	none
5	3	5	2	0.027	(2,1)
6	8	5	2	0.027	(4,4)
7	8	4	1	0.028	none
8	4	6	3	0.028	(2,2), (3,1)
9	3	6	1	0.029	(2,1,1)
10	5	5	2	0.029	several

The ten best ARMA equations, and corresponding AMZ models, based on measurements at 250 mm and 550 mm are shown in Table 5.5. In this particular case, the ARMA equation with the lowest mse which is also structurally factorisable is the equation with the third lowest mse. The mse associated with this equation is however only a little higher than that of the best model. This is will represent the data almost as well as the top-ranked equation.

This ARMA equation has n_a=3, n_b=6, and n_k=5. This may be factorised into an AMZ model of three pathways. One pathway will have two tanks, one will have one tank, and the last will have a single tank with no mixing volume. Graphical analysis of the cubic polynomial in the denominator of the ARMA equation indicates a double root near -0.9, and a single root close to 0. Solution of the

appropriate equation, assuming that the two tanks in the first pathway are equal, which is justified by the graph of the polynomial, resulted in $\alpha_{11}=\alpha_{12}=-0.884$, $\alpha_2=-0.781$, and of course, $\alpha_3=0$. Now, expansion of the AMZ model described above yields a numerator of,

$$\begin{aligned}&\beta_{11}\beta_{12}q^{-(k_{11}+k_{12})}+\beta_{11}\beta_{12}\alpha_2 q^{-(k_{11}+k_{12}+1)}+\beta_2 q^{-k_2}+\beta_2(\alpha_{11}+\alpha_{12})q^{-(k_2+1)}+\\&\beta_2\alpha_{11}\alpha_{12}q^{-(k_2+2)}+\beta_{11}q^{-k_3}+\beta_3(\alpha_{11}+\alpha_{12}+\alpha_2)q^{-(k_3+1)}+\\&\beta_3(\alpha_{11}\alpha_{12}+\alpha_{11}\alpha_2+\alpha_{12}\alpha_2)q^{-(k_3+2)}+\beta_3\alpha_{11}\alpha_{12}\alpha_2 q^{-(k_3+3)}\end{aligned} \qquad (5.27)$$

$$= b_1q^{-5}+b_2q^{-6}+b_3q^{-7}+b_4q^{-8}+b_5q^{-9}+b_6q^{-10} \quad .$$

As none of the b's are equal to 0, the values of the k's must be such that all the delays between 5 and 10 have an AMZ parameter associated with them. There are 48 possible combinations of the k's that would produce delays within the bounds of 5 and 10. Of these 36 may be ruled out as the combination would result in one or more of the b parameters being equal to 0. Thus 12 combinations remain to be tested. This testing involves the determination of the β parameters. A successful test requires that equations (5.13) and (5.15) are satisfied. One by one these 12 possible models were tested. Sequentially they were rejected on the grounds that application of equations (5.13) and (5.15) led to physically-impossible parameter values.

The $n_a=3$, $n_b=5$, and $n_k=2$, ARMA equation was also a good fit to the site 10 data. However a graph of the denominator polynomial showed that two of the roots, and hence the α's, were complex. Thus this ARMA equation can not be algebraically factorised into an AMZ model.

The sixth-ranked ARMA equation had a structure of $n_a=8$, $n_b=5$, and $n_k=2$. This particular ARMA equation structure may be factorised into an AMZ model with two solute transport pathways, each with four tanks. Application of Descartes' rule-of-signs to the A polynomial showed that, at most, there could be two negative

roots. Further graphical analysis showed that all the roots were complex. However the uncertainty in the a_8 parameter was such that at the lower limit of a_8, the polynomial would have two real roots, with the reminder complex. This was taken as sufficient justification to attempt to factorise the ARMA equation as two pathways, each with four equal tanks. This is obviously an approximation. But without this, due to the complex roots, the ARMA equation could not be factorised.

The a_1 and a_2 parameters from the ARMA equation were used to determine that the α_1 and α_2 parameters of the AMZ model were 0.055 and -0.443. In order to compare the ARMA equation and the AMZ model, thereby testing the validity of the equal tank assumption, the AMZ parameters were used to recalculate the parameters of an ARMA equation which corresponded to that originally fitted to the data. The parameters from the fitted ARMA equation are compared with those back-calculated from the AMZ model in Table 5.6. Figure 5.12 shows the data at 550 mm at site 10, along with the ARMA and AMZ simulations.

The first point to note about this AMZ model is that one of the α parameters is positive, thus a mixed volume cannot be calculated from this parameter. The a_i parameters are, in general, closer than the b_i parameters. This may simply reflect the fact that only the α parameters were calculated directly from the ARMA equation. The β_i parameters were instead calculated from the α_i parameters using equation (5.13). An attempt could have been made to calculate both the β and α parameters from the ARMA equation by solving a system of five equations. However, due to the existence of complex roots to the ARMA equation, the success of this would be doubtful. More importantly, the relationship between the α_i and β_i parameters must preserve the relationship in equation (5.13). Otherwise the simulated solute mass will not be preserved. It would seem preferable to retain these equations rather than attempt to reconcile the relationship *a posteriori*.

Excepting the a_3 parameter, the a_i parameters calculated from the AMZ model are well within the limits of uncertainty of the ARMA equation parameters. In fact all except a_3 and b_1 are within 1 standard deviation of the fitted parameter. However as can be seen from Figure 5.12, this difference is quite significant in terms of simulated solute transport. The simulated output, although similar in shape to the ARMA equation, produces a much earlier arrival of solute at 550 mm than is

Table 5.6 Calibrated ARMA equation parameters and equivalent ARMA equation parameters back-calculated from the AMZ model for site 10 between 250 mm and 550 mm. (* parameters used to calculate the AMZ model)

ARMA equation parameter	Parameter value		
	Fitted ARMA equation (standard deviation)		back-calculated from AMZ
a_1	-1.5506*	(0.0963)	-1.5508
a_2	0.8046*	(0.1746)	0.8047
a_3	-0.3129	(0.1858)	-0.1201
a_4	0.0545	(0.1886)	-0.0177
a_5	0.0529	(0.1857)	0.0029
a_6	0.0531	(0.1798)	0.0005
a_7	-0.0483	(0.1631)	0.0000
a_8	0.0244	(0.0814)	0.0000
b_1	-0.0551	(0.1001)	0.6674
b_2	-0.1258	(0.9160)	-1.0856
b_3	0.6671	(0.2032)	0.7286
b_4	-0.7638	(0.1677)	-0.2147
b_5	0.3347	(0.0923)	0.0238

evident from either the data or the ARMA equation. If the transport volume were to be calculated from the simulated output of the AMZ model it would be smaller than that calculated from either the data or the ARMA equation simulation. It is of course not possible, in this instance, to use the AMZ model parameter values to calculate the transport volume. The calculation would in this case involve taking the log of a negative number!

There is obviously little point in making predictions of solute transport based on the AMZ model calculated for the site 10 data shown. The discrepancy between the AMZ simulation and the fitted ARMA equation was in part at least due to the approximation of equal tanks within a pathway However, due to the existence of

complex roots for the ARMA equation, an exact AMZ model could not be found. As detailed earlier, it would be possible to make predictions, under rather restrictive conditions, using the ARMA equation alone.

If the problem of factorising the ARMA equation were evident in just a few sites, it may not raise a significant problem. Unfortunately, however, data from many sites exhibited the same difficulty as outlined above.

5.6 CONCLUSION

The above sections have described the AMZ model of solute transport developed from that introduced by Beven and Young (1988). This model has been tested using data derived from field experimentation.

The basis of the AMZ model is that solute transport through soil can be described as being equivalent to an arrangement of delayed-input, continuously-stirred tanks. This part of the model is conceptually appealing and relatively simple. The AMZ model is parameterised by matching the equation for solute transport through these tanks to an ARMA equation which has been fitted to the data. This matching or factorisation process is however not straight forward. Firstly it might not be possible to find a form of the AMZ model which is indeed a factorisation of the ARMA equation. But if this is possible, the model is then deemed structurally factorisable. Once structural factorisability had been established it then might be that the AMZ model parameters are not physically sensible. If the parameters are physically sensible, then the model is said to be algebraically factorisable.

If the factorisation of the ARMA equation is successful then the AMZ model has been demonstrated to describe and predict well solute transport. The model indicates the volume of pores active in solute transport. It further separates these into those which transport solute via dispersion-free plug flow and those which are more active in the transport process. Not all soil pores may be involved in solute transport. Those involved in transport might do so via dispersion-free plug flow, or may be more active in creating dispersion. An AMZ model, by virtue of its

separation of the transport volume into convective and mixed volumes, may be useful in interpreting these processes if these volumes can be related to some physical property of the soil pores.

If the aim of the fitting of the ARMA equation to the data is to provide the means by which to parameterise the AMZ equation, then the ARMA may not be the most appropriate method by which to do this parameterisation. An alternative that might be worth investigation is to fit equation (5.3) directly to the data. This could be done by picking a particular arrangement of tanks to be tested. Given input data and initial parameter values, this would allow, by means of least-squares parameter fitting, determination of the convective and mixed volumes. A variety of tank arrangements would need to be tested and usually the equal tank assumption would be needed to ensure that the number of parameters was not excessive. *A priori* it is difficult to anticipate the success of this technique, but if it can sensibly sub-divide θ_{st} it may reveal more of solute transport in the complex surface soil.

Chapter Six

DISCUSSION AND CONCLUSIONS

In the first chapter of this thesis a framework for discussing our current research philosophy was presented, and several questions posed. This introductory chapter was followed by chapters dealing with experimental details, the results of the experiments, convection-dispersion equation (CDE) modelling of those results, and Aggregated Mixing Zone (AMZ) modelling of the results. This concluding chapter summarises the information and understanding gained from this experimentation and modelling, and discusses the implications of this new understanding both for users of solute transport models as well as for researchers. The chapter will conclude with a discussion of the findings in relation to the philosophic framework developed initially.

6.1 INTRODUCTION

The main aim of this study was to study the effect of soil layering on solute transport during unsaturated water flow. A secondary aim was to examine spatial, both horizontal and vertical, and temporal variability of solute transport. The experimental work was field-based. To this end experiments were established, in both a lysimeter and the surrounding field. The soil contained several sharply defined layers. The experiment in the lysimeter was under more controlled conditions of solute and water application, while the water input during the field experiment was considerably more variable. This variation was reflected in the results.

Following the experiments, there were three stages of extraction of information and understanding of the solute transport process. First by direct examination of the data, secondly as a result of application of the CDE model, and finally further understanding was sought through the use of the AMZ model.

The next three sections in this chapter will consider each of these stages separately. These will then be followed by two sections in which the implications for users and researchers of solute transport models or information are drawn out.

6.2 INFORMATION GAINED EMPIRICALLY

It is difficult to distinguish between that insight that has been gained from the data, and that understanding that has been learned from application of models to the data. We can only think about experimental data in the light cast from the history of modelling and experimentation. Indeed, we initially had to have some sort of model in order to design the experiment. The CDE model is particularly pervasive as a mind tool. Historically the CDE has been thought to describe well solute transport through soil. Even when not specifically applied to data, the terminology of the model has become the *lingua franca* of solute transport discussions.

Solute transport in the lysimeter was more controlled and controllable than in the field experiment.

Solute transport in the lysimeter during the 1988 experiment was such that more drainage was found to be required to pass the mean of the breakthrough curve (BTC) than was observed during the 1990 experiment. The BTC was considerably more dispersed in 1988 than in 1990. These effects were attributed to the more spatially-variable water application of the 1988 experiment and movement of the solute immediately following application into immobile water.

The 1988 field data indicated that solute transport was spatially variable at horizontal separations of less than 0.5 m as well as at 10 m separations. This lateral variabilitywas considerably greater than any longitudinal variability. It was not clear if this lateral variability was due to variability in water application, soil properties, or a combination of both. Evidence from the comparison of the 1988 and 1990 lysimeter BTC's suggested that water application variability was important.

The mass balance of solute in the experiments was good in both experiments, indicating that sufficient measurements were taken. Further analysis of the expected value and variance of the BTC's indicated that reducing the number of measurements sites at any one depth from 20 to 10 would not have significantly compromised estimates of either the expected value or variance of field-scale transport.

Samples collected from porous cups and from soil cores differed in concentration. These differences conformed to the expectations that would result from assuming that the porous cups collect a flux-averaged sample and soil cores a resident sample. This could not however be conclusively determined.

Not all of the soil's water-filled pores were found to be active in moving solute through the soil. This was true even in the fine sand layer where the soil was essentially structureless.

Either the transport properties of the surface soil, or the boundary and initial conditions, were such that solute transport in the top 250 mm of soil was slower and more dispersed than elsewhere in the soil. This difference was far greater than any changes in solute transport caused by the widely-different texture of the soil layers.

Soon after application of the solid fertiliser, the solute must have moved, either by mass flow or diffusion, into some part of the pore space to be rendered somewhat resistant to leaching.

This information was extracted from the data without formally fitting a solute transport model to the data. By comparison of these observations with the known physical properties of the soil considerable knowledge has already been gained. When a process-based model such as the ubiquitous CDE is applied to the data what further understanding may be gained?

6.3 UNDERSTANDING GAINED FROM THE CDE MODEL

As already mentioned the CDE model is so pervasive in our thinking that it is difficult to separate this section from the previous one. However there is a difference in that new understanding can results from fitting the CDE model to the data.

The CDE was applied, albeit with considerable simplification, to the data gathered during the experiments. Temporal variation in water application was disregarded. This input was both intermittent and spatially variable. To apply the CDE the independent variable of cumulative drainage density was simply transformed to that

of time by assuming a constant water flux of 10 mm day^{-1}. Any variation in water content with either time or depth was ignored. Although there was evidence that a mobile-immobile CDE might have been more appropriate, nonetheless the simpler option of the classic CDE was employed.

Solute transport in the lysimeter during the 1990 experiment, with the exception of the surface soil, was well-described by a CDE calibrated between 250 mm and 550 mm. The variance of the BTC grew linearly with depth. This implies that transverse dispersion was sufficient to smooth lateral differences in solute concentration. The excellent fit between the CDE prediction and the 760 mm and 1000 mm data further shows that the soil layering was unimportant to solute transport here. Within the limits of the range of water fluxes applied to the lysimeter in 1990, and acknowledging that the water balance was dominated by drainage, the transient nature of the water input did not seem to affect solute transport.

Application of the CDE to the field data was not as successful. Although the CDE equation could be fitted to the measured BTC's, the changes in the coefficients with depth were not in accord with the dictates of the model. The velocity when calibrated between the soil surface and any depth greater than 250 mm was constant as expected. However calibration to the 250 mm data indicated a very much slower velocity. This did not appear logical. Also, there was no rational pattern to the dispersion coefficient.

These observations suggested our understanding of solute transport in the lysimeter had been enhanced through the process of fitting the CDE to the data. However our understanding of the processes that might have led to the BTC's observed in the field was limited. The CDE could not describe solute transport here. The reason for this remained unclear. Although the spatially-variable water input could explain some of the differences observed between the lysimeter outflow in 1988 and 1990, such variability does not help explain the field data. Neither could the results be explained adequately by other models which demand that the variance of the BTC grow with the square of depth.

Therefore it is unlikely that existing models of solute transport are capable of predicting the solute concentrations observed during this field experiment.

Application of the process-based CDE model gave little understanding as to why the model could not mimic observed solute transport.

In order to gain further understanding a non-mechanistic model, the AMZ, was applied to the data. The aim was not to predict solute transport *per se*, rather to obtain information about the volumes of the soil's wetted pore space which transports solute. Understanding gained from this model is now discussed.

6.4 UNDERSTANDING GAINED FROM THE AMZ MODEL

There are a large number of non-mechanistic models, many perhaps most, are easier to apply and interpret than the AMZ model. These other models are already established in the soil science literature. Given this, why use the AMZ model?

The answer is that although the AMZ model is not based on processes, rather on the notion that solute transport can be mimicked by flow through water-filled tanks and pipes, the model purports to divide the soil's wetted volume into non-interacting transport pathways. These volumes are then further categorised into those that actively disperse the solute and those which transport solute via plug flow. If this model could sensibly so divide the soil's pores, then certain patterns may become evident. This in turn may enhance our understanding of the apparently-chaotic field data. Furthermore if these volumes could then be related to measurable physical properties then this understanding might be propagated into improved models and so lead to better understanding of the solute transport process.

Application of the AMZ model to the 1990 lysimeter data revealed the transport porosity of the soil between 250 mm and 550 mm was 0.26. This was in agreement with that resulting from the CDE model. This porosity could be further sub-divided. One half apparently transported solute via plug flow and the other half was active in dispersing solute as well as transporting it. One might speculate that this might represent some division of solute transport between the macropores and the matrix of the soil. From the fitted model there was no evidence of parallel transport of solute, rather that the macropores and matrix interacted with each other. This was also in accord with the findings from the CDE model. Predictions of solute transport to greater depths in the lysimeter were also successful. Thus the

AMZ model was at least capable of mimicking well-behaved data as faithfully as the CDE model.

When applied to the field data the performance of the model was even more disappointing than the CDE, albeit for different reasons. The auto-regressive moving-average (ARMA) equation, which was used to parameterise the AMZ model, could rarely be successfully factorised in order that the AMZ model could be formed. Without the AMZ model the ARMA equation itself does little to enhance our understanding of the solute transport processes operating in the field. It was unclear whether this failure to factorise the ARMA equation was because solute transport was not acting in accordance with the model, or whether the combination of the variability of the data and the parameterisation technique were inappropriate. An alternative suggested for future work would be to try to fit the AMZ model directly to the data. For this to be a profitable research direction it would be necessary to ally closely the modelling with a critical examination of the nature of the soil's pores.

6.5 EMPIRICISM AND MODELLING: IMPLICATIONS FOR USERS

In the following sections a separation is proposed between people interested in solute transport experiments, understanding, and models. Users can be defined as those who seek primarily to predict either the agricultural or environmental consequences following the application of a substance to a soil. They may be concerned that the chemical remain accessible to plants, or that the chemical does not result in contamination of surface or ground waters as required by the Resource Management Act. Users may be primarily concerned with either the peak of solute concentration or the how the leading edge of the BTC will behave. The priorities forced on the users are such that their attitudes are considerably different to most researchers. Myers (1990) in an address to a symposium concerned with solute transport and water quality stated this as

> "I understand that we haven't been able to characterise preferential flow well enough to allow its incorporation into models. ... While processes such as preferential flow may deserve additional attention in model development and water quality research, the time available for model improvement is limited. Those of us facing the political

> realities of a concerned community can't wait for perfect models. We need to put what we know now into practice. Even though existing models need further refinement, they can and should be used in selecting and evaluating solutions to specific problems."

Unfortunately the implications that are drawn from this work are not particularly auspicious for those who wish to predict real-world problems. Roth *et al.* (1991) have stated that because of preferential flow they do not believe that it will be possible to predict solute transport from the measurement of soil physical properties alone. The experience here also suggests that the influence of the initial state of the surface soil is critical. So if it is not possible to determine this accurately, as well as to interpret its effect on subsequent solute movement, then even empiricism itself will not assist much in the prediction of solute transport. The minute detail of solute transport in the first minutes or hours after surface application may indeed be more important than the conditions that prevail over the next year or so.

Thus there will be a need for new field measurement techniques that will better reveal what has happened to the applied solute at early time in the top few centimetres of soil. If the water application is as variable as was experienced during the 1988 experiment, prediction may well be very difficult. It may however be possible to predict of the approximate location of the centre of mass of the solute. Given that lawyers regard the balance of doubt to lie at 50% whereas researchers of solute transport in the field regard 'success' as being when predictions are within an order of magnitude, the probability of existing models of solute transport being appropriate legislative tools is poor.

Users of solute transport understanding will therefore be dependent upon experimental data resulting from appropriately-designed field experiments, as well as models such as the CDE model which are simplified to make them manageable in practice. Models such as the AMZ will not be useful here as their predictive ability is in general no better than that of the CDE. They are however in return considerably more difficult to apply. Perhaps they may be useful where there is clear evidence of multi-modal transport.

6.6 EMPIRICISM AND MODELLING: IMPLICATIONS FOR RESEARCHERS

Researchers are different to users of solute transport understanding in that their primary goal is to understand the properties and process at work. It is through such understanding that empirical information can be applied to conditions 'different' from the original. They need to know what properties and process are important so as to know indeed what 'different' means . Then they can apply the knowledge gained. Society demands that models of solute transport be applied to real-world problems. Such understanding of solute transport will allow the development of better management tools, whether these be for nutrient studies or for water quality modelling and control.

We need to develop experimental techniques that will allow us to examine not only the position and concentration of solute in the soil but also the status of the solute with regard to the invading solution. These techniques will need to be such that they do not disturb the soil. This is particulary true of the top few centimetres of the soil. For a given mode of application of solute, say either as a solid or in solution, what factors influence where the solute will immediately move to? The detail of the immediate movement of water through the surface soil is likely to be important, and bulk techniques may not be appropriate. Techniques such as the use of the disc permeameter of Perroux and White (1988) filled with solute-laden water as described by Clothier *et al.* (1992) are promising in this respect.

After the initial application of solute it would appear that the small-scale local variability in water transport is important. It has been shown that spatially-variable water application not only increases the spread of the BTC but also affects the amount of water required to move solute through the soil. This variability must be characterised and its effect on solute transport quantified.

In this study the layering and the behaviour of the solute at the interfaces between the layers appeared to be unimportant in solute transport. However this cannot perhaps be regarded as universally true. It is likely to be more important in cultivated soils and under saturated flow conditions. The latter could be especially true if the soil physical properties are such that flow instabilities are likely to develop. Because the water application rate is frequently above the matrix

conductivity, macropores are likely to be important in influencing the movement of water and solutes.

The work of Jury and co-workers, and this study, reinforce how vitally important it is to examine solute concentrations at more than one depth and time in order to derive meaningful information and thereby understanding of solute transport processes. Not to do so merely results in a curve fitting exercise in which the most-flexible function will win!

Examination of the expectation and variance of the BTC's in the field experiment revealed that we would lose little information about the field-averaged BTC had only 10 sites, rather than the full 20, been sampled. However it would have been interesting to have had measurements at the same depth at a range of horizontal separations in order to perform a geostatistical analysis.

With regard to the number of depths monitored, each depth provided new and vital information about the processes operating. Sometimes this information only served to refute that a model, such as the CDE or AMZ, could explain solute movement at that place and time. Such information is however essential. Given the number of depths measured and the form of their measurement, it is unlikely that if the soil layering had influenced solute transport, we would have been able to deduce the correlation structure of solute transport across the interface.

The question as to whether solute transport experiments should be conducted using porous cups or soil cores remains open. If, as was one of the intentions of this study, the aim of an experiment is to deduce the correlation structure of solute transport across an interface, then as Jury and Roth (1990) argued it is inappropriate to use data from flux-averaged samples. They show that flux-averaged samples differentiate only poorly between the extremes of correlation.

This might be good news for users of solute transport theory, as a corollary of this is that for the leaching of solutes the correlation structure is unimportant. But where the structure is important to our understanding of the process involved, soil cores should then be collected. However, as it is not possible to sequentially collect soils cores from the same location, problems of spatial variability and stationarity must then be addressed. Soil cores do not reveal the status of the solute sampled

with respect to its ability to move. Perhaps porous cup samples do not either. Interpretation of the data for leaching processes thus remains difficult. In practice a well-designed experiment will probably employ some mix of both type of measurements. A greater understanding of the factors influencing solute transport on the small scale will enhance our ability to relate the concentrations measured via soil cores to those sampled via porous cups. Perhaps new technology will also assist in this, such as the use of time domain reflectometry technology to measure solute flux (Kachanoski *et al.*, 1992).

Researchers of solute transport processes are reliant on a melange of data gathering and interpretation via direct and critical examination of that data, as well as by use of process-based models. Non-mechanistic models which can account for certain observed patterns may have a contribution. Ultimately the aim should be to understand solute transport from the perspective of a process-based model. This enhances our ability to extrapolate without the aid of complex numerical manipulations.

6.7 SUMMARY

The lament of Chapter One that we need more data has been bolstered by the experience in this thesis. Here the data, interpreted nonetheless in the light of understanding developed from process-based models, has revealed more than the fitting of either model tested. However it should not be forgotten that the gathering, understanding, and modelling of data are iterative processes. Dagan stated in 1986 that ...

> "First, field data, existing and newly acquired by carefully designed experiments, have to be collected and analysed with the aid of the theoretical tools already developed or under development."

Despite a recent increase in field experiments, there still appears to be a large number of models which are not independently tested.

It would appear that textural differences within the soil are overwhelmed by the small-scale heterogeneity of water and solute application and the position of the solute in the soil in relation to the moving water. This could not be anticipated *a priori* from existing models, or from laboratory experimentation. It only became

evident from the data. This agrees with Knight's (1988) comment that it is still the experimental data that are limiting. Although awareness of the need for data may have increased, that need remains unrequited.

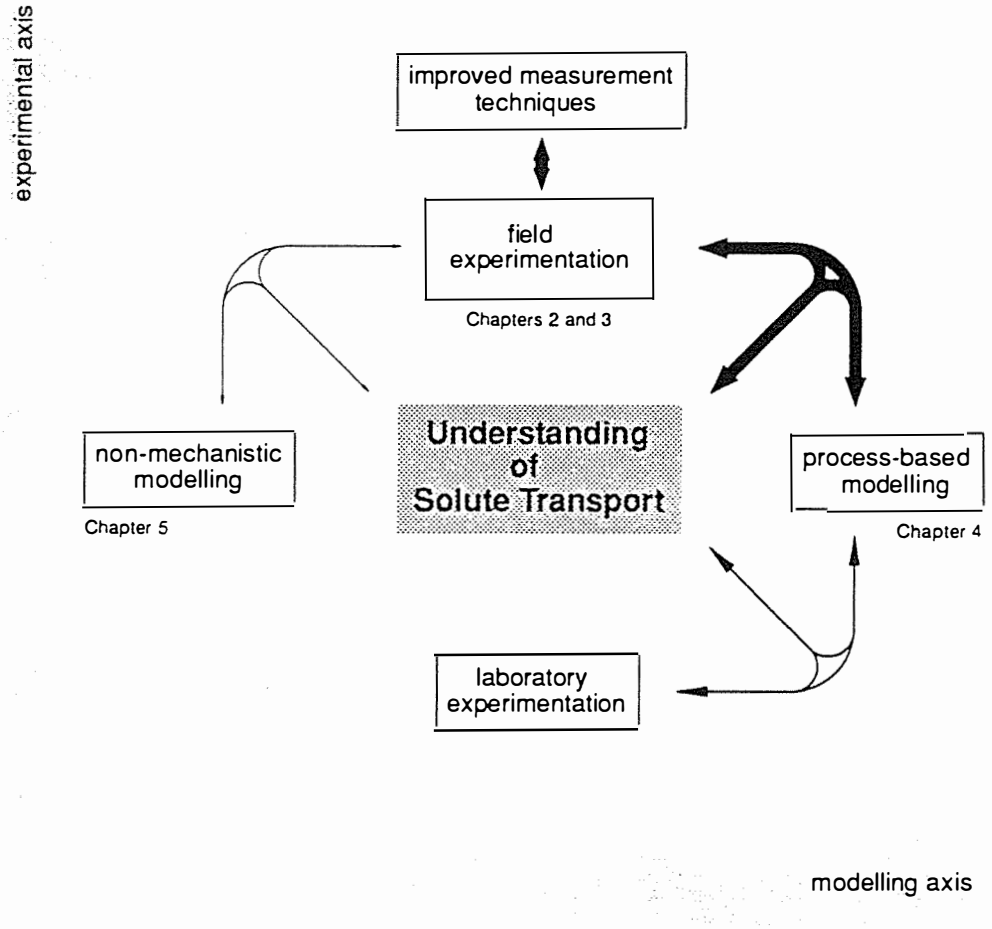

Figure 6.1 A philosophical framework for the understanding of solute transport modified by the experience of this thesis.

Armed with this understanding we can now re-examine the philosophic framework of solute transport research developed in Chapter One. These lessons indeed suggest that the structure of the diagram presented in Figure 1.1 is appropriate. There should however be more emphasis on the collaboration of process-based modelling and field experimentation with understanding. Figure 1.1 has now been re-presented as Figure 6.1 with this emphasis indicated. It also seems that an increased effort in improving measurement techniques will be advantageous. The

non-mechanistic AMZ modelling, of the data yielded little information or understanding.

One last conclusion from this thesis is that the small-scale local heterogeneities at the soil surface require more attention. For effective progress in understanding, we must concentrate this attention using a combination of field-based experimentation and process-based modelling.

Appendix A

DERIVATION OF EQUATION (5.3)

The equation describing the mass balance of solute in a tank is taken from equation (5.3),

$$V_m \frac{\mathrm{d}\, c_o(Q)}{\mathrm{d}Q} = c_i(Q - V_c) - c_o(Q) \quad . \tag{A.1}$$

Equation (A.1) may solved using Laplace transforms, where the transform of $f(Q)$ is written as $F(s)$ and is defined by,

$$F(s) = \mathcal{L}\{f(Q)\} = \int_0^\infty \mathrm{e}^{-sQ} f(Q)\, \mathrm{d}Q \quad . \tag{A.2}$$

Further defining,

$$\mathcal{L}\{c(Q)\} = C(s) \quad , \tag{A.3}$$

and using the properties,

$$\mathcal{L}\{\mathrm{e}^{-s\alpha} F\} = f(Q-\alpha) \quad , \tag{A.4}$$

and

$$\mathcal{L}\left\{\frac{\mathrm{d}f}{\mathrm{d}q}\right\} = sf - f(0) \quad , \tag{A.5}$$

we can now take the transform of equation (A.1) so that,

$$V_m s\, C_o(s) - V_m c_o(0) = \mathrm{e}^{-sV_c} C_i(s) - C_o(s) \quad . \tag{A.6}$$

Rearranging equation (A.6) leads to,

$$C_o(s) = \frac{\mathrm{e}^{-sV_c} C_i(s)}{1 + V_m s} + \frac{V_m c_o(0)}{1 + V_m s} \quad . \tag{A.7}$$

Now find the inverse Laplace transform of the first term on the right-hand side of equation (A.7). Let,

$$F(s) = \frac{1}{1 + V_m s} \quad \Rightarrow \quad f(Q) = \frac{1}{V_m} e^{-\frac{Q}{V_m}} \quad , \tag{A.8}$$

and,

$$G(s) = e^{-s V_c} C_i(s) \quad \rightarrow \quad g(Q) = c_i(Q - V_c) \quad . \tag{A.9}$$

Applying the convolution theorem it follows that,

$$\begin{aligned} \mathcal{L}^{-1}\left\{\frac{e^{-s V_c}}{1 + V_m s} C_i(s)\right\} &= \int_0^Q f(Q-Q')g(Q')dQ' \\ &= \int_0^Q \frac{1}{V_m} e^{-\frac{Q-Q'}{V_m}} c_i(Q'-V_c)dQ' \\ &= \frac{1}{V_m} e^{-\frac{Q}{V_m}} \int_0^Q e^{\frac{Q'}{V_m}} c_i(Q'-V_c)dQ' \quad . \end{aligned} \tag{A.10}$$

For the second term on the right-hand side of equation (A.7),

$$\mathcal{L}^{-1}\left\{\frac{V_m}{1 + V_m s} c_o(0)\right\} = c_o(0)\, e^{-\frac{Q}{V_m}} \quad . \tag{A.11}$$

Thus,

$$c_o(Q) = c_o(0) e^{-\frac{Q}{V_m}} + \frac{1}{V_m} e^{-\frac{Q}{V_m}} \int_0^Q e^{\frac{Q'}{V_m}} c_i(Q'-V_c)\, dQ' \quad . \tag{A.12}$$

Appendix B

DERIVATION OF EQUATION (5.5)

The equation describing the outflow concentration of solute from a tank was given in equation (5.3) as,

$$c_o(Q) = c_o(0)e^{-\frac{Q}{V_m}} + \frac{1}{V_m}e^{-\frac{Q}{V_m}}\int_0^Q e^{\frac{Q'}{V_m}} c_i(Q'-V_c)\,dQ' \quad . \qquad \text{(B.1)}$$

This equation may be discretised by first considering an interval of cumulative drainage, ΔQ, which is sufficiently small that c_o and c_i may be considered to be constant throughout the interval.

Expressed over the interval $0 \leq Q < \Delta Q$, equation (B.1) becomes,

$$c_o(\Delta Q) = c_o(0)e^{-\frac{\Delta Q}{V_m}} + \frac{1}{V_m}e^{-\frac{\Delta Q}{V_m}}\int_0^{\Delta Q} e^{\frac{Q'}{V_m}} c_i(\Delta Q-V_c)\,dQ' \quad . \qquad \text{(B.2)}$$

Generalising equation (B.2) to the interval $n\Delta Q \leq Q < (n+1)\Delta Q$, equation (B.1) becomes,

$$c_o([n+1]\Delta Q) = c_o(n\Delta Q)e^{-\frac{\Delta Q}{V_m}} + \frac{1}{V_m}e^{-\frac{(n+1)\Delta Q}{V_m}}\int_{n\Delta Q}^{(n+1)\Delta Q} e^{\frac{Q'}{V_m}} c_i([(n+1)\Delta Q]-V_c)\,dQ' \quad . \qquad \text{(B.3)}$$

It follows that,

$$c_o((n+1)\Delta Q) = c_o(n\Delta Q)e^{-\frac{\Delta Q}{V_m}} + \frac{1}{V_m}e^{-\frac{(n+1)\Delta Q}{V_m}}\left[V_m e^{\frac{Q'}{V_m}}\right]_{n\Delta Q}^{(n+1)\Delta Q} c_i([(n+1)\Delta Q]-V_c) \quad , \tag{B.4}$$

and,

$$c_o((n+1)\Delta Q) = c_o(n\Delta Q)e^{-\frac{\Delta Q}{V_m}} + \left(1-e^{-\frac{\Delta Q}{V_m}}\right) c_i([(n+1)\Delta Q]-V_c) \quad . \tag{B.5}$$

If <> stands for the nearest integer, j stands for $\langle(n+1)\Delta Q\rangle$, and k the number of drainage intervals in V_c, $\langle V_c/\Delta Q\rangle$, then equation (B.5) may be written as,

$$c_o(j) = e^{-\frac{\Delta Q}{V_m}} c_o(j-1) + \left(1 - e^{-\frac{\Delta Q}{V_m}}\right) c_i(j-k) \quad . \tag{B.6}$$

Appendix C

FACTORISATION OF THE ARMA EQUATION

Once an ARMA equation suitable for describing the calibration data had been found, the specific form of the general ARMA equation,

$$c_o(j) = \left[\frac{b_1 + b_2 q^{-1} + \ldots + b_{n_b} q^{-(n_b-1)}}{1 + a_1 q^{-1} + \ldots + a_{n_a} q^{-n_a}} \right] c_i(j - n_k) \quad , \qquad \text{(C.1)}$$

will be known. That is the parameters defining the form of the equation (n_a, n_b, n_k) as well as the parameter values (a_i and b_i) have been determined.

Factorisation is the process of finding the AMZ parameter values that correspond to the fitted ARMA equation. Stated mathematically, we want to find x, n_i, and k_i followed by α_i, and β_i, such that,

$$\left[\frac{b_1 + b_2 q^{-1} + \ldots + b_{n_b} q^{-(n_b-1)}}{1 + a_1 q^{-1} + \ldots + a_{n_a} q^{-n_a}} \right] c_i(j - n_k) = \left[\left(\frac{\beta_1 \, q^{-k_1}}{1 + \alpha_1 q^{-1}} \right)^{n_1} + \ldots + \left(\frac{\beta_x \, q^{-k_x}}{1 + \alpha_x q^{-1}} \right)^{n_x} \right] c_i(j) \quad . \qquad \text{(C.2)}$$

This process may be divided into two parts. Structural factorisation is the process of finding values of the parameters n_1 to n_x, and k_1 to k_x. These parameters equate to n_i, n_b, and n_k in the ARMA equation. Structural factorisability is established when the RHS of equation (C.2) can be expanded to match the numerator and denominator orders in equation (C.1). Once this has been done the values of α_1 to α_x can be found. First we will consider AMZ models where all tanks have a mixing volume.

It can be seen that the form of the RHS of equation (C.2) which, when expanded, will form the lowest degree of q in the numerator is when the total convective delay on each pathway is equal, or when,

$$k_1 n_1 = k_2 n_2 = \ldots = n_k \quad . \tag{C.3}$$

First consider an AMZ model which is subject to equation (C.3). In this case, because for all i,

$$q^{-n_i k_i} c_i(j) = c_i(j-n_k) \quad , \tag{C.4}$$

structural factorisation reduces to finding the n_i parameters of the AMZ such that,

$$\frac{b_1+b_2q^{-1}+\ldots+b_{n_b}q^{-(n_b-1)}}{1+a_1q^{-1}+\ldots+a_{n_a}q^{-n_a}} = \left(\frac{\beta_1}{1+\alpha_1 q^{-1}}\right)^{n_1}+\ldots+\left(\frac{\beta_x}{1+\alpha_x q^{-1}}\right)^{n_x} \quad . \tag{C.5}$$

The denominators of all the elements on the RHS of equation (C.5) must be multiplied together to form the denominator of the LHS of equation (C.5). Thus, the power to which q will be raised in the denominator of the LHS of equation (C.5) is the negative sum of the n_i's. Therefore,

$$n_a = \sum_{i=1}^{x} n_i \quad . \tag{C.6}$$

Equation (C.6) holds whether or not the AMZ is subject to equation (C.3).

The power to which q is raised on the numerator of the LHS of equation (C.5) is $-(n_b-1)$. On the RHS of equation (C.5) the numerator power of q will be the negative sum of the n_i's excluding the lowest n_i. If the AMZ is not subject to equation (C.3) then the resultant ARMA equation numerator must have an order equal to, or more negative than this. So that,

$$\begin{aligned} -(n_b-1) &\leq -\left(\sum_{i=1}^{x} n_i - \min[n_i]\right) \quad , \\ &\leq -(n_a-\min[n_i]) \quad , \\ n_b &\geq n_a+1-\min[n_i] \quad . \end{aligned} \tag{C.7}$$

Now, if $x=1$, it can be seen that $n_a=n_1$, and $n_b=1$.

If $x=2$, because there are only two terms on the RHS of equation (C.5), it can be seen that $(n_b\text{-}1)\geq\max[n_i]$. Further,

$$\begin{aligned} \max[n_i] &\geq \min[n_i] \quad , \\ n_b-1 &\geq n_a+1-n_b \quad , \\ n_b &\geq \frac{n_a+2}{2} \quad . \end{aligned} \tag{C.8}$$

Finally if $x\geq 3$, there must be at least two denominator terms from the RHS equation (C.5) being multiplied together to form the numerator of the LHS. In this case the minimum power to which q is raised on the numerator of the LHS must be greater than, or equal to, twice the minimum n_i value. Therefore,

$$\begin{aligned} n_b-1 &\geq 2\min[n_i] \quad , \\ n_b-1 &\geq 2(n_a+1-n_b) \quad , \\ n_b &\geq \frac{2n_a+3}{3} \quad . \end{aligned} \tag{C.9}$$

Additionally, provided α does not equal 0 and none of the b parameters in the ARMA are 0 then,

$$n_b \leq \sum_{i=1}^{x}\left(1+\sum_{j=1,j\neq i}^{x} n_j\right) \quad . \tag{C.10}$$

The inequality (C.10) will help decide if dispersion-free tanks are in the AMZ model.

The above analysis has implicitly assumed that all α's are greater than 0. This corresponds to an assumption that each tank has a mixing volume. Tanks without mixing volumes transport solute with dispersion-free flow only. If the case where the possibility of $V_m=0$ is considered, then n_a equals not the number of tanks as represented in equation (C.3), but the number of tanks with mixing volumes. In this case, the relationships outlined above still are valid. As the addition of a pathway

with $\alpha=0$ will increase n_b but leave n_a unaffected, the above arguments apply also to AMZ models with dispersion-free tanks.

These requirements establish only structural factorisability and are unaffected by any assumption of equal tanks within a pathway. To establish algebraic factorisability the values of the α's must all lie within the range, $-1 \leq \alpha \leq 0$. If any α falls outside this range, either a mixed volume cannot be calculated or will be physically nonsensical. It may, for example, be negative. Graphical analysis of the A polynomial will assist in the determination of the α values.

REFERENCES

Addiscott T.M., Wagenet R.J., 1985, Concepts of solute leaching in soils: A review of modelling approaches. *J. Soil Sci.* 36:411-424.

Al-Niami A.N.S. Rushton K.R., 1979, Dispersion in stratified porous media: Analytical solutions. *Water Resources Res.* 15:1044-1048.

Barry D.A., Parker J.C., 1987, Approximations for solute transport through porous media with flow transverse to layering. *Transport in Porous Media.* 2:65-82.

Beer T., Young P.C., 1983, Longitudinal dispersion in natural streams. *J. Environmental Engineering* 109:1049-1067.

Beven K.J., Young P.C., 1988, An aggregated mixing zone model of solute transport through porous media. *J. Contaminant Hydrology* 3:129-143.

Biggar J.W., Nielsen D.R., 1967, Miscible displacement and leaching phenomenon. In *Irrigation of Agricultural Lands.* Eds Hagan R.M., Haise H.R., Edminster T.W. Agronomy 11. Pub. A.S.A., Madison, Wisconsin, pp254-274.

Biggar J.W., Nielsen D.R., 1976, Spatial variability of the leaching characteristics of a field soil. *Water Resources Res.* 12:78-84.

Bond W.J., Smiles D.E., 1983, Influence of velocity in hydrodynamic dispersion during unsteady soil water flow. *Soil Sci. Soc. Am. J.* 47:438-441.

Bresler E, Dagan G., 1981, Unsaturated flow in spatially variable fields. 3. Solute transport models and their application to two fields. *Water Resources Res.* 19:429-435.

Bruch J.C., 1970, Two-dimensional dispersion in short laboratory cores. *Soc. Pet. Eng. J.* 17:91-99.

Burns I.G., 1975, An equation to predict the leaching of nitrate uniformly incorporated to a known depth or uniformly distributed throughout a soil profile. *J. Soil Sci.* 31:175-202.

Butters G.L., Jury W.A., Ernst F.E., 1989, Field scale transport of bromide in an unsaturated soil. 1. Experimental methodology and results. *Water Resources Res.* 25:1575-1581.

Butters G.L., Jury W.A., 1988, *Bromide transport through an unsaturated field soil.* EPRI-EA-5939.

Butters G.L., Jury W.A., 1989, Field scale transport of bromide in an unsaturated soil. 2. Dispersion modelling. *Water Resources Res.* 25:1583-1589.

Cassel D.K., van Genuchten M. Th., Wierenga P.J., 1975, Predicting anion movement in disturbed and undisturbed soils. *Soil Sci. Soc. Am. J.* 39:1015-1019.

Christiansen J.E., 1942, *Irrigation by sprinkling.* Univ. of Calif. Agr. Exp. Stat. Report. 670pp.

Clothier B.E., 1977, *Aspects of the water balance of an oats crop grown on a layered soil.* Unpublished PhD Thesis. Massey University, Palmerston North, New Zealand.

Clothier B.E., Kirkham M.B., McLean J.E., 1992, *In situ* measurements of the effective transport volume for solute moving through soil. *Soil Sci. Soc. Am. J.* 56:733-736.

Clothier B.E., Pollock J.P., Scotter D.R., 1978, Mottling in soil profiles containing a coarse-textured horizon. *Soil Sci. Soc. Am. J.* 42:761-763.

Clothier B.E., Scotter D.R., Kerr J.P., 1977a, Water retention in a soil underlain by a coarse-textured layer. *Soil Science* 123:392-390.

Clothier B.E., Scotter D.R. Kerr J.P., 1977b, Drainage flux in a permeable soil underlain by a coarse-textured layer. *Soil Sci. Soc. Am. J.* 41:671-676.

Coats K.H., Smith B.D., 1964, Dead-end pore volume and dispersion in porous media. *Soc. Pet. Eng. J.* 4:74-84.

Coulson J.M., Richardson J.F., 1978, *Chemical Engineering, Vol 2, Unit operations. 3rd Ed.* London, Pergamon Press.

Dagan G., 1984, Solute transport in heterogenous porous formations. *J. Fluid Mech.* 145:151-177.

Dagan G., 1986, Statistical theory of ground water flow and transport: Pore to laboratory, laboratory to formation, and formation to regional scale. *Water Resources Res.* 22:120S-134S.

Dagan G., Bresler E., 1981, Unsaturated flow in spatially variable fields. 1. Derivation of models of infiltration and redistribution. *Water Resources Res.* 19:413-420.

De Lisle J.E., 1966, Mean insolation in New Zealand. *N. Z. J. Sci.* 9:992-1005.

De Smedt F., Wierenga P.J., 1979, A generalised solution for solute flow in soils with mobile and immobile water. *Water Resources Res.* 15:1137-1141.

Dyson J.S., Jury W.A., Butters G.L., 1990, *The prediction and interpretation of chemical movement through porous media: The transfer function model approach. EPRI EN-6853.*

Dyson J.S., White R.E., 1989, A simple predictive approach to solute transport in layered soils. *J. Soil Sci.* 40:525-542.

Elrick D.E., Laryea K.B., Greonvelt P.H., 1979, Hydrodynamic dispersion during infiltration of water into soil. *Soil Sci. Soc. Am. J.* 43:856-865.

FAO-Unesco, 1974, *Soil maps of the world. Vol I. Legend.* Pub. FAO-Unesco, Paris.

Feynman R.P., 1967, *The Character of Physical Law.* MIT Press, Cambridge, Mass.

Field T.R.O., Theobald P.W., Ball P.R., Clothier B.E., 1985, Leaching losses of nitrate from cattle urine applied to a lysimeter. *Proc. Agron. Soc. N. Z.* 15:137-141.

Florence T.M., Farrar Y.S., 1971, Spectrophotometric determination of chloride at the parts-per-billion level by the mercury II, thiocyanate method. *Analytica Chemica Acta* 54:373-377.

Freyberg D.L., 1986, A natural gradient experiment on solute transport in a sand aquifer. 2. Spatial moments and the advection and dispersion of nonreactive tracers. *Water Resources Res.* 22:2031-2046.

Garabedian S.P., Le Blanc D.R., Gelhar L.W., Celia M.A., 1991, Large-scale, natural-gradient tracer test in sand and gravel, Cape Cod, Masachusetts. 2. Analysis of spatial moments for nonreactive tracer. *Water Resources Res.* 27:991-924.

Gardner W.R., 1965, Movement of nitrogen in soil. In *Soil Nitrogen* Agronomy Monographs 10., eds Bartholomew W.V., Clark F.E. Pub. A.S.A. Wisconsin, pp550-572.

Green A.E., 1983, *Some measurements and estimates of evapotranspiration from pasture.* Dip. Agr. Sci dissertation, Massey University, Palmerston North, New Zealand.

Green A.E., Clothier B.E., Kerr J.P., Scotter D.R., 1984, Evapotranspiration from pasture: A comparison of lysimeter and Bowen ratio measurements with Priestley-Taylor estimates. *N. Z. J. Agr. Res.* 27:321-327.

Gureghian A.B., Jansen G., 1985, One-dimensional analytical solutions for the migration of a three-member radionuclide decay chain in a multi-layered geologic medium. *Water Resources Res.* 21:733-742.

Hassan H.M., Warrick A.W., Amoozegar-Fard A., 1983, Sampling volume effects on determining salt in a soil profile. *Soil Sci. Soc. Am. J.* 47:1265-1267.

Heng L.K., 1991, *Measurement and modelling of chloride and sulphate leaching from a mole drained soil.* Unpublished PhD thesis, Massey University, Palmerston North, New Zealand.

Hornberger G.M., Beven K.J., Germann P.F., 1990, Inferences about solute transport in macroporous forest soils from times series models. *Geoderma* 46:249-262.

Jury W.A., 1982, Simulation of solute transport using a transfer function model. *Water Resources Res.* 18:363-368.

Jury W.A., 1988, Solute movement and dispersion. In *Flow and Transport in the Natural Environment: Advances and Applications.* Eds Steffan W.L., Denmead O.T. Springer-Verlag, pp1-16.

Jury W.A., Dyson J.S., Butters G.L., 1990, A transfer function model of field scale solute transport under transient water flow. *Soil Sci. Soc. Am. J.* 54:327-350.

Jury W.A., Fluhler H., 1992, Transport of chemicals through soil: Mechanisms, models, and field applications. *Advances in Agronomy* 47:141-201.

Jury W.A., Gardner W.R., Saffigna P.G., Tanner C.B., 1976, Model for predicting simultaneous movement of nitrate and water through a loamy sand. *Soil Science* 122:36-43.

Jury W.A., Roth K., 1990, *Transfer Functions and Solute Movement Through Soil: Theory and Applications.* Birkhauser, Basel, Switzerland.

Jury W.A., Sposito G., White R.E., 1986, A transfer function model of solute transport through soil. 1. Fundamental concepts. *Water Resources Res.* 22:243-247.

Jury W.A., Stolzy L.H., Shouse P., 1982, A field test of the transfer function model for predicting solute transport. *Water Resources Res.* 18:369-375.

Kahn A.U., Jury W.A., 1990, A laboratory study of the dispersion scale effect in column outflow experiments. *J. Contam. Hydrol.* 5:119-131.

Kachanoski R.G., Pringle E., Ward A., 1992, Field measurement of solute travel times using time domain reflectometry. *Soil Sci. Soc. Am. J.* 56:47-52.

Kissel D.E., Ritchie J.T., Burnett E., 1973, Chloride movement in undisturbed clay soil. *Soil Sci. Soc. Am. J.* 37:21-24.

Knight J.H., 1988, Solute movement and dispersion - Commentary. In *Flow and Transport in the Natural Environment: Advances and Applications.* Eds Steffan W.L., Denmead O.T. Springer-Verlag, pp17-29.

Kreft A., Zuber A., 1978, On the physical meaning of the dispersion equation and it's solutions for different boundary conditions. *Chem. Eng. Sci.* 33:1471-1480.

Leij F.J., Dance J.H., van Genuchten M.Th., 1991, Mathematical analysis of one-dimensional solute transport in a layered soil profile. *Soil Sci. Soc. Am. J.* 55:944-953.

Ljung L., 1987, *System Identification - Theory for the user.* Prentice-Hall, Englewood Cliffs, N.J.

Ljung L., 1988, System identification toolbox users guide. The Mathworks Inc.

Matheron G., de Marsily G., 1980, Is transport in porous media always diffusive? A counter-example. *Water Resources Res.* 16:901-917.

Myers P.C., 1990, Symposium challenge from deputy secretary of agriculture. In *Proceedings of the International Symposium on Water Quality Modelling of Agricultural Non-Point Sources. Part 1. June 19-23 1988, Utah State University, Logan, Utah*, pp7-10.

Moore E.C.S., 1898, *Sanitary engineering: a practical treatise on the collection, removal and final disposal of sewage and the design and construction of works of drainage and sewerage.* B.T. Batsford, London.

Morrison R.D., 1982, A modified vacuum-pressure lysimeter for soil water sampling. *Soil Science* 134:206-210.

Nielsen D.R., van Genuchten M.T., Biggar J.W., 1986, Water flow and solute transport in the unsaturated zone. *Water Resources Res.* 22:89S-108S.

Parker J.C., van Genuchten M.Th., 1984, Flux-averaged and volume-averaged concentrations in continuum approaches to solute transport. *Water Resources Res.* 20:866-872.

Parkin T.B., Meisinger J.J., Chester S.T., Starr J.L., Robinson J.A., 1988, Evaluation of statistical estimation methods for lognormally distributed variables. *Soil Sci. Soc. Am. J.* 52:323-329.

Perroux K.M., White I., 1988, Designs for disc permeameters. *Soil Sci. Soc. Am. J.* 52:1205-1215.

Philip J.R., 1991, Soils, natural science, and models. *Soil Science.* 151:91-98.

Priestley C.H.B., Taylor R.J., 1976, Assessment of the surface heat flux and evaporation using large scale parameters. *Monthly Weather Review* 100:81-92.

Raats P.A.C., 1978a, Convective transport of solutes by steady flows. I. General theory. *Ag. Water Management* 1:201-218.

Raats P.A.C., 1978b, Convective transport of solutes by steady flows. II. Specific flow examples. *Ag. Water Management* 1:201-218.

Rahardjo P., 1989, *Water use by apple trees.* Unpublished M.Agr.Sci. thesis, Massey University, Palmerston North, New Zealand.

Rao P.S.C., Green R.E., Ahuja L.R., Davidson J.M., 1976, Evaluation of a capillary bundle model for describing solute dispersion in aggregated soils. *Soil Sci. Soc. Am. J.* 40:815-820.

Resource Management Act, 1991, GPH Print.

Richter G., Jury W.A., 1986, A microlysimeter field study of solute transport through a structured sandy loam soil. *Soil Sci. Soc. Am. J.* 50:863-868.

Riekerk H., Morris L.A., 1983, A constant potential soil water sampler. *Soil Sci. Soc. Am. J.* 47:606-608.

Robinson N., 1966, *Solar Radiation.* Elsevier, Amsterdam.

Rosenberg N.J., Blaine L.B., Verma S.B., 1974, *Microclimate: The biological environment. 2nd Edition.* Wiley Interscience.

Roth K., Jury W.A., Fluhler H., Attinger W., 1991, Transport of chloride through an unsaturated field soil. *Water Resources Res.* 27:2533-2541.

Scotter D.R., Clothier B.E., Turner M.A., 1979, The soil water balance of a fragiaqualf and its effect on pasture growth in central New Zealand. *Aust. J. Soil Res.* 17:455-465.

Selim H.M., Davidson J.M., Rao P.S.C., 1977, Transport of reactive solutes through multi-layered soils. *Soil Sci. Soc. Am. J.* 41:3-10.

Sellers W.D., 1965, *Physical Climatology.* University of Chicago Press, Chicago.

Shamir U.Y., Harleman D.R.F., 1967, Dispersion in layered porous media. *Proc. Am. Soc. Civil Eng. Hydr. Div.* 93:236-260.

Sichel H.S., 1952, New methods in the statistical evaluation of mine sampling data. *Trans. London Inst. Mining Metallurgy* 61:261-288.

Simmons C.S., 1982, A stochastic-convective transport representation of dispersion in one-dimensional porous media systems. *Water Resources Res.* 18:1193-1214.

Smiles D.E., Philip J.R., 1978, Solute transport during absorbtion of water: Laboratory studies and their practical implications. *Soil Sci. Soc. Am. J.* 42:537-544.

Smiles D.E., Philip J.R., Knight J.H., Elrick D.E., 1978, Hydrodynamic dispersion during absorption of water by soil. *Soil Sci. Soc. Am. J.* 42:229-234.

Smith L., Schwartz F.W., 1980, Mass transport. 1. A stochastic analysis of macroscopic dispersion. *Water Resources Res.* 16:303-313.

Sposito G., Jury W.A., Gupta V.J., 1986, Fundamental problems in the stochastic convection-dispersion model of solute transport in aquifers and field soils. *Water Resources Res.* 22:77-88.

Sposito G., White R.E., Darrah P.R., Jury W.A., 1986, A transfer function model of solute transport through soil. 3. The convection-dispersion equation. *Water Resources Res.* 22:255-262.

Starr J.L., de Roo H.C., Frink C.R., Parlange J-Y., 1978, Leaching characteristics of a layered soil. *Soil Sci. Soc. Am. J.* 42:386-391.

Starr J.L., Parlange J-Y., Frink C.R., 1986, Water and chloride movement through a layered field soil. *Soil Sci. Soc. Am. J.* 50:1284-1390.

Taylor G., 1953, Dispersion of soluble matter in solvent flowing slowly through a tube. *Proc. Royal Soc. London. Series A.* 219:186-203.

Tillman R.W., 1991, *Solute movement associated with intermittent water flow.* Unpublished PhD thesis, Massey University, New Zealand.

Tillman R.W., Scotter D.R., Clothier B.E., White R.E., 1991, Solute movement during intermittent water flow in a field soil and some implications for irrigation and fertiliser application. *Ag. Water Manage.* 20:119-133.

Tyler D.D., Thomas G.W., 1981, Chloride movement in undisturbed soil columns. *Soil Sci. Soc. Am. J.* 45:459-461.

Van Genuchten M.Th., Wierenga P.J., 1976, Mass transfer in sorbing porous media. I. Analytical solutions. *Soil Sci. Soc. Am. Proc.* 40:473-480.

Van Wesenbeeck I.J., Kachanoski R.G., 1991, Spatial scale dependence of *in situ* solute transport. *Soil Sci. Soc. Am. J.* 55:3-7.

Wagner G.H., 1962, Use of porous ceramic cups to sample soil water within the profile. *Soil Science* 94:379-386.

Wallis S.G., Young P.C., Beven K.J., 1989, Experimental investigation of the aggregated dead zone model for longitudinal solute transport in stream channels. *Proc. Inst. Civ. Eng.* 87:1-22.

Warrick A.W., Amoozegar-Fard A., 1977, Soil water regimes near porous cup water samplers. *Water Resources Res.* 13:203-207.

Warrick A.W., Biggar J.W., Nielsen D.R., 1971, Simultaneous solute and water transfer for an unsaturated soil. *Water Resources Res.* 7:1216-1225.

White R.E., Ayoub A.T., 1983, Decomposition of plant residues of variable C/P ratio and the effect on soil phosphate availability. *Plant and Soil.* 74:163-173.

White R.E., Dyson J.S., Haigh R.A., Jury W.A., Sposito G., 1986, A transfer function model of solute transport through soil. 2. Illustrative applications. *Water Resources Res.* 22:248-254.

White R.E., Thomas G.W., Smith M.S., 1984, Modelling water flow through undisturbed soil cores using a transfer function model derived from ^{3}HOH and Cl transport. *J. Soil Sci.* 35:159-168.

Wood W.W., 1973, A technique using porous cups for water sampling at any depth in the unsaturated zone. *Water Resources Res.* 9:486-488.